

DISCOVERY AND CHARACTERIZATION OF SMALL MOLECULE INHIBITORS
OF THE ALDEHYDE DEHYDROGENASE 1/2 FAMILY

Cameron D. Buchman

Submitted to the faculty of the University Graduate School
in partial fulfillment of the requirements
for the degree
Doctor of Philosophy
in the Department of Biochemistry and Molecular Biology,
Indiana University

December 2016

Accepted by the Graduate Faculty, Indiana University, in partial fulfillment of the requirements for the degree of Doctor of Philosophy

Thomas D. Hurley, Ph.D., Chairman

Jeffrey S. Elmendorf, Ph.D.

Doctoral Committee

Quyen Q. Hoang, Ph.D.

September 1, 2016

Ronald C. Wek, Ph.D.

Dedication

To my mother, who has always supported my dreams and encouraged me to fulfill them,
and to my sister, who has always kept me level-headed while pursuing them.

Acknowledgements

I would like to start by thanking my graduate advisor, Dr. Thomas Hurley, for being an outstanding mentor and friend. I am grateful to him for allowing me to complete my research thesis with him and for providing me with multiple learning opportunities.

Despite my limited prior experience, he allowed me to pursue this project independently, while always being there when I needed help. Above all, I thank him for his patience and wisdom. I firmly believe that he is the best mentor I could ever have had for my graduate studies. I also thank the other members of my committee; Dr. Jeffrey Elmendorf, Dr. Quyen Hoang, and Dr. Ronald Wek; for their guidance, suggestions, and constructive criticism, and challenging me to think beyond the test tube, or this case, the cuvette.

Science is a highly collaborative endeavor, and as such multiple individuals and laboratories helped me complete this project. I thank the Chemical Genomics Core facility, especially Dr. Lan Chen, for providing the use of their facilities and compound libraries and assisting with the high-throughput screens. I thank Dr. Maureen Harrington and Dr. Danielle Matei for the use of their cell culture facilities, and Dr. Donghui Zhou and Dr. Salvatore Condello for teaching me cell culture techniques. I thank Dr. Clark Wells for providing the MDA-MB-468 cells. I also thank Dr. John Turchi for the use of his fluorimeter.

My colleagues in Dr. Hurley's laboratory have also aided me in this project. I thank Dr. Bibek Parajuli for aiding me in my rotation and helping me get started in the lab; Dr. May

Khanna, Dr. Vimbai Chikwana, Dr. Ann Kimble Hill, and Dr. Cindy Morgan for their answers to my many questions; Lanmin Zhai for assistance with multiple protein purifications, and Krishna Kishore Mahalinghan for completing Screen 1 of the high-throughput screen. I also thank all of them, and Mikhail Chtcherbinine, for their friendship, support, and providing the necessary distractions from an often hectic schedule.

I would also like to thank members of the Department of Biochemistry and Molecular office, Sandy, Melissa, Jack, Patty, Darlene, and Sheila, for their assistance and working behind-the-scenes to make my graduate studies run smoothly.

This research was supported by the U.S. National Institutes of Health (grants RO1AA018123 and R21CA198409 to T.D.H.). Results shown in this report are derived from work performed at Argonne National Laboratory, Structural Biology Center at the Advanced Photon Source. Argonne is operated by UChicago Argonne, LLC, for the U.S. Department of Energy, Office of Biological and Environmental Research under contract DE-AC02-06CH11357. This research used resources of the Advanced Photon Source, a U.S. Department of Energy (DOE) Office of Science User Facility operated for the DOE Office of Science by Argonne National Laboratory under Contract No. DE-AC02-06CH11357.

Cameron D. Buchman

DISCOVERY AND CHARACTERIZATION OF SMALL MOLECULE INHIBITORS
OF THE ALDEHYDE DEHYDROGENASE 1/2 FAMILY

The human aldehyde dehydrogenase (ALDH) superfamily consists of 19 isoenzymes that are critical for normal physiology as well as the removal of toxic aldehydes. Members of the ALDH1/2 family have vital roles in cell signaling during early development, ethanol metabolism, and the removal of aldehydes derived from oxidative stress. We sought to develop selective compounds toward ALDH2 to help determine its individual contribution to biological function, as many of the ALDH1/2 family possess overlapping substrate preferences. A high-throughput screen of over 100,000 compounds uncovered a class of aromatic lactones which inhibit the ALDH1/2 enzyme family. The lactones were then characterized using a combination of enzyme kinetics, X-ray crystallography, and cell culture experiments. We found that many of the lactones are over ten times more potent toward ALDH2 than daidzin, a previously described ALDH2 inhibitor. Our ability to produce many more ALDH isoenzymes allowed us to determine that daidzin is not as selective as previously believed, inhibiting ALDH2, ALDH1B1, and ALDH1A2 with equal potency. This inhibition pattern was seen with several of the aromatic lactones as well. Structural studies show that many of the lactones bind between key aromatic residues in the ALDH1/2 enzyme substrate-binding sites. One lactone in particular mimics the position of an aldehyde substrate and alters the position of the catalytic

cysteine to interfere with the productive binding of NAD^+ for enzyme catalysis. Further characterization of related compounds led to the realization that the mechanism of inhibition, potency, and selectivity differs amongst the lactones based off the substituents on the aromatic scaffold and its precise binding location. Two of these compounds were found to be selective for one of the ALDH1/2 family members, BUC22, selective for ALDH1A1, and BUC27, selective for ALDH2. BUC22 demonstrates ten-fold selectivity for ALDH1A1 over ALDH1A2 and does not inhibit the remaining ALDH1/2 enzymes. Additionally, treatment with BUC22 led to decreased growth of triple-negative breast cancer cells in culture. BUC27 inhibits ALDH2 with the same potency as daidzin. Both BUC22 and BUC27 could be further developed to use as chemical tools to better understand the functional roles of ALDH1A1 and ALDH2 in biological systems.

Thomas D. Hurley, Ph.D., Chairman

Table of Contents

List of Tables	xi
List of Figures	xii
I. Introduction	1
A. Aldehydes.....	1
B. Aldehyde Dehydrogenase Superfamily.....	5
C. Aldehyde Dehydrogenase 1/2 Family	13
D. ALDH1A1, Cancer, and Cancer Stem Cells.....	19
E. ALDH2, ALDH2*2, and Alcohol-Induced Pathophysiology	22
F. ALDH2 and Cardiovascular Disease.....	25
G. ALDH1A1, ALDH2, and Neurological Disease	27
H. ALDH1/2 Activators and Inhibitors	29
I. Hypothesis and Approach.....	31
II. Materials and Methods	34
A. Materials.....	34
B. Methods	34
1. Production and Purification of ALDH Isoenzymes	34

2. Esterase High-Throughput Screen	37
3. Aldehyde Oxidation Activity Assays for ALDH Isoenzymes	39
4. Steady-state Kinetic Characterization with ALDH1A1 and ALDH2	41
5. Characterization of 2BS4's Inhibition of ALDH2	43
6. Crystallization of ALDH1A1 and ALDH2 Complexes	44
7. Cellular Effect of the Coumarin Derivative BUC22	47
III. Results	48
A. Esterase High-Throughput Screen for ALDH2 Modulators	48
1. Z'-factor Calculation	48
2. High-Throughput Screen Results	50
B. Hit Compound Validation and Initial Determination of Selectivity	52
C. EC ₅₀ Determination of Hit Compounds	57
1. Alda-1 Mimics	57
2. Coumarin and Psoralen Derivatives, in Comparison to Daidzin	59
D. Characterization of Interaction of Aromatic Lactones with ALDH2	62
1. Kinetic Characterization of 2P4	62
2. 2P3-ALDH2 Crystal Structure	64

3. Kinetic Characterization of 2BS4	66
E. Characterization of Additional Psoralen and Coumarin Analogs	69
1. Single Concentration Selectivity for Structure-Activity Relationships	69
2. EC ₅₀ Determination.....	76
3. Characterization of BUC11's Interaction with ALDH1A1 and ALDH2	78
4. Characterization of BUC25's Interaction with ALDH1A1	81
5. Characterization of BUC22's Interaction with ALDH1A1	83
6. Characterization of BUC27's Interaction with ALDH2	85
F. Effect of BUC22 on Viability of Breast Cancer Cells in 3D Culture.....	86
IV. Discussion.....	88
V. Conclusion and Future Directions.....	108
References.....	113
Curriculum vitae	

List of Tables

Table 1: Common sources of aldehydes	2
Table 2: The 19 human aldehyde dehydrogenase isoenzymes	7
Table 3: AC ₅₀ determination of Alda-1 mimics with ALDH2	59
Table 4: IC ₅₀ values for four aromatic lactones with nine ALDH isoenzymes	61
Table 5: Collection and refinement statistics for the 2P3-ALDH2 complex.....	65
Table 6: Structure activity relationships for psoralen derivatives	71
Table 7: Structure activity relationships for coumarin derivatives.....	72
Table 8: IC ₅₀ values for four analogs with ALDH1A1, ALDH2, and ALDH3A1	76
Table 9: EC ₅₀ values for seven analogs with the ALDH1/2 family and ALDH3A1	78
Table 10: Collection and refinement statistics for the BUC11-ALDH1A1 complex....	79
Table 11: Collection and refinement statistics for the BUC25-ALDH1A1 complex....	82
Table 12: Collection and refinement statistics for the BUC22-ALDH1A1 complex....	83

List of Figures

Figure 1: Aldehyde detoxification enzymes	4
Figure 2: ALDH nomenclature	5
Figure 3: Phylogenetic tree for human ALDH superfamily	6
Figure 4: Catalytic mechanisms for ALDH isoenzymes	11
Figure 5: Multiple conformations of cofactor bound to ALDH isoenzymes.....	12
Figure 6: Structural characteristics of ALDH isoenzymes	13
Figure 7: Retinoic acid signaling pathway.....	15
Figure 8: Structure of ALDH2 versus ALDH2*2.....	24
Figure 9: Research approach to identifying compound that alter ALDH activity	33
Figure 10: Z'-factor determination for Screen 1	49
Figure 11: Z'-factor determination for Screen 2.....	50
Figure 12: Example plate from Screen 1 for compounds that modify ALDH activity..	51
Figure 13: Effect on aldehyde oxidation of hit compounds from HTS	54
Figure 14: Effects of four aromatic lactones on activity of nine ALDH isoenzymes....	57
Figure 15: Three Alda-1 mimics identified via the HTS	58
Figure 16: Four aromatic lactone inhibitors identified via the HTS.....	60

Figure 17: Standard curve for fluorescence of NADH	63
Figure 18: Substrate K_m determination using fluorescence assay	63
Figure 19: Steady-state kinetic characterization of inhibition of ALDH2 by 2P4	64
Figure 20: Crystal structure of 2P3-ALDH2 complex.....	66
Figure 21: Steady-state kinetic characterization of inhibition of ALDH2 by 2BS4.....	67
Figure 22: Incubation of ALDH2 with 2BS4	68
Figure 23: IC_{50} values for BUC22 with ALDH2 after different incubation periods	69
Figure 24: Compound scaffolds of psoralen- and coumarin-derived analogs	70
Figure 25: Crystal structure of BUC11-ALDH1A1 complex.....	80
Figure 26: Steady-state kinetic characterization of BUC11 with ALDH enzymes	81
Figure 27: Crystal structure of BUC25-ALDH1A1 complex.....	82
Figure 28: Crystal structure of BUC22-ALDH1A1 complex.....	84
Figure 29: Steady-state kinetic characterization of inhibition by BUC22 and BUC20.	85
Figure 30: Steady-state kinetic characterization of inhibition of ALDH2 by BUC27 ..	86
Figure 31: Effect of BUC22 treatment on proliferation of breast cancer cells.....	87
Figure 32: Effect of different compounds on esterase and dehydrogenase assays	90
Figure 33: Orientation of 2P3 in catalytic tunnel of ALDH2	92

Figure 34: Comparison of NAD ⁺ and 2P3 binding to ALDH2	93
Figure 35: Schematic of 2P3/4 inhibition of ALDH2.....	95
Figure 36: Comparison of BUC22 binding to ALDH1A1 versus ALDH2	100
Figure 37: Docking of BUC27 in substrate binding site of ALDH2	102
Figure 38: Alignment of three enzyme-inhibitor complexes	104

I. Introduction

A. Aldehydes

Aldehydes are organic compounds which contain a terminal carbonyl carbon (RCHO) where the R group can range from a hydrogen atom to complex organic structures.

Aldehydes are found in a variety of endogenous and exogenous sources (**Table 1**).

Amino acid catabolism produces aldehyde intermediates such as glutamic γ -semialdehyde. The catabolism of various neurotransmitters including gamma-aminobutyric acid (GABA), dopamine, adrenaline, and serotonin also produces several aldehyde intermediates.¹ Many open chain forms of carbohydrates contain an aldehyde group, or contain a ketone which can tautomerize in solution to form an aldehyde group. The metabolism of ethanol and other foods can generate acetaldehyde as well as other aldehyde products. Aldehydes such as citral and benzaldehyde are also added to foods to provide flavor and odor.² Several aldehydes play important roles in normal physiological processes. Retinaldehydes are an example that has multiple functions; as transcription factors critical for cellular growth and differentiation pathways, or as the ligand for rhodopsin, which covalently binds 11-cis-retinal and enables vision in low-light conditions.^{3, 4}

Despite being critical for many biological functions, many aldehydes are carcinogenic and cytotoxic. Oxidative degradation of membrane lipids, or lipid peroxidation, can produce over 200 aldehyde species, including 4-hydroxynonenal (4-HNE) and malondialdehyde (MDA).⁵ Environmental exposure to smog, cigarette smoke, and motor vehicle exhaust are potential sources for formaldehyde, acetaldehyde, and acrolein,

Table 1 Common sources of aldehydes.

Endogenous Source	Aldehyde
Lipid peroxidation	4-hydroxynonenal, malondialdehyde, hexanal
Dopamine catabolism	3-4-Dihydroxyphenylacetaldehyde
GABA metabolism	succinic semialdehyde
Serotonin metabolism	4-hydroxyindoleacetaldehyde
Putrescine catabolism	γ -amino butyraldehyde
Vitamin A metabolism	retinaldehyde
Carbohydrate metabolism	glyceralehyde, glycolaldehyde, glyoxal

Exogenous Source	Aldehyde
Ethanol	acetaldehyde
Foods	citral, benzaldehyde, crotonaldehyde
Combustion	formaldehyde, acetaldehyde, acrolein
Cigarettes	γ -3-pyridyl- γ -methylbutyraldehyde

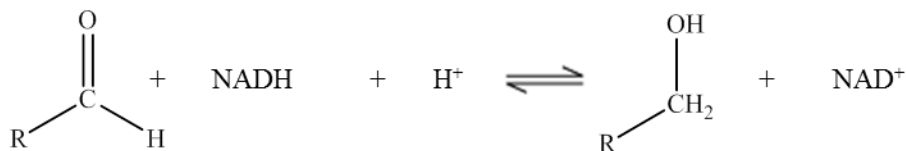
amongst other aldehydes.⁶ Aldehydes are also used or produced in various industrial applications including the production of resins, polyurethane, and polyester plastics. Each of these sources can contribute to the aldehydic load within the body. Highly reactive and electrophilic carbonyl groups in aldehydes can form adducts with various macromolecules including proteins, nucleic acids, and glutathione. Unlike reactive oxygen species and free radicals, aldehydes have relatively long lifespans and once formed, can react with both nearby cellular components and targets some distance away via diffusion or molecular transport.⁵ Aldehydes can form a covalent adduct with proteins either by formation of a Schiff base via the ϵ -amino of lysine or by a Michael addition to cysteine, histidine, or lysine residues in a process called protein carbonylation.⁷ These reactions will typically result in a loss of function due to the importance of cysteine, histidine, and lysine in many enzyme catalytic mechanisms. Although moderate amounts

of carbonylation can be accommodated by cells, increasing amounts of carbonylation will eventually lead to protein dysfunction, cell death, and ultimately disease progression. It is important to note that protein carbonylation is elevated during oxidative stress and correspondingly a high proportion of carbonylated proteins are found in the mitochondria.⁸ Aldehydes have also been shown to inactivate antioxidant enzymes such as glutathione reductase and glutathione peroxidase by protein carbonylation, which as a consequence perpetuates oxidative stress in a positive feedback loop.^{9, 10} Aldehydes can also form adducts with DNA creating DNA-DNA and DNA-protein crosslinks, chromosomal aberrations, and other DNA damage.^{11, 12}

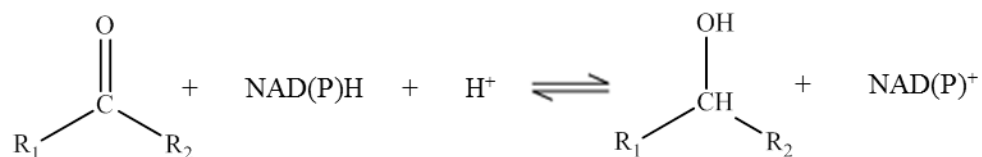
Cells have several mechanisms to alleviate aldehyde stress. Aldehydes can be reduced to an alcohol, oxidized to a carboxylic acid, or eliminated via interaction with glutathione. The main enzyme classes that reduce aldehydes to alcohols are alcohol dehydrogenases and aldo-keto reductases, and the main enzyme classes that oxidize aldehyde to carboxylic acids are aldehyde/xanthine oxidases and aldehyde dehydrogenases (**Figure 1**). Alcohol dehydrogenases can catalyze the reversible reduction of aldehydes and ketones to an alcohol. The direction of this reaction is heavily dependent on the NAD^+/NADH ratio. Oxidation of an alcohol to an aldehyde is the predominant reaction due to the normal 500:1 ratio of NAD^+ to NADH found within cells.¹³ The aldo-keto reductase superfamily consists of 13 human enzymes and catalyzes the reversible reduction of a variety of aldehydes and ketones to their corresponding alcohols.¹⁴ Aldehyde/xanthine oxidases catalyze the conversion of aromatic and heterocyclic aldehydes to their corresponding carboxylic acids.¹⁵ Aldehyde dehydrogenases catalyze

the NAD(P)^+ -dependent oxidation of an aldehyde to its corresponding carboxylic acid or ester CoA.¹⁶ Short-chain dehydrogenases/reductases compose a large subset of all dehydrogenases and can catalyze the NAD(P)H -dependent oxidation or reduction of aldehydes depending on the individual enzyme.¹⁷ Lipid peroxidation products can be eliminated via conjugation to glutathione via glutathione S-transferase.¹⁸ Although all of these enzymes contribute to the alleviation of the aldehydic load, aldehyde dehydrogenases are capable of oxidizing a variety of aromatic and aliphatic aldehydes and thus contribute to a wide range of physiological functions and generation of biological products.

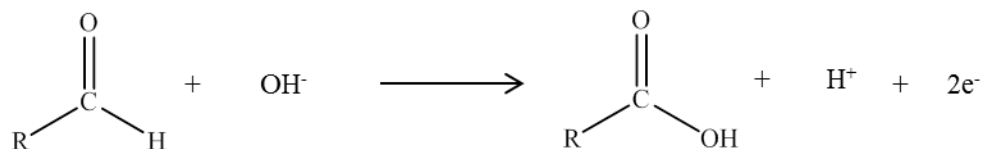
Alcohol Dehydrogenase



Aldo-Keto Reductase



Aldehyde/Xanthine Oxidase



Aldehyde Dehydrogenase

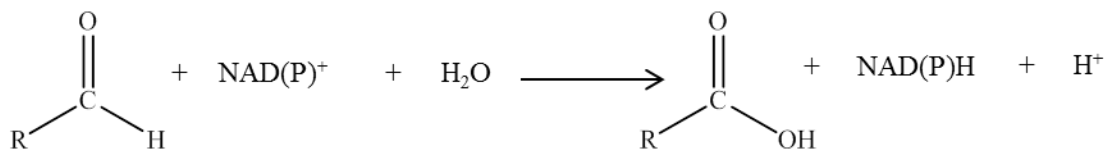


Figure 1 Aldehyde detoxification enzymes.

B. Aldehyde Dehydrogenase Superfamily

The aldehyde dehydrogenase (ALDH) superfamily exists in all three taxonomic domains, *Archaea*, *Eubacteria*, and *Eukarya*, highlighting the important role that these enzymes have had throughout evolution.¹⁹ A nomenclature system based on sequence alignments and evolutionary relationships was established in 1999 and is used primarily in *Eukarya* (**Figure 2**).²⁰ By convention members of different ALDH families have less than 40% protein sequence identity, while members of the same subfamily have more than 60% protein sequence identity. Due to the extensive amount of research done on ALDH2 in the field of ethanol metabolism prior to 1999, its name was grandfathered into the system, despite its amino acid sequence placing it in the ALDH1B subfamily.

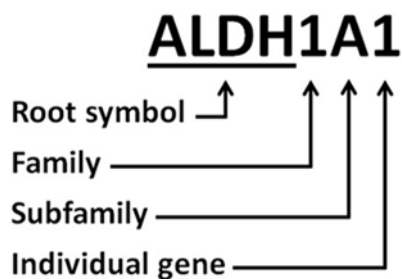


Figure 2 ALDH nomenclature

Currently there are 24 recognized ALDH families in eukaryotes; 11 of these families are represented in the human genome totaling 19 isoenzymes (**Figure 3**).²¹ ALDH isoenzymes differ in tissue location, subcellular location, substrate specificity, and structure. Many ALDH isoenzymes possess leader sequences that direct their translocation to specific subcellular locations.²² ALDHs have a variety of functions. ALDHs contribute to the synthesis of numerous important biological molecules including GABA, retinal, and tetrahydrofolate, and the removal of toxic aldehydes through their aldehyde oxidation activity.²³ Physiological roles for ALDHs are not limited to enzymatic function. ALDHs in the eye function as structural proteins called crystallins which absorb

harmful UV light.²⁴ ALDH16A1 may also serve as a structural protein as it lacks a functional nucleophile in its active site.²⁵ A summary of the 19 ALDH isoenzymes is shown in **Table 2**.

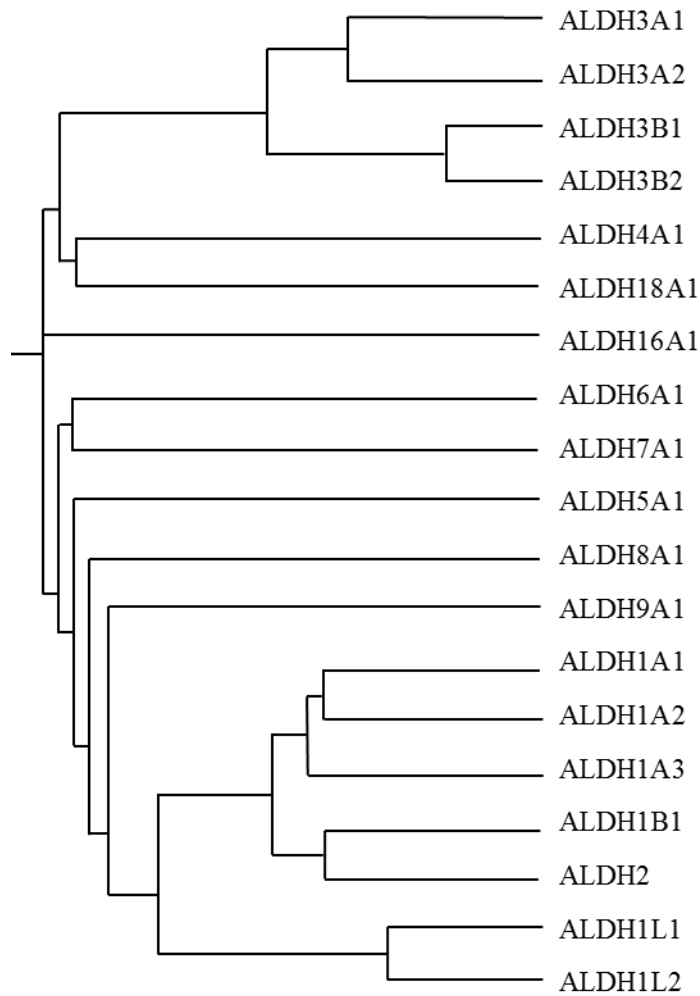


Figure 3 Phylogenetic tree for the human ALDH superfamily. Dendrogram of the 19 human ALDH members. Branch lengths depict degree of evolutionary divergence between isoenzymes.²⁶

Table 2 The 19 human aldehyde dehydrogenase isoenzymes.

Name	% ID to ALDH2	Chr Loc	Structure (PDB ID)	Common substrate(s)	Associated Diseases	Activators (A)/ Inhibitors (I)
ALDH1A1	68	9q21.13	Human (4WJ9)	Retinal, acetaldehyde, DOPAL	Parkinson's disease, cancer	citral (I), disulfiram (I), CM037 (I), CM039 (I)
ALDH1A2	67	15q21.3	Human (4X2Q)	Retinal	Cancer, spina bifida	WIN 18446 (I)
ALDH1A3	66	15q26.3		Retinal	Cancer	
ALDH1B1	73	9p13.1		Acetaldehyde	Diabetes, cancer	
ALDH1L1	48	3q21.3	ct-Rat (2O2P)	10-formyltetrahydrofolate	Cancer	
ALDH1L2	49	12q23.3		Unknown		
ALDH2	100	12q24.12	Human (3N80)	Acetaldehyde, DOPAL	Alcoholism, heart disease, Alzheimer's disease	Alda-1 (A), daidzin (I), disulfiram (I), citral (I), benomy1 (I)
ALDH3A1	28	17p11.2	Human (3SZA)	Aromatic and aliphatic aldehydes	Cancer	citral (I), gossypol (I)
ALDH3A2	28	17p11.2	Human (4QGK)	Fatty aldehydes	Sjögren-Larsson Syndrome	

% ID to ALDH2 represents percent protein sequence identity to ALDH2 calculated by NCBI Blast

Table 2, continued The 19 human aldehyde dehydrogenase isoenzymes.

Name	%ID to ALDH2	Chr Loc	Structure (PDB ID)	Common substrate(s)	Associated Diseases	Activators (A)/ Inhibitors (I)
ALDH3B1	25	11q13.2		Medium and long chained aliphatic aldehydes	Schizophrenia	
ALDH3B2	26	11q13.2		Unknown		
ALDH4A1	27	1p36.13	Human (4OE5)	Glutamate γ -semialdehyde	Type II hyperprolinemia	
ALDH5A1	35	6p22.3	Human (2W8R)	Succinate semialdehyde	γ -hydroxy-butyric aciduria	
ALDH6A1	30	14q24.3	Bacteria (4E4G)	Malonate semialdehyde, methylmalonate semialdehyde	Metabolic abnormalities	
ALDH7A1	30	5q23.2	Human (4ZUK)	α -aminoadipic semialdehyde	pyridoxine-dependent epilepsy	
ALDH8A1	39	6q23.3		2-amino-mucinate semialdehyde?		
ALDH9A1	43	1q24.1	Cod (1A4S)	γ -amino-butyraldehyde		
ALDH16A1	29	19q13.33		Unknown	Gout	
ALDH18A1	30	10q24.1	Human (2H5G)	Glutamic Acid	Metabolic and neurologic abnormalities	

% ID to ALDH2 represents percent protein sequence identity to ALDH2 calculated by NCBI Blast

Human ALDHs are associated with a number of diseases due to their involvement in a variety of physiological processes (**Table 2**). Mutations in multiple ALDHs (ALDH1A1, ALDH1A2, ALDH1A3, ALDH1B1, ALDH1L1, ALDH2, and ALDH3A1) are associated with cancer, and overexpression of ALDH1A1 and ALDH3A1 in cancer is linked to poor prognosis and decreased efficacy of certain chemotherapeutics, including cyclophosphamide.^{23, 27} *Aldh1a1*^{-/-} and *Aldh3a1*^{-/-} single knockout mice as well as *Aldh1a1*^{-/-} *Aldh3a1*^{-/-} double knockout mice develop cataracts prematurely as ALDH1A1 and ALDH3A1 both protect ocular tissue from UV radiation.²⁸ The ALDH1A subfamily is significantly involved in retinoic acid signaling and mutations in these genes are often detrimental to embryogenesis and can lead to spina bifida.^{23, 29} ALDH1A1 and ALDH2 have been linked to neurodegenerative diseases due to their involvement in dopamine metabolism.³⁰ ALDH1B1 has been shown to be important in beta cell development; mutations may contribute to the eventual development of diabetes.³¹

ALDH3A2 metabolizes the oxidization of fatty aldehydes and mutations are associated with Sjögren-Larsson Syndrome, an autosomal recessive disorder that leads to skin, cognitive, and neurological defects.³² A single nucleotide polymorphism in ALDH3B1 has been linked to the development of paranoid schizophrenia.³³ ALDH4A1 is involved in proline degradation and mutations in this gene lead to Type II hyperprolinemia characterized by seizures and mental retardation.³⁴ ALDH5A1 is involved in the metabolism of the neurotransmitter GABA; mutations lead to γ -hydroxybutyric aciduria characterized by neurological and cognitive defects.³⁵ ALDH6A1 is the only known CoA-dependent human ALDH and this enzyme catalyzes the conversion of malonate

semialdehyde and methymalonate semialdehyde to acetyl-CoA and propionyl-CoA, respectively, in valine and pyrimidine catabolism.³⁶ Mutations in the ALDH6A1 gene lead to a variety of metabolic abnormalities, which are typically accompanied by psychomotor delay.³⁷ ALDH7A1 catalyzes the oxidation of α -amino adipic semialdehyde during lysine metabolism; mutations are linked to pyridoxine-dependent epilepsy which causes severe seizures during infancy and early childhood.³⁸ ALDH16A1 is unique amongst the human ALDH enzymes as the active site lacks key catalytic residues. Although the enzyme does not have aldehyde oxidation activity, ALDH16A1 may act as a binding partner to other proteins and has been linked to gout.²⁵ ALDH18A1 catalyzes the reduction of glutamate to Δ -pyrroline-5-carboxylate during the *de novo* synthesis of the amino acids proline and arginine.³⁹ Mutations in the ALDH18A1 gene result in various metabolic and neurologic abnormalities characterized by cataract formation, neurodegeneration, and connective tissue disorders.⁴⁰

The primary function for ALDH enzymes is aldehyde oxidation. Sequence alignment of 145 ALDHs indicated that there is a small number of residues conserved in catalytically active enzymes, which include the catalytic cysteine and residues involved in cofactor binding.⁴¹ The reaction mechanism for aldehyde oxidation by ALDH isoenzymes is shown in **Figure 4A**. The process begins with binding of the cofactor NAD(P)⁺ in the Rossmann fold of the enzyme.^{42, 43} NAD(P)⁺ can adopt multiple conformations when bound to ALDHs (**Figure 5**).^{44, 45} Cys302 is the active site nucleophile and Glu268 acts as a general base (numbering based on mature ALDH2 sequence).^{46, 47} Cys302 is activated either directly by Glu268 or by a hydroxyl ion generated by Glu268 to perform

a nucleophilic attack on the carbonyl carbon of the aldehyde which yields the formation of a thioacyl-enzyme intermediate and hydride transfer to NAD(P)^+ . Glu268 then activates a water molecule that performs a nucleophilic attack on the carbonyl carbon of the thioacyl-enzyme intermediate which, after rearrangement, yields the reduced cofactor NAD(P)H and carboxylic acid product. The reduced cofactor is thought to be released after the carboxylic acid.⁴⁸ Due to structural differences, the rate limiting step differs between enzymes. For example, the rate limiting step is cofactor dissociation for the ALDH1A subfamily, deacylation for ALDH2, and hydride transfer for ALDH3A1.⁴⁹⁻⁵¹ Many ALDHs, including ALDH2, also have a NAD(P)^+ -independent esterase activity which uses the same active site residues and is the same reaction that hydrolyzes the thioacyl-enzyme intermediate to regenerate the free enzyme (**Figure 4B**).^{52, 53}

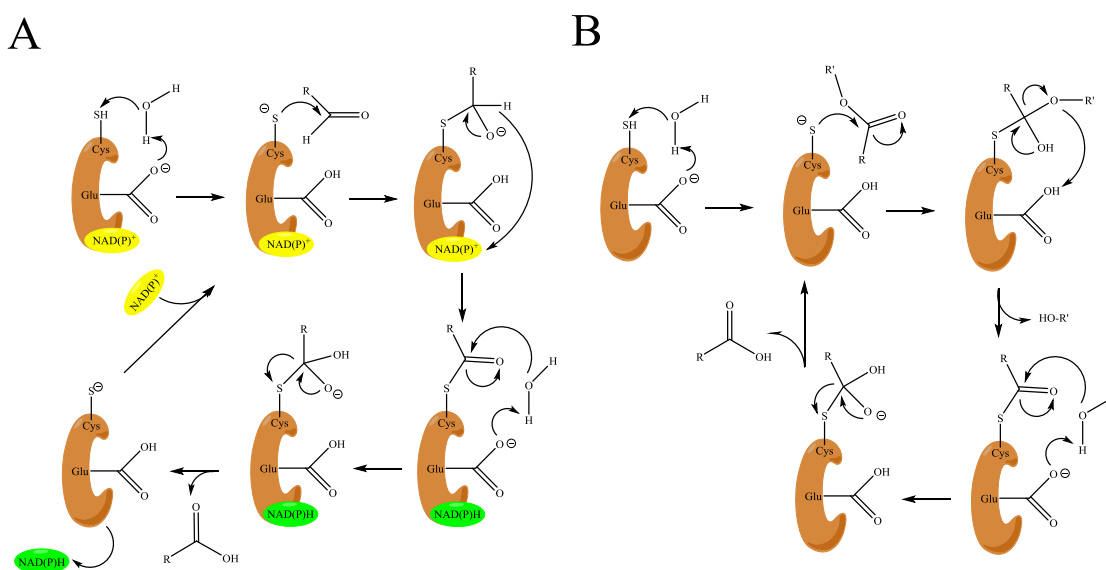


Figure 4 Catalytic mechanisms for ALDH isoenzymes. Aldehyde oxidation (A) requires cofactor NAD^+ , while ester hydrolysis (B) does not.

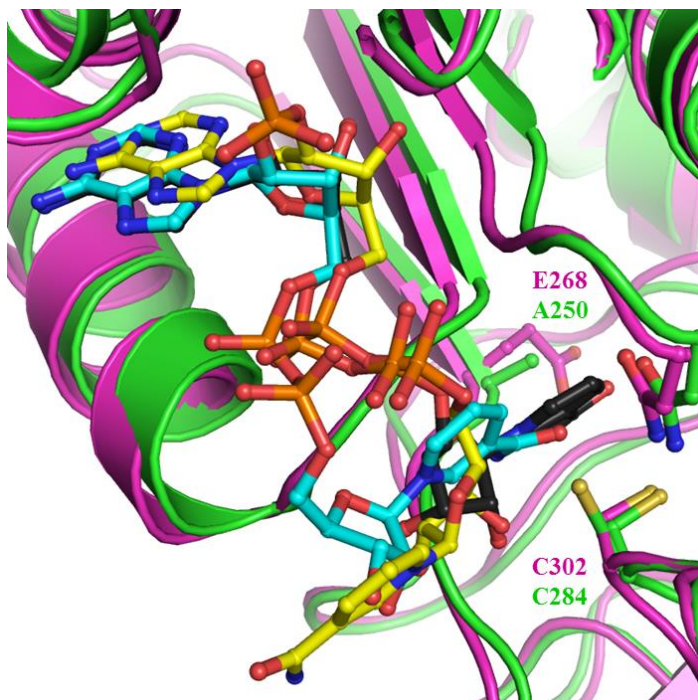


Figure 5 Multiple conformations of cofactor bound to ALDH isoenzymes. NAD⁺ (black) and NADH (cyan) bound to human ALDH2 (purple) and NADP⁺ (yellow) bound to glyceraldehyde 3-phosphate dehydrogenase (E250A) from *Streptococcus mutans* (green). PDB codes 1O00, 1O02, 1O04, 2QE0.

However, the presence of cofactor can stimulate esterase activity by either enhancing the nucleophilicity of Cys302 or increasing the frequency of productive encounters with Cys302.^{54, 55} Cofactor's effect on esterase activity is due in part to the shape of the active site. Mammalian ALDHs function as either dimers or tetramers, with each monomer containing a catalytic domain, a cofactor binding domain (Rossmann fold), and an oligomerization domain (**Figure 6A & B**).⁵⁶ The active site of ALDH enzymes contains a tunnel where the cofactor binding site is located on one end, with the substrate site at the other end of the tunnel and the catalytic cysteine situated in the middle (**Figure 6C**). The ALDHs have evolved to recognize different aldehyde substrates due to differences in the size and shape of their respective binding site.^{56, 57}

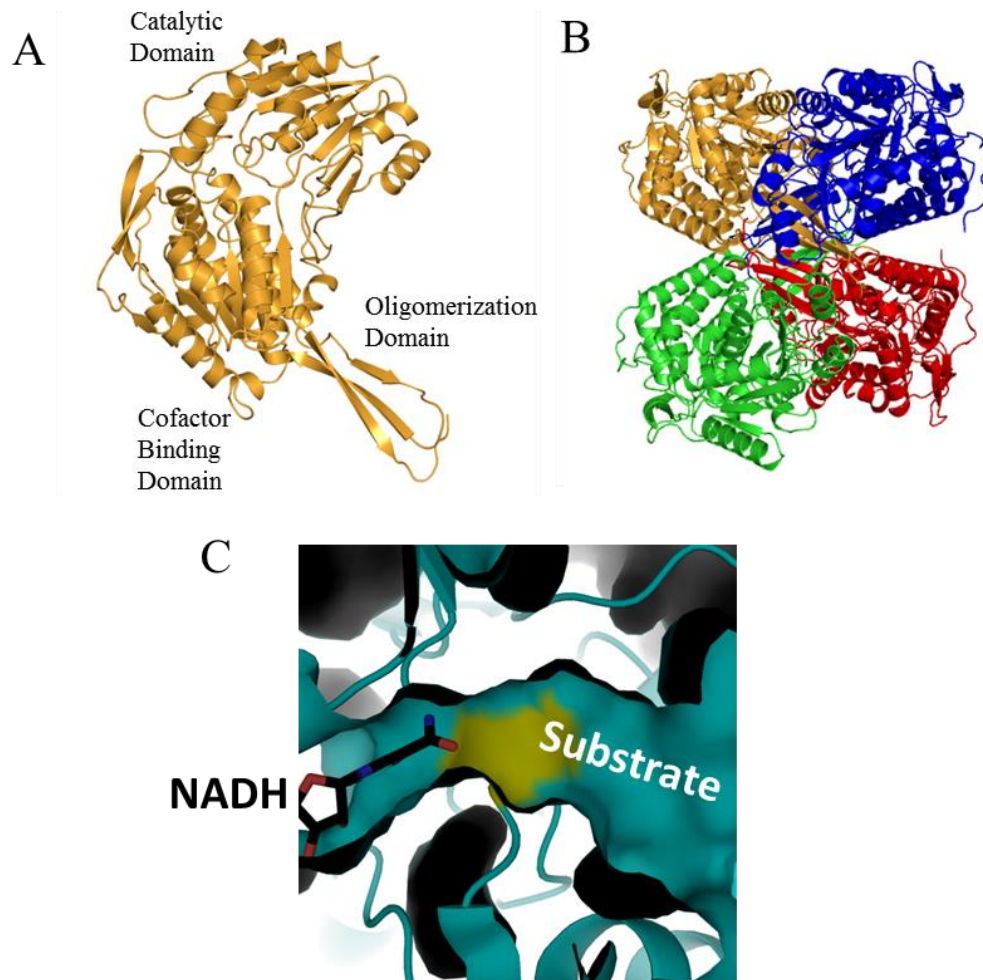


Figure 6 Structural characteristics of ALDH isoenzymes. (A) Ribbon diagram of the ALDH2 monomer. (B) Ribbon diagram of ALDH2 homotetramer with each monomer colored individually. (C) Surface representation of tunnel connecting cofactor binding site and catalytic site of ALDH1A1. Region of catalytic cysteine colored in yellow. NADH (black) bound to cofactor binding site. (PDB Code 4WB9).

C. Aldehyde Dehydrogenase 1/2 Family

The aldehyde dehydrogenase 1/2 family in humans consists of seven isoenzymes:

ALDH1A1, ALDH1A2, ALDH1A3, ALDH1B1, ALDH2, ALDH1L1, and ALDH1L2.

These enzymes are present among different tissues, and each can have variable expression patterns, along with oxidizing a variety of aldehydes. Thus the ALDHs have a diverse set of physiological functions.

The ALDH1A subfamily consists of the cytosolic ALDH1A1, ALDH1A2, and ALDH1A3 that share ~70% sequence identity. Each of the three isoenzymes can facilitate oxidation of retinal to retinoic acid (RA), though the substrate specificity for each of these enzymes differs. ALDH1A1 catalyzes the oxidation of all-trans-, 9-cis-, and 13-cis-retinal with K_m values ranging from 2 – 6 μ M.⁵⁸ ALDH1A2 and ALDH1A3 prefer the all-trans isomer, but also can utilize the cis-isomers as substrates.^{23, 59} The RA products can then act on other cells in an endocrine or paracrine manner.⁶⁰ Once in the nucleus of the target cell, the RA products then bind to retinoic acid (RAR) and retinoic X receptors (RXR) (**Figure 7**). Both RAR and RXR are type II nuclear receptors and as such are retained in the nucleus regardless of the presence or absence of ligand. RA products will bind to heterodimers of RAR and RXR, which interact with the retinoic acid response element (RARE), a specific DNA sequence in the promoter region of the target gene to regulate gene expression and cellular phenotype. RXRs also can form heterodimers with other nuclear receptors such as thyroid hormone receptors and peroxisomal proliferator activated receptors. Retinoid metabolism and signaling are involved in embryogenesis, cell cycle control, cell growth, and differentiation.^{61, 62} Dysregulation of these functions has been linked to obesity, diabetes, cardiovascular disease, cancer, and fetal/birth defects.^{61, 62} Whereas *Aldh1a1* knockout mice are viable, both *Aldh1a2* and *Aldh1a3* knockout mice do not produce viable animals, suggesting that ALDH1A2 and ALDH1A3 are more involved in embryogenesis and tissue patterning.⁶³ *Aldh1a2*^{-/-} knockout mice are characterized by defects in heart development and death at midgestation, while *Aldh1a3*^{-/-} knockout mice are characterized by nasal and ocular

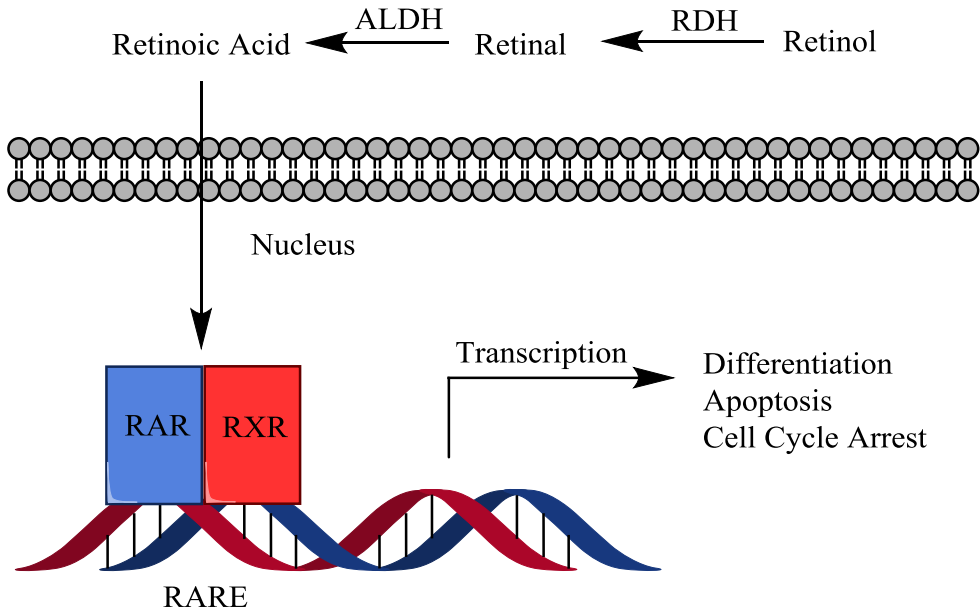


Figure 7 Retinoic acid signaling pathway.

Retinol (vitamin A) is oxidized by retinal dehydrogenases (RDH) to produce retinal, which is further oxidized by ALDH1A enzymes to produce retinoic acid (RA). RA then diffuses into the nucleus and initiates transcription of target genes which contain RARE elements in their target genes via activation of heterodimers of RAR and RXR. Depending on the cellular context, the increased transcription can lead to differentiation, apoptosis, or cell cycle arrest. Adapted from Marcato *et al.*⁶⁴

defects, similar to RAR mutants, which lead to respiratory failure shortly after birth.^{65, 66}

Although *Aldh1a1*^{-/-} knockout mice are viable, the absence of Aldh1a1 activity results in reduced retinoic acid synthesis later in life.⁶⁷ Mouse Aldh1a7, an ALDH1A1 paralog not found in humans, may partially rescue the *Aldh1a1*^{-/-} knockout mouse phenotype.⁶⁸

Aldh1a1^{-/-} knockout mice are also resistant to diet-induced obesity and insulin resistance.⁶⁹ Based on *in vitro* studies, the major enzyme expressed during adipogenesis is ALDH1A1, compared to other vitamin-A metabolizing enzymes.⁷⁰ The increased levels of retinaldehyde in the *Aldh1a1*^{-/-} knockout mice could have several beneficial effects in regards to adipogenesis. Retinaldehyde decreased fat levels and increased

insulin sensitivity in an obese mouse model.⁶⁹ Retinaldehyde is also an inhibitor of peroxisomal proliferator activated receptors gamma (PPAR γ), a transcription factor heavily involved in adipogenesis, and in activation of RXRs.⁶⁹ There is a fourth possible retinal dehydrogenase in humans, ALDH8A1, though it shares only 40% sequence identity with ALDH1A1 and is most similar to bacterial tryptophan metabolism enzymes.⁷¹

The function of ALDH1A1 is not limited to retinoid signaling. ALDH1A1 can also catalyze the oxidation of 3-4-dihydroxyphenylacetaldehyde (DOPAL) to 3-4-dihydroxyphenylacetic acid (DOPAC) and the conversion of acetaldehyde to acetic acid during ethanol metabolism; both of these processes will be discussed further in later sections concerning neurodegenerative diseases and alcohol abuse.^{30, 72} ALDH1A1, as well as ALDH1A2 and ALDH1A3, contribute to the oxidation of lipid peroxidation products such as 4-hydroxynonenal (4-HNE), malondialdehyde (MDA), and hexanal.²³ ALDH1A1 will act as corneal and lens crystallins in eye tissue alongside other ALDHs.⁷³ In this role, ALDH1A1 protects the tissue from ultraviolet radiation damage and contributes to transparent and refractive properties of the eye tissue.⁷⁴ ALDH1A1 can also bind to androgens, thyroid hormone, and cholesterol and interact with drugs like quinolone and flavopiridol.^{21, 75, 76}

ALDH2 is a mitochondrial homotetramer with 67% sequence identity to the ALDH1A subfamily. ALDH2 is ubiquitously expressed, though the expression levels are variable with the heart, liver, kidney, lung, and brain having high levels.²³ ALDH2 is well-known

for being the primary enzyme responsible for the catalysis of acetaldehyde to acetic acid during ethanol metabolism.⁷⁷ ALDH2 is involved in the metabolism of lipid peroxidation derived aldehydes, including 4-HNE and MDA.¹⁶ ALDH2 also can oxidize DOPAL to DOPAC and bioactivate nitroglycerin.^{30, 78} The various functions of ALDH2 and how each contribute to various disease states will be discussed further in later sections.

ALDH1B1 is a mitochondrial homotetramer that has 72% sequence identity to ALDH2. Although the physiological function of ALDH1B1 is still unknown, ALDH1B1 was reported to oxidize acetaldehyde with a low K_M (55 μ M) suggesting that this enzyme has a role in ethanol metabolism, especially when ALDH2 activity is low.⁷⁹ ALDH1B1 can also catalyze the oxidation of 4-HNE and MDA, like ALDH2 and members of the ALDH1A subfamily.⁷⁹ *Aldh1b1*^{-/-} knockout mice displayed increased blood acetaldehyde levels post ethanol consumption and higher fasted blood glucose levels.⁸⁰ ALDH1B1 also influences the transition from the pancreas endocrine progenitor to the mature beta cell.³¹ Expression of ALDH1B1 was found to be increased in pancreatic adenocarcinoma, suggesting that this enzyme contributes to cancer proliferation.⁸¹ Furthermore, ALDH1B1 has been proposed to be a biomarker for colon cancer.⁸² ALDH1B1 may contribute to colon cancer growth by helping regulate the Wnt/ β -catenin, Notch, and phosphoinositide 3-kinase (PI3K)/Akt signaling pathways.⁸³

ALDH1L1 and ALDH1L2 are two enzymes that are the fusion of two or more distinct activities. Both are included in the aldehyde dehydrogenase 1/2 family due to the sequence similarity in their aldehyde dehydrogenase domains. ALDH1L1 is a multi-

domain protein with two distinct catalytic domains, an amino-terminal formyl transferase domain and a carboxy-terminal aldehyde dehydrogenase domain.⁸⁴ Unlike the aforementioned members of the ALDH1/2 family, ALDH1L1 prefers NADP⁺ as a substrate.⁸⁵ ALDH1L1, also known as 10-formyltetrahydrofolate (10-FTHF) dehydrogenase, catalyzes the conversion of 10-FTHF to tetrahydrofolate (THF).⁸⁶ THF, the major metabolite of dietary folate, is important in one-carbon metabolism and 10-FTHF is involved in purine synthesis and may have an impact on DNA replication and repair.⁸⁷ ALDH1L1 is suggested to have a role in cancer development. Overexpression of ALDH1L1 in multiple cancer cell lines suppressed cellular proliferation and increased cytotoxicity.⁸⁸ In keeping with the idea that ALDH1L1 may suppress cancer progression, ALDH1L1 was reported to be downregulated in human liver, lung, prostate, pancreas, and ovarian cancers.⁸⁸ ALDH1L1 also contributes to alleviating methanol toxicity. Methanol is metabolized in the liver by two steps to form formate, with formaldehyde as the intermediate product.⁸⁹ Accumulation of formate is believed to cause the majority of the deleterious effects associated with methanol poisoning.⁸⁹ Formate is oxidized to carbon dioxide by first being condensed with THF to form 10-FTHF by methylenetetrahydrofolate dehydrogenase. 10-FTHF is then converted to THF by ALDH1L1 to regenerate THF while releasing carbon dioxide as a product.²³

ALDH1L2 shares 72% sequence identity with ALDH1L1 and has a mitochondrial leader sequence. ALDH1L2 is also a multi-domain protein containing an amino-terminal formyl-trans-N-formyl transferase domain, a formyltransferase domain in the middle, and a carboxy-terminal aldehyde dehydrogenase domain.²⁶ The physiological function of

ALDH1L2 is still unknown, though it likely relates to folate metabolism in the mitochondria.

D. ALDH1A1, Cancer, and Cancer Stem Cells

According to the National Cancer Institute, approximately 40% of all men and women will be diagnosed with cancer at some point in their lifetime and national expenditures for cancer care totaled nearly \$125 billion in 2010 and could reach \$150 billion by 2020. The longstanding model for development of solid tumors stated that these tissues are heterogeneous and most, if not all, cells are capable of metastasis. The cancer stem cell model states that a small subset of cells, called cancer stem cells, have the ability to proliferate extensively while the vast majority of cancer cells are differentiated and have a limited capacity for tumor formation.⁹⁰ Cancer stem cells, also known as tumor-initiating cells, are defined by enhanced tumorigenicity and the capacity for self-renewal/differentiation.⁶⁴ Some cancer stem cells may arise from dedifferentiation of differentiated cancer cells through the right combination of transcription factors.⁹¹ Though the idea that cancer may originate from a small population of cells with stem cell-like properties was first proposed in the 19th century, cancer stem cells were first identified in 1994 in acute myeloid leukemia.^{92, 93} Cancer stem cells were later found in solid tumors as well.⁹⁴ Signal transduction pathways involved in oncogenesis, including those featuring Notch, Sonic hedgehog, and Wnt, are also important for stem cell self-renewal.⁹⁵ Many current cancer treatments utilize a stochastic approach, targeting all cells to minimize tumor size. However, if cancer stem cells are inherently resistant to chemotherapeutics and represent a minority of the total tumor cell population, then

cancer stem cells may still be present in the smaller tumor and be able to regenerate the cancer. This may explain why tumor regression does not correlate with increases in patient survival in clinical trials for advanced cancers.⁹⁶ Specifically targeting cancer stem cells, while sparing normal stem cells, is one way to treat cancer by eliminating the tumor-initiating cell population.

ALDHs are widely used to identify cancer stem cells and ALDH1A1 is considered a cancer stem cell marker.⁹⁷ ALDH1A1 is overexpressed in many cancers, including lung, ovarian, stomach, and breast, and is associated with poor outcomes in many cases.⁹⁸ The manner in which ALDH1A1 contributes to stem cell biology is not well understood as *Aldh1a1* deficient mice have no noticeable disruption in stem cell function, though ALDH1A1's function in retinoid metabolism is worth noting as retinoids effect cellular differentiation.⁹⁹ Retinoic signaling has been shown to play a major role in embryonic stem cells and cancer cells.^{100, 101} Breast cancer stem cells treated with the non-selective ALDH inhibitor diethylaminobenzaldehyde showed enrichment with genes involved with cell self-renewal while cancer stem cells treated with all-trans retinoic acid had similar gene expression profiles as differentiated cancer cells.¹⁰² ALDH enzymes also protect cancer stem cells from reactive oxygen species generated under oxidative stress conditions.¹⁰³ Tumor cells can undergo hypoxia and a loss of oxygen tension, giving rise to reactive oxygen species and oxidative stress.¹⁰⁴ ALDH1A1, alongside ALDH3A1, also helps provide cellular protection from cytotoxic drugs; for example, both ALDH1A1 and ALDH3A1 can convert cyclophosphamide, an alkylating agent, to the inactive product carboxyphosphamide.^{105, 106}

Mammary cancer cells form spheroids in 3D culture that are rich in progenitor cells and have metastatic capacity.¹⁰⁷ These spheroids are rich in ALDH1A1 enzymatic activity and have been associated with poorer clinical outcome in breast cancer cases.¹⁰⁸ Other cancers, including prostate and ovarian, have also been shown to form spheroids.^{109, 110} The ability of ovarian cancer cells to form spheroids may facilitate metastases and enable cancers to survive chemotherapy.¹¹¹ Spheroids grown in 3D culture *in vitro* represent a better approximation of tumor cells *in vivo* compared to cancer cells grown in monolayer culture.¹¹¹ Ovarian cancer spheroids have elevated ALDH1A1 enzyme activity, but not elevated transcription of other ALDHs linked to cancer, such as ALDH1A2, ALDH1A3, ALDH2, and ALDH3A1.¹¹¹ Although the exact role of ALDH1A1 in cancer stem cell viability is unclear, it is not related to its role in retinoic acid signaling as these cells remain dedifferentiated. The elevation in ALDH1A1 activity may be in response to increased oxidative stress due to decreased oxygen tension in the interior of the spheroids.

The role of ALDH1A1 in cancer stem cells may also be related to various signaling pathways. Inhibition of the β -catenin/Wnt pathway prevented multicellular aggregation in cancer spheroids. Given that ALDH1A1 is important for spheroid formation, and ALDH1A1 is a direct target of the transcription factor β -catenin, it is likely that this ALDH enzyme functions downstream of the β -catenin/Wnt pathway in cancer progression.¹¹¹ Likewise activation of β -catenin and dysregulation of the Wnt pathway is common in cancer.¹¹² ALDH1A1 expression and activity have also been connected to the Hippo pathway. Inhibition of ALDH1A1 led to growth attenuation of MDA-MB-468

cells in 3D culture as well as a decrease in the activity of YAP, a transcription factor in the Hippo pathway.¹¹³ Overexpression of YAP is also correlated with an increase in *ALDH1A1* expression in MDA-MB-468 cells. YAP binds to TEAD elements in promoters of target genes and the *ALDH1A1* promoter region contains a TEAD element.¹¹³ Compounds which selectively inhibit *ALDH1A1* could be used as chemical probes to better understand the role *ALDH1A1* plays in cancer stem cell function and tumor metastasis.

E. ALDH2, ALDH2*2, and Alcohol-Induced Pathophysiology

Aldehyde dehydrogenase 2 (*ALDH2*) is a mitochondrial enzyme that adopts a homotetramer structure. The enzyme functions more accurately as a dimer of dimers as only two of the catalytic sites seem to be active at any given time.¹¹⁴ An N-terminal mitochondrial targeting sequence (MTS) directs the protein to the mitochondria, where upon entrance of the enzyme into this organelle, the sequence is cleaved to form the mature protein.²² *ALDH2* is the primary *ALDH* isoenzyme responsible for the oxidation of acetaldehyde ($K_m < 1 \mu\text{M}$) during ethanol metabolism.¹¹⁵ Other isoenzymes, such as *ALDH1A1* and *ALDH1B1*, can also contribute to the oxidation of acetaldehyde, especially in the case of the *ALDH2*2* variant.^{72, 116} The *ALDH2*2* allele is among the most prevalent human enzyme deficiencies, affecting ~540 million people worldwide.¹¹⁷ Found in ~40% of individuals of East Asian descent, the *ALDH2*2* allele can be traced back to the Han Chinese population over 2000 years ago.^{118, 119} Individuals with the *ALDH2*2* allele will develop nausea, dizziness, headaches, and vasodilation (facial flushing), also known as alcohol flush reaction, after ethanol consumption due to

decreased ALDH2 enzymatic activity.¹¹⁷ The lower activity is caused by a single nucleotide change (G→A) that results in an E487K substitution (E504K with the MTS included), which causes a 10-fold reduction in k_{cat} and increases the K_{m} for coenzyme (NAD⁺) above physiological levels.¹²⁰ Glu487 appears to maintain a stable structural scaffold and facilitate catalysis by connecting the cofactor binding domain and substrate binding domains in ALDH2 through interactions with other residues in the enzyme.¹²¹ The crystal structure of ALDH2*2 lacks density for the helix α G of the Rossmann fold and a loop in the active site (**Figure 8A**).¹²² The *ALDH2*2* allele is dominant as *ALDH2*2* homozygotes have little to no ALDH2 activity and ALDH2 activity in heterozygotes is severely reduced.¹²³ If one ALDH2*2 monomer is present in the tetrameric unit the entire tetrameric unit is enzymatically compromised due to Glu487 being located along the interface between monomers (**Figure 8B**).¹²¹ The *ALDH2*2* allele is associated with a lower risk of alcoholism due in part to the adverse physiological response upon alcohol consumption.¹²⁴ However, societal pressure can overcome this reduced risk.^{125, 126} *ALDH2*2* has also been associated with alcoholic liver disease and cirrhosis.¹²⁷

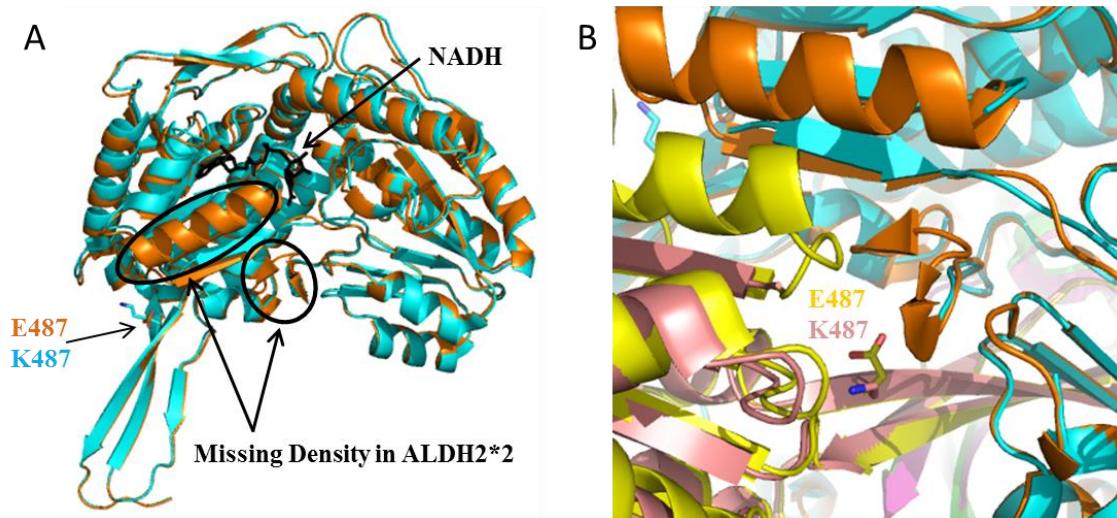


Figure 8 Structure of ALDH2 versus ALDH2*2.

(A) Monomer of ALDH2 (orange) vs ALDH2*2 (cyan). The E487K substitution is located in the oligomerization domain. (B) E487K substitution is located at the dimer interface. The E487K residue (yellow/mauve) faces the active-site loop of the neighboring monomer (orange/cyan). PDB Code 1O02 and 1ZUM.

Approximately 16 million people in the United States have an Alcohol Use Disorder, which encompasses both alcohol abuse and alcohol dependence, and the misuse of alcohol costs the United States over \$200 billion annually.^{128, 129} Ethanol was classified as a group 1 carcinogen by the International Agency for Research on Cancer in 2007; however, acetaldehyde is most likely the chemical species that leads to malignancy.¹³⁰ Blood acetaldehyde levels are significantly higher after moderate ethanol consumption in ALDH2-deficient individuals.¹³¹⁻¹³³ Acetaldehyde can form DNA-DNA and DNA-protein crosslinks.^{134, 135} Multiple DNA adducts have been seen in human cells and in mice exposed to acetaldehyde.^{136, 137} DNA damage contributing to the development of upper aerodigestive track (UADT) cancers is most likely caused by acetaldehydes.^{138, 139} ALDH2*2 carriers have an increased risk of developing UADT cancers and have increased levels of acetaldehyde-induced DNA damage.^{140, 141} Acetaldehyde-induced DNA damage may also contribute to the diseases phenotypes seen in Fetal Alcohol

Syndrome and Fanconi Anemia.^{142, 143} Fanconi Anemia (FA) is caused by a recessive mutation to one of many identified FA genes, including FANCD2, which function to repair DNA cross-links.¹⁴⁴ A maternal functional copy of ALDH2 was necessary to counteract aldehyde toxicity in the development of *Aldh2*^{-/-} *Fancd2*^{-/-} double knockout mouse embryos. *Aldh2*^{-/-} *Fancd2*^{-/-} mouse embryos were also sensitive to developmental deformities in the uterus when the mothers were exposed to ethanol.¹⁴³ Interestingly, the most common cancers in adult FA patients are UADT or head and neck cancers.¹⁴⁵

Accumulation of acetaldehyde can also lead to cardiotoxicity. Acetaldehyde can cause cardiac hypertrophy and contractile dysfunction.^{146, 147} Adult mice overexpressing ALDH2 are more resistant to acute ethanol cardiotoxicity.¹⁴⁸ ALDH2 confers cardiac protection partly through the regulation of Akt and AMPK signaling and mTOR and thereby autophagic flux.¹⁴⁹ Pharmacological activation of ALDH2 reversed ethanol-induced cardiac defects and apoptosis, as did the AMPK inhibitor compound C.¹⁵⁰ Although an excess amount of alcohol will lead to cardiotoxicity, a moderate amount of ethanol will activate ALDH2 through phosphorylation by PKC ϵ to alleviate cardiac stress.¹⁵¹

F. ALDH2 and Cardiovascular Disease

Cardiovascular diseases are a major cause of morbidity and mortality worldwide. The role of ALDH2 in cardiac health is not limited to acetaldehyde-induced cardiotoxicity. Other cardiotoxic aldehydes originating from reactive oxygen species-induced stress can also cause myocardial dysfunction.^{152, 153} Reactive oxygen species generate lipid

peroxidation products, such as 4-hydroxynonenal (4-HNE) and malondialdehyde, which will form adducts with various proteins, which can culminate in cardiac dysfunction.¹⁵⁴ 4-HNE modified proteins are elevated in patients with hypertrophic and dilated cardiomyopathy, hypertension, and peripheral artery disease.¹⁵⁵ Mice overexpressing *ALDH2*2* exhibited impaired mitochondrial bioenergetics and elevated levels of 4-HNE protein adducts.¹⁵⁶ Overexpression of ALDH2 prevented 4-HNE protein adduct formation and alleviated myocardial damage from ischemia reperfusion.¹⁵⁷ However, 4-HNE can form adducts with ALDH2 itself and inactivate the enzyme.¹⁵⁸ Pharmacological activation of ALDH2 offers cardioprotection from lipid peroxidation aldehydes, and can prevent the inactivation of the enzyme by 4-HNE.¹⁵¹ Specifically, Alda-1, an ALDH2 activator, decreased ischemic damage after a myocardial infarction.¹⁵¹ The *ALDH2*2* allele is also a risk factor for acute coronary syndrome and hypertension.¹⁵⁹⁻¹⁶¹

Nitroglycerin (GTN) is often used to treat angina and heart failure.¹⁶² GTN works by increasing blood flow to the heart through the vasodilator nitric oxide (NO).¹⁶³ ALDH2 is the key enzyme that catalyzes the bioactivation of GTN to 1,2-glyceryl dinitrite (1,2-GDN).¹⁶⁴ The proposed mechanism involves the formation a thionitrate on the catalytic cysteine (Cys302) and release of 1,2-GDN. A disulfide bond is then formed between Cys302 and one of the two adjacent cysteine residues and nitrite is released.¹⁶⁵ Sustained GTN treatment leads to tolerance and is associated with pro-oxidant effects and endothelial dysfunction.^{166, 167} Tolerance is mainly mediated by the inability of ALDH2 to catalyze the conversion of GTN to 1,2-GDN and nitrite, which is then further reduced to NO.¹⁶⁸ Acetaldehyde, acting as a competitive substrate, and the ALDH2 inhibitor

daidzin both suppress the bioactivation of GTN by ALDH2.^{169, 170} Individuals with the ALDH2*2 mutation have a reduced vasodilatory response to GTN and have higher incidences of GTN tolerance.^{171, 172} Pharmacological activation of ALDH2 or ALDH2*2 by Alda-1 did not increase the denitration and bioactivation of GTN, though Alda-1 does help prevent the development of GTN tolerance by preventing inactivation by produced NO, similar to the protection from 4-HNE adduct formation by Alda-1.^{173, 174}

G. ALDH1A1, ALDH2, and Neurological Disease

Multiple neurological diseases are highlighted by the accumulation of aldehyde products and mitochondrial dysfunction.^{175, 176} Two of these diseases are Parkinson's disease (PD) and Alzheimer's disease. PD is a neurodegenerative disorder that is found in 1% of the population over 65 years old and is characterized by the intracellular aggregation of α -synuclein in so-called Lewy bodies and the loss of dopaminergic neurons in the substantia nigra.^{177, 178} 3,4-dihydroxyphenylacetaldehyde (DOPAL) has been identified as a neurotoxin that will induce Parkinsonism.¹⁷⁹ DOPAL is a metabolic product of the neurotransmitter dopamine formed via monoamine oxidase. Most DOPAL is then converted by an ALDH to the carboxylic acid 3,4-dihydrophenylacetic acid (DOPAC), though reduction to the alcohol 3,4-dihydrophenylethanol (DOPET) also occurs. One of the most prevalent treatments for PD is the dopamine precursor levodopa, which serves to increase the levels of dopamine in the brain, but does not halt the progression of the disease.¹⁸⁰ Accumulation of the lipid peroxidation product 4-HNE can also contribute to the symptoms of PD.¹⁸¹ Both ALDH1A1 and ALDH2 have been linked to the progression of PD. Although DOPAL is a substrate, DOPAL can also inhibit ALDH1A1

and ALDH2 decreasing its own catabolism.^{30, 182, 183} 4-HNE also will inhibit the conversion of DOPAL to DOPAC, presumably by covalently binding to ALDH2.¹⁸³ Exposure to benomyl, a fungicide and potent inhibitor of ALDH2, led to increased development of PD in factory workers.¹⁸⁴ ALDH1A1 mRNA and protein have been found to be downregulated in PD as well.^{185, 186} Double knockout mice of ALDH1A1 and ALDH2 have elevated levels of DOPAL and 4-HNE, loss of dopaminergic neurons in the substantia nigra, and age-dependent deficits in motor performance.¹⁸⁷ As neither single knockout develop substantial neurodegeneration, it remains unclear which enzyme, ALDH1A1 or ALDH2, is the major contributor to the metabolism of dopamine with regards to PD.^{188, 189}

Alzheimer's disease (AD) is a progressive neurodegenerative disease characterized by a loss of cortical neurons that results in the onset of dementia.¹⁹⁰ By 2050 it is estimated that 13.2 million Americans will have the disease.¹⁹¹ 4-HNE accumulates in the hippocampus of patients with early AD.¹⁹² 4-HNE adduct formation is believed to contribute to amyloid plaque formation seen in the later stages of AD.¹⁹³ Individuals with the *ALDH2**2 allele have a higher incidence of AD.^{194 195} Likely this is due to the decreased ability of the *ALDH2**2 allele to oxidize 4-HNE and prevent adduct formation.¹⁹⁶ *ALDH2**2 transgenic mice developed age-related neuronal loss associated with memory loss, premature aging, and shortened life span.¹⁹⁷ Pharmacological activation of ALDH2 prevented amyloid β peptide-induced impairment of angiogenesis in cultured endothelial cells.¹⁹⁸

Dopamine metabolism, and thereby ALDH2, is also linked to the development of addiction. Addictive drugs lead to increased dopamine release in the nucleus accumbens.¹⁹⁹ Inhibition of ALDH2 led to a decrease in cocaine seeking behavior in rats through the formation of tetrahydropapaveroline (THP).²⁰⁰ Inhibition of ALDH2 causes an increase in DOPAL concentration leading to the condensation of DOPAL and dopamine to form THP. THP selectively inhibits tyrosine hydroxylase to reduce dopamine signaling via a negative-feedback loop.²⁰⁰ Inhibition of ALDH2 has also been found to prevent alcohol-induced dopamine release.²⁰¹

H. ALDH1/2 Activators and Inhibitors

Activating and/or inhibiting the function of various ALDHs are potential pharmacological approaches for the treatment of human pathologies. Development of inhibitors/activators has so far been primarily limited to three isoenzymes: ALDH1A1, ALDH2, and ALDH3A1.⁵⁶ However, selectivity amongst the ALDH isoenzymes has remained a challenge. One of the first clinical applications for the inhibition of ALDHs was the inhibition of ALDH2 as an antidipsotropic therapy.²⁰² ALDH2 inhibitors, like daidzin and disulfiram, cause a buildup in acetaldehyde during consumption of alcohol, which yields symptoms similar to the alcohol flush reaction seen with ALDH2*2. As a consequence the drug decreases the consumption of alcohol. Daidzin is an isoflavone derived from the kudzu plant and is a 100x more potent inhibitor of ALDH2 compared to ALDH1A1.^{203, 204} Analogs of daidzin including CVT-10216 are being developed to be more selective for ALDH2.²⁰¹ However, the effects of daidzin and its analogs on the activity of ALDH1A2, ALDH1A3, and ALDH1B1 are understudied. Disulfiram, itself,

inhibits ALDH1A1 more strongly than ALDH2, although its *in vivo* metabolites are more potent towards ALDH2.^{205, 206} Disulfiram will also inhibit ALDH1B1.⁷⁹ The sulfur atoms in disulfiram also make it a copper chelator and disulfiram will inhibit tyrosine β -hydroxylase and other copper-dependent enzymes.²⁰⁷ Disulfiram has been used to treat cocaine addiction by decreasing norepinephrine release and as an anti-cancer agent utilizing some of these non-ALDH effects.^{208, 209} Several ALDH inhibitors act as slow substrates for the target enzyme(s). Citral is a volatile α,β -unsaturated aldehyde found naturally in herbs and citrus fruits. Citral can inhibit multiple ALDH isoenzymes by acting as a slow substrate thereby inhibiting the oxidation of faster substrates.⁵⁶ 4-(Diethylamino)benzaldehyde, the control inhibitor for the Aldeflour Assay for cancer stem cell detection, also acts as a slow substrate for many of the ALDH isoenzymes and as a mechanism-based inhibitor for others.²¹⁰ Gossypol is also an aldehyde, though its inhibition does not seem to be derived from being a slow substrate. Gossypol is more selective for ALDH3A1 compared to the ALDH1/2 family, and also inhibits other NAD(P)⁺-dependent enzymes. Gossypol most likely interacts with the cofactor binding sites of these enzymes.²¹¹ Many biocides, including benomyl, also inhibit ALDH isoenzymes.²¹² WIN 18446, a potent inhibitor of spermatogenesis, has been found to inhibit the activity of ALDH1A2; the activity of WIN 18446 on other ALDH isoenzymes remains unknown.²¹³

Although achieving selectivity for one of the ALDHs is challenging, a few compounds have recently been discovered via high throughput screening (HTS). HTS has been used to develop more selective ALDH3A1 inhibitors in use for sensitizing ALDH3A1-positive

cancer cells to oxazaphosphorine treatment.^{214, 215} HTS has also been used to discover ALDH1A1 inhibitors such as CM037. CM037, a benzothienopyrimidinone with an ester side chain, is a selective inhibitor of ALDH1A1 by competitively interfering with propionaldehyde binding to the enzyme. CM037 takes advantage of Gly458 in the active site of ALDH1A1, which is a much larger residue in the other catalytically active ALDH isoenzymes.²¹⁶ However, as an ester, CM037 will most likely be hydrolyzed quickly *in vivo*.

Activators can also serve as chemical probes to elucidate the function of the various ALDH isoenzymes. There are only a few small molecular activators of ALDHs compared to the large number of ALDH inhibitors. Tamoxifen has been found to induce the activity of ALDH1A1 by 2-fold.²¹⁷ Alda-1 also activates ALDH2 by 2-fold and can prevent inactivation by toxic aldehyde substrates, such as 4-HNE, increasing protection from oxidative stress.¹⁵¹ Alda-1 can also act as a chemical chaperone and restore ALDH2*2 to near-normal function.⁵⁵ Alda-1 may also activate ALDH1A1 activity after DOPAL-induced inactivation.²¹⁸ Alda-1 and its analogs are being further developed as ALDH2-selective activators; however, this compound series has solubility issues which most likely will preclude its use in a clinical setting.

I. Hypothesis and Approach

Even though ALDH2 has been targeted for the treatment of alcoholism since 1948, there remains a lack of selective ALDH2 inhibitors.²¹⁹ Additionally, the selective ALDH2 activator Alda-1 has solubility issues which limit its use. We hypothesized that the unique

topologies of the substrate sites in ALDH isoenzymes will permit the discovery and optimization of inhibitors that can specifically probe the function of selected ALDHs, in this case ALDH2. These selective compounds could then be used to better elucidate the individual function of ALDH2 in both health and disease.

As selective compounds for ALDH1A1 and ALDH3A1 have been previously found through *in vitro* high-throughput screening (HTS), we used an *in vitro* HTS to identify potential selective inhibitors for ALDH2.^{214, 220} Normally ALDH activity is measured by oxidation of aldehyde substrate by measuring the production of NADH at 340 nm on a spectrophotometer ($\epsilon = 6220 \text{ M}^{-1} \text{ cm}^{-1}$). However, this assay is not ideal for high-throughput screening of chemical libraries as many compounds have similar absorption properties as NADH and provide interference. Although measuring the fluorescence of NADH is one alternative option, we utilized the esterase activity of ALDH2 to perform a high-throughput screen. In this reaction para-nitrophenylacetate is hydrolyzed to para-nitrophenol, the production of which is measured spectrophotometrically at 405 nm. Both the dehydrogenase and esterase reactions utilize the same critical residues, with Glu268 acting as a general base to activate Cys302, thus any compound that modulates esterase activity will also likely modulate aldehyde oxidation activity.⁵⁶ The esterase reaction also has the advantage of being NAD^+ -independent, meaning compounds which bind to the coenzyme-binding site are less likely to be identified.

Once compounds were identified via the HTS, several additional approaches were used to characterize and determine compound selectivity: (1) steady state competition assays to

determine mode of inhibition, (2) X-ray crystallographic studies of compound-inhibitor complexes, (3) structure activity relationship experiments to help determine the basis of selectivity and potency, and (4) cell culture experiments to determine effects of compound on proliferation of cancer cells (**Figure 9**).

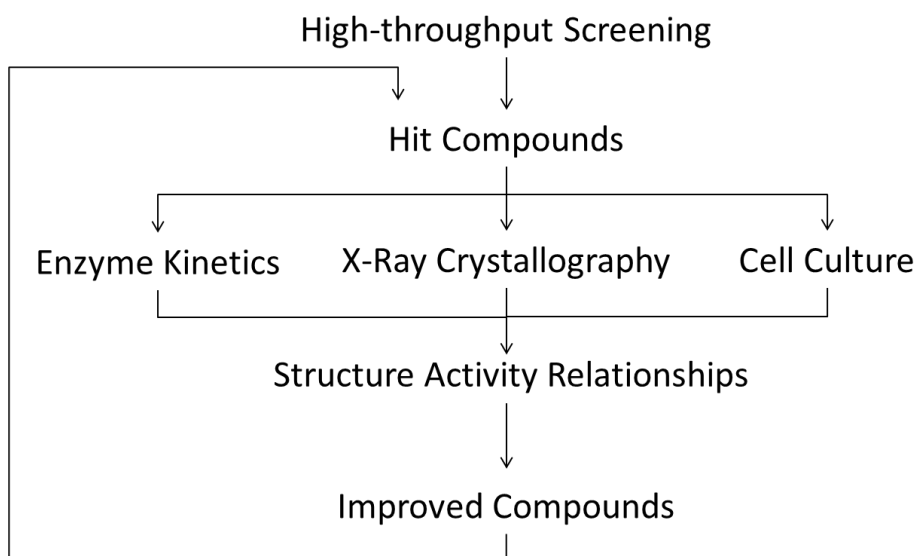


Figure 9 Research approach to identifying compounds that alter ALDH activity. Hit compounds are identified through high-throughput screening. Hit compounds are then analyzed via enzyme kinetic, X-crystallographic, and cell culture experiments to form structure activity relationships to guide the basis for improved compounds. These improved compounds can then be considered new hit compounds and be analyzed using the same means. Eventually, the improved compounds would be tested in an animal model for effects *in vivo*.

II. Materials and Methods

A. Materials

Chemicals and reagents used for protein expression and purification, enzyme kinetics, X-ray crystallography, and cell culture were purchased from Sigma-Aldrich (St. Louis, MO) unless otherwise noted. Compounds were purchased from ChemDiv Corporation (San Diego, CA), ChemBridge Corporation (San Diego, CA), InterBioScreen Limited (Moscow, Russia), Life Chemicals (Burlington, ON), and Princeton BioMolecular Research Inc. (Princeton, NJ). Dithiothreitol (DTT) was purchased from GoldBio (St. Louis, MO). Sitting drop plates for crystallography were purchased from Charles Supper Co (Natick, MA).

B. Methods

1. Production and Purification of ALDH Isoenzymes

The full-length cDNA for human ALDH2 was generously provided by Dr. Henry Weiner, Purdue University, in a pT7-7 vector and used to transform *E. coli* BL21 cells for subsequent expression and purification of the enzyme.²²¹ The general protocol for the production and purification for ALDH1A1, ALDH1A2, and ALDH2 has been published previously.^{214, 221} Specifically, a single transformed BL21 colony was transferred to 10 mL 2xTY broth containing 100 µg/mL ampicillin and grown overnight in culture at 37°C while shaking. A 5 mL aliquot of the overnight culture was used to inoculate 100 mL 2xTY containing 100 µg/mL ampicillin the next morning and was grown at 37°C while shaking. After 1-2 hours 10 mL of the 100 mL was added to 8 x 1L 2xTY broth containing 100 µg/mL ampicillin and incubated at 37°C with shaking at 200 rpm. Once

the culture reached an optical density of 0.6 to 0.8 at 600 nm, isopropyl- β -D-thiogalactopyranoside was added to a final concentration of 100 μ M to induce the synthesis of the enzyme. Cultures were incubated overnight at 16°C while shaking at 200 rpm and then collected via centrifugation, flash frozen in liquid nitrogen and then stored at -80°C. Cell pellets were thawed at room temperature and then resuspended in lysis buffer (10 mM sodium phosphate (NaP_i) pH 7.0, 2 mM EDTA, 1 mM benzamidine, 1 mM DTT). Cells were lysed via three passages through a microfluidizer (DivTech Equipment). Cell lysate was clarified by centrifugation at 35,000 rpm for 25 min at 4°C (Beckman-Coulter Optima L-90K Ultracentrifuge, Ti-45 Rotor). The clarified lysate was dialyzed against 2 x 4 L changes of lysis buffer at 4°C each for at least 5 hours. The lysate was then loaded onto a DEAE-sepharose column and eluted using gradient from 0-250 mM NaCl in lysis buffer. The eluted fractions from the DEAE-sepharose column were analyzed by SDS gel and an activity assay to confirm the presence of active enzyme. In the activity assay 20 μ L of the eluted fraction was added to saturating amounts of NAD⁺ (75 mM) and propionaldehyde (10 mM) in 100 mM sodium pyrophosphate buffer, pH 9.5 and activity determined by measuring the change in absorbance at $\lambda=340$ nm due to NADH production. Fractions containing protein were pooled and dialyzed into 4L 4-hydroxyacetophenone (4-HAP) column buffer (20 mM NaP_i pH 7.5, 1 mM EDTA, 50 mM NaCl, 1 mM DTT) overnight. The dialyzed enzyme was then loaded onto the 4-HAP column and eluted in a single step with approximately 75 mL of 4-HAP buffer containing 10 mM 4-hydroxyacetophenone. The protein preparations were then dialyzed exhaustively against 10 mM ACES, pH 6.6 with 1 mM DTT at 4°C. Enzyme was concentrated to 5-10 mg/mL using Amicon Ultra Centrifugal

Devices (Millipore Corp, Bedford, MA). Prior to storage, the protein concentration was measured using the BioRad Protein Assay (BioRad Laboratories, Hercules, CA) and its aldehyde oxidation activity measured using saturating amounts of NAD⁺ and propionaldehyde to determine specific activity. An 8 L preparation generated ~150 mg ALDH1A1, ~60 mg ALDH2, or ~35 mg ALDH1A2. Aliquots were flash frozen in liquid nitrogen and stored at -80°C. Portions of the ALDH1A1 and ALDH2 preparation were stored at -20°C in a 50% (v/v) solution with glycerol for future crystallization. Prior to crystallization set-up the enzyme was dialyzed against 3 X 4L changes of 10 mM sodium ACES, pH 6.6 with 1 mM DTT at 4°C for at least 5 hours each. All solutions were sparged with helium to remove dissolved oxygen before use to help prevent oxidation of cysteine residues in addition to the DTT already present.

ALDH1B1 and ALDH3A1 were produced and purified as previously described.^{214, 222} ALDH3A1 was purified and provided by Dr. Bibek Parajuli and a portion of ALDH1B1 used was purified and provided by Lanmin Zhai. The full length cDNA for human ALDH4A1 and ALDH5A1 was generously provided by Dr. Daria Mochly-Rosen and the carboxyl terminus of rat ALDH1L1 was generously provided by Dr. Sergey Krupenko in the pRSET expression plasmid. ALDH1L1 was expressed and purified as previously described for ALDH3A1 with the following modifications: 1) the medium contained 100 µg/mL ampicillin, 2) cells were lysed via passage through a microfluidizer, 3) the second passage through a Q-sepharose column was not included. The purification of ALDH4A1 and ALDH5A1 followed the same protocol as ALDH1L1.²¹⁰ The purification of ALDH1A3 followed one of two protocols. The first is consistent with that of ALDH1A1,

ALDH1A2, and ALDH2 and produced very small amounts of ALDH1A3.²¹⁴ Dr. Jaume Ferrer (Barcelona, Spain) generously provided a His-tagged construct for full length ALDH1A3. The His-tagged ALDH1A3 was produced and purified by a single passage through a nickel-NTA column similar to the purification of ALDH4A1, ALDH5A1, and ALDH1L1 and yielded ~120 mg per 8 L culture for enzymatic study.

2. Esterase High-Throughput Screen

The high-throughput screen (HTS) was performed using a reaction where para-nitrophenyl acetate (pNPA) is hydrolyzed to form para-nitrophenol and acetic acid. The esterase assay was used for screening as it is cofactor independent and the spectral properties of para-nitrophenol do not overlap with the absorbance characteristics of the majority of compounds within the tested libraries. The substrate was prepared by adding 0.0725 g of pNPA to 6 mL of 100% DMSO. This mixture was added slowly to 94 mL of water with continuous stirring for a final concentration of 4 mM pNPA in 6% (v/v) DMSO. Screens were completed with two different libraries at the Indiana University Chemical Genomics Core Facility in 384-well, clear-bottomed plates. Screen 1 consisted of 63,000 compounds from ChemDiv Corporation (San Diego, CA) and utilized 75 nM ALDH2, 0.8 mM pNPA, 10 μ M library compound, 2% DMSO, and 25 mM HEPES buffer, pH 7.5 for a final reaction volume of 50 μ L. Screen 2 consisted of 50,000 compounds from ChemBridge Corporation (San Diego, CA) and utilized 75 nM ALDH2, 1.6 mM pNPA, 10 μ M library compound, 3.2% DMSO, and 25 mM HEPES buffer, pH 7.5 also in a final volume of 50 μ L. The concentration of library compound is an approximation based upon the average mass of the compounds in the entire library. The

production of para-nitrophenol was monitored by measuring the increase in absorbance at $\lambda=405$ nm (molar extinction coefficient of $18,000 \text{ M}^{-1} \text{ cm}^{-1}$) on a Spectromax Plus 384 plate reader for 10 minutes. Additional wells on each plate either had an inhibitor control or no compound present to determine the normal rate. The inhibitor control for Screen 1 was $100 \mu\text{M}$ daidzin. Screen 2 used $1 \mu\text{M}$ 2,3,5-trimethyl-6-propyl-7H-furo[3,2-g]chromen-7-one (2P3), an inhibitor discovered in the Screen 1. A multichannel pipet was used to add either $20\mu\text{L}$ of 2% DMSO solution, $20\mu\text{L}$ of $250 \mu\text{M}$ daidzin in 2% DMSO, or $20\mu\text{L}$ of $2.5 \mu\text{M}$ 2P3 in 2% DMSO to their respective control column. The Genesis (Tecan) Workstation TeMO with a 96-channel pipetting head was used to make all subsequent reagent additions. The rate of reaction was used to determine a ratio to control for each compound with control being the average of the rates for the positive control (wells with no compound) on that compound's plate ($n=16$):

$$\text{Equation 1: } \textit{Ratio to Control} = \frac{\textit{Rate of reaction with compound}}{\textit{Average rate of reaction of control}}$$

Compounds which had ratios to control less than 0.60 (>40% inhibition) were considered inhibitors and those with a value greater than 1.25 (1.25-fold activation) were considered activators in Screen 1. Compounds which met these selection criteria were rescreened for validation using the same protocol. Selection criteria for Screen 2 was greater than 40% inhibition or 2-fold activation in both the primary and secondary screens.

A Z' -factor was calculated for the screening conditions prior to completion of each HTS by comparing the values of ALDH2 plus/minus the control inhibitor (each $n=384$) under the conditions of that particular HTS using the following formula:

$$\text{Equation 2: } \textit{Z'-factor} = 1 - \frac{3(\delta_p + \delta_n)}{|\mu_p - \mu_n|}$$

where μ_p and δ_p are the mean and standard deviation of the control reaction and μ_n and δ_n are the mean and standard deviation of the inhibition reaction. A Z' -factor was also calculated using 1 mM NAD^+ as an esterase activator during Screen 2. A Z' -factor between 0.5 and 1.0 indicates a good assay that is statistically strong enough to detect inhibitors and/or activators. Confirmed chemical hits that were commercially available were purchased from ChemDiv Corporation (San Diego, CA), ChemBridge Corporation (San Diego, CA), Interbioscreen Limited (Moscow, Russia), Life Chemicals (Burlington, ON) or Princeton BioMolecular Research Inc. (Princeton, NJ) to determine their effect on aldehyde oxidation.

3. Aldehyde Oxidation Activity Assays for ALDH Isoenzymes

The effect on the aldehyde oxidation activity of ALDH isoenzymes by the hit compounds from the screens was determined by measuring the formation of NAD(P)H spectrophotometrically at $\lambda=340$ nm (molar extinction coefficient of $6220 \text{ M}^{-1} \text{ cm}^{-1}$) on a Beckman DU-640 spectrophotometer using purified recombinant enzyme. Compounds were initially tested for their effect against ALDH1A1, ALDH2, and ALDH3A1. For ALDH1A1 and ALDH2, the reaction contained 100-200 nM enzyme, 200 μM NAD^+ , 100 μM propionaldehyde, and 1% DMSO in 50 mM BES, pH 7.5 at room temperature. For ALDH3A1, the reaction contained 20-25 nM enzyme, 300 μM NADP^+ , 300 μM benzaldehyde, and 1% DMSO in 100 mM NaPi buffer, pH 7.5. The reaction was initiated by addition of aldehyde substrate after a 2 min pre-incubation of enzyme, coenzyme, and compound. Compounds were initially screened at a concentration of 10 μM . Measurements at higher concentrations of compound were occasionally used to aid in

interpretation of data. Compounds that were potentially selective for ALDH1A1 and/or ALDH2 were then tested with other ALDH isoenzymes. For ALDH1A2 and ALDH1A3, the reaction contained 100-400 nM enzyme, 200 μM NAD^+ , 100 μM propionaldehyde, and 1% DMSO. The assay for ALDH1B1 used 500 μM NAD^+ and 200 μM propionaldehyde. For ALDH4A1 the assay included 500 μM NAD^+ and 20 mM propionaldehyde. For ALDH5A1 the assay included 200 μM NAD^+ and 2 mM propionaldehyde. For rat ALDH1L1 the assay included 500 μM NADP^+ and 4 mM propionaldehyde. The assay components for the selectivity assays were designed to provide the maximal stringency toward ALDH2, such that the substrate concentration utilized was >500-fold above K_M for ALDH2 while keeping below 15-fold over K_m for the other isoenzymes. All reactions were initiated with the addition of aldehyde substrate after a 2 min pre-incubation period. EC_{50} values for aldehyde oxidation were calculated by varying the concentration of compound from 0 - 100 μM for compounds which showed greater than 50% activation/inhibition at 10 μM concentration of compound. Assay parameters for EC_{50} calculation were the same as for the initial selectivity screen, with the use of 500 μM acetaldehyde as an additional aldehyde substrate for AC_{50} calculations with ALDH2. Data were fit to the four parameter EC_{50} equation using SigmaPlot (v12):

$$\text{Equation 3: } y = \text{min} + \frac{(\text{max} - \text{min})}{1 + \left(\frac{x}{\text{EC}_{50}}\right)^{-\text{HillSlope}}}$$

where y is the rate of activity and x is the concentration of compound. The values represent the mean/SEM of three independent experiments, with each experiment n = 3.

Thirty-four additional psoralen and coumarin derivatives were ordered from ChemDiv Corporation (San Diego, CA) and ChemBridge Corporation (San Diego, CA) to build structure-activity relationships for the hit compounds. Analogs were selected as a representative sample of the 600+ commercially available compounds which had >95% structure similarity. EC₅₀ values for aldehyde oxidation for these compounds were calculated using the same protocol as the initial hit compounds. Data were fit to the four parameter EC₅₀ equation (Equation 3) using SigmaPlot (v12). The values represent the mean/SEM of three independent experiments, with each experiment n=3.

4. Steady-State Kinetic Characterization with ALDH1A1 and ALDH2

The mode of inhibition of the compounds was characterized by steady state kinetics through covariance of compound and either aldehyde substrate or coenzyme concentration. The secondary substrate was kept at a saturating amount. The mode of inhibition towards NAD⁺ binding with ALDH1A1 was determined by covarying inhibitor and coenzyme concentrations at a fixed aldehyde substrate concentration. Dehydrogenase activity was measured spectrophotometrically by measuring the formation of NADH at 340 nm (molar extinction coefficient of 6200 M⁻¹ cm⁻¹) on a Beckman DU-640 spectrophotometer for 3 min. The assay included 100-200 nM ALDH1A1, 20-200 μM NAD⁺, 1 mM propionaldehyde, and 1% DMSO in 25 mM BES buffer, pH 7.5. The reaction was initiated by the addition of propionaldehyde after a 2 minute pre-incubation with enzyme, NAD⁺, and compound. The mode of inhibition towards NAD⁺ binding with ALDH2 was determined in a similar fashion. The activity of ALDH2 was determined in a reaction containing 100-200 nM ALDH2, 15-400 μM NAD⁺, 1 mM propionaldehyde,

and 1% DMSO in 25 mM BES buffer, pH 7.5. All data were fit to the tight binding or single substrate-single inhibitor non-linear velocity expressions for competitive, non-competitive, mixed type non-competitive, and uncompetitive inhibition using SigmaPlot (v12, Enzyme Kinetics Module). Lineweaver-Burk plots were generated using SigmaPlot (v12) to better visualize the model fit. The appropriate model was selected through analysis of goodness-of fit. Values shown represent the mean/SEM of three independent experiments (each n=3).

The mode of inhibition towards aldehyde substrate binding for ALDH2 was measured via fluorescence spectroscopy. The K_M of ALDH2 for propionaldehyde (<1 μM) is so low that measurement of activity at near K_M concentrations is nearly impossible by measurement of absorbance.²²³ Utilizing the fluorescent characteristics of NADH allowed for the measurement of these activities. A standard curve of the fluorescence of NADH from 10 nM to 3000 nM was first measured for use in converting the arbitrary fluorescence units into the amount of NADH produced during the experiment. The K_M values for propionaldehyde and cofactor NAD^+ for ALDH2 were then determined for ALDH2 using the fluorescence assay as these values may differ from those obtained using the absorbance assay. Dehydrogenase activity was measured by monitored the fluorescence of NADH at $\lambda = 470$ nm after excitation at $\lambda = 320$ nm for 2 min measuring every five seconds. Reactions for K_M calculations contained 5 nM ALDH2 in 100 mM NaPi, pH 7.0 in a reaction volume of 3 mL. The K_M for NAD^+ was determined by plotting increasing concentrations of NAD^+ (10-400 μM) versus the velocity of the reaction with a saturating amount of propionaldehyde (1 μM). The K_M for

propionaldehyde was determined by plotting increasing concentrations of propionaldehyde (50-750 nM) versus the velocity of the reaction with a saturating amount of NAD⁺ (400 μM). Data were plotted using the Simple Ligand Binding Toolbox in SigmaPlot (v12) and the values represent the mean/SEM of a single experiment (n=3). Steady-state kinetics were used to measure the mode of inhibition towards propionaldehyde binding in ALDH2. Assay solutions included 5 nM ALDH2, 400 μM NAD⁺, 75-600 nM propionaldehyde, 0.2% DMSO, and 0-80 nM inhibitor in 100 mM NaPi, pH 7.0. Due to low concentrations of substrate used in the assay, all reagents were filtered to remove additional aldehyde contaminants. All data were fit to the tight binding non-linear velocity expressions for competitive, non-competitive, mixed-type non-competitive and uncompetitive inhibition using SigmaPlot (v12, Enzyme Kinetics Module) to evaluate goodness of fit. Lineweaver-Burk plots were generate using SigmaPlot (v12) to better visualize the mode of inhibition. All data represent the mean/SEM of the four independent experiments (n=4) of duplicate assays at each concentration.

5. Characterization of 2BS4's Inhibition of ALDH2

IC₅₀ curves were measured for the inhibition of ALDH2 by 2BS4 utilizing different incubation times. The rate of aldehyde oxidation was determined by measuring the formation of NADH spectrophotometrically at λ=340 nm (molar extinction coefficient of 6220 M⁻¹ cm⁻¹) on a Beckman DU-640 spectrophotometer using purified recombinant enzyme. The assay solutions included 150 nM ALDH2, 200 μM NAD⁺, 100 μM propionaldehyde, 0 – 50 μM 2BS4, and 1% DMSO in 25 mM BES buffer, pH 7.5. The

reaction was initiated by addition of enzyme to coenzyme, compound, and substrate (0 min incubation) or by addition of aldehyde substrate after either a 2 or 10 min pre-incubation of enzyme, coenzyme, and compound. Data were fit to the four parameter EC_{50} equation (Equation 3) using SigmaPlot (v12). Values represent the mean/SEM of one experiment with three replicates for each data point (n=3).

The interaction of the compound 2BS4 with ALDH2 was characterized further by incubating 2BS4 with ALDH2 before the addition of NAD^+ and aldehyde substrate. Dehydrogenase activity was measured spectrophotometrically by determining the formation of NADH at 340 nm (molar extinction coefficient of $6200 \text{ M}^{-1} \text{ cm}^{-1}$) using a Beckman DU-640 spectrophotometer for 3 min. The assay included 200 nM ALDH2, 0.3 μM or 1.5 μM 2BS4, 200 μM NAD^+ , 1 mM propionaldehyde, and 1% DMSO in 25 mM BES buffer, pH 7.5. ALDH2 was incubated with either 3 μM or 15 μM 2BS4 in 10% DMSO for various time periods before subsequent 10-fold dilution into the assay. After dilution of the ALDH2/2BS4 solution, the reaction was initiated by the addition of propionaldehyde after 2 minute incubation with ALDH2/2BS4 and NAD^+ . The measurement at zero hour(s) incubation was taken by diluting the enzyme-compound mixture immediately after addition of compound. Each data point represents the average of two measurements. (n=2)

6. Crystallization of ALDH1A1 and ALDH2 Complexes

The general crystallization conditions for both ALDH1A1 and ALDH2 have been reported previously.^{44, 220} Crystals of ALDH1A1 were grown by equilibrating 3 mg/mL

ALDH1A1 with 100 mM sodium BisTris, pH 6.2 – 6.6, 9 – 11% PEG 3350, 200 mM NaCl, and 5 mM YbCl₃ using the sitting drop method with 500 μL mother liquor. Drop composition consisted of 2 – 4 μL protein mixed with 2 – 4 μL crystallization solution. The drop was then mixed by agitation. Crystallization was allowed to proceed at 22°C in an incubation chamber and crystals grew in 1 – 2 weeks. BUC11 and BUC22 complexes were prepared by growing ALDH1A1 crystals in the presence of 200 μM compound and 2% (v/v) DMSO (co-crystallization). Compound was first added to the protein solution before mixing with the crystallization solution. The BUC25 complex was prepared by soaking an apo-ALDH1A1 crystal overnight with crystallization solution containing 500 μM BUC25 with 2% (v/v) DMSO. All ALDH1A1 crystals were cryoprotected for flash-freezing by adding 20% (v/v) ethylene glycol to the final crystallization solution. Crystals were frozen in a liquid nitrogen cryostream and were tested on the home source Bruker D8 system for diffraction quality. Crystals with good diffraction were stored in liquid nitrogen until data collection at a synchrotron source.

Crystals of the 2P3-ALDH2 complex were grown by equilibrating 8 mg/mL ALDH2 and 200 μM 2P3 in 2% DMSO with 100 mM sodium ACES, pH 6.4, 100 mM guanidine-HCl, 10 mM MgCl₂, 4 mM dithiothreitol, and 18% PEG 6000 using the sitting drop method with 500 μL mother liquor. Crystal plates were set up in a glove box then transferred to an incubation chamber at 22°C for crystal growth. Crystals typically grew in 1 – 2 weeks. Crystals were cryoprotected for flash-freezing by adding 18% (v/v) ethylene glycol to the final crystallization solution. Crystals were frozen in a liquid nitrogen cryostream and were tested on the home source Bruker D8 system for diffraction

quality. Crystals with good diffraction were stored in liquid nitrogen until data collection at a synchrotron source.

Diffraction data was collected at Beamline 19-ID operated by the Structural Biology Consortium at the Advanced Photon Source, Argonne National Laboratory, Chicago, IL. Diffraction data was indexed, integrated, and scaled using the HKL2000 or HKL3000 program suites.²²⁴ The CCP4 program suite was used for molecular replacement and refinement.²²⁵ The human apo-ALDH2 structure (PDB Code 3N80) was used as a model for ALDH2 and the human apo-ALDH1A1 structure (PDB Code 4WJ9) was used as a model for ALDH1A1. Molecular replacement was necessary as both the ALDH1A1-BUC22 and ALDH2-2P3 complexes were obtained in orientations and/or space groups not seen previously using the same conditions. The ALDH2-2P3 complex was obtained in the previously seen $P2_12_12_1$ crystal lattice but with different unit cell dimensions. The ALDH1A1-BUC22 complex was obtained in a previously unseen P1 crystal lattice that contained two tetramers in the asymmetric unit. Previous ALDH1A1 structures, and the ALDH1A1-BUC25 and ALDH1A1-BUC11 structures, were obtained in a P422 space group with a single monomer in the asymmetric unit. The molecular graphics application Coot was used for model building.²²⁶ Ligand maps were generated using Sketcher (CCP4) to use for refinement. The TLSMD (Translation/Libration/Screw Motion Determination) server was used to determine dynamic properties of ALDH1A1.^{227, 228}

7. Cellular Effect of the Coumarin Derivative BUC22

MDA-MB-468 (ER-/PR-/HER-) breast cancer cells were generously provided by Dr. Clark Wells (IUSM). MDA-MB-468 cells were cultured in 1X DMEM (Cellgro, Mediatech Inc, Manassa, VA) supplemented with 10% fetal bovine serum (FBS) (Cell Applications Inc, San Diego, CA) and 100 Units/mL penicillin and 100 µg/mL streptomycin (P/S)(Lona, Walkersville, MD). Cells were passaged after every 80-90% confluence (normally every 3-4 days).

The 3-(4,5-dimethylthiazol-2-yl)-2,5-diphenyltetrazolium bromide (MTT) assay was used to measure the proliferative potential of cancer cells after treatment with BUC22. Cells were plated at 5000 cells/well density in 96-well clear bottom cell culture plates on 40 µL ~7mg/mL Matrigel Matrix Basement Membrane (Corning, Bedford, MA). Cells were treated starting on the day of plating (Day 1) by adding compound in 0.5% (v/v) DMSO to 200 µL DMEM supplemented with FBS and P/S. One set of wells contained Matrigel alone and one set contained cells on Matrigel, both in compound-free media. Media was changed on Day 3 and Day 5. On Day 6 media was aspirated and 0.1 mL of MTT (0.5 mg/mL in PBS) was added to each well followed by incubation for 4 hours at 37°C to allow for reduction of MTT to its formazan. After reduction 100 µL 0.05N HCl in 10% SDS was added to each well followed by incubation for 4 hours at 37°C to lyse the cells. After the second incubation the absorbance of each well was measured at $\lambda=595$ nm. Each experiment had three duplicate wells of each condition. Values were normalized by subtracting absorbance values of wells which contained only Matrigel. Data represent the mean/SEM of three independent experiments, each n=3.

III. Results

A. Esterase High-Throughput Screen for ALDH2 Modulators

Two high-throughput screens (HTS) were performed to identify activators and inhibitors of ALDH2 as measured by its *in vitro* esterase activity. Screen 1 consisted of 63,000 compounds from ChemDiv Corporation (San Diego, CA) and Screen 2 consisted of 50,000 compounds from ChemBridge Corporation (San Diego, CA). Both the esterase hydrolysis and aldehyde oxidation reactions use the same catalytic residues. The use of the esterase reaction for screening purposes has two advantages over the aldehyde oxidation reaction. First, interference from compounds with overlapping UV absorbance characteristics with NADH is minimized. Secondly, the esterase reaction does not require NAD⁺ and thus the esterase reaction limits identification of compounds that interfere with cofactor binding. The cofactor binding site is highly conserved among ALDH isoenzymes, thus compounds that bind in the cofactor binding site are less likely to be selective and options to achieve selectivity are limited.

1. Z'-factor Calculation

A Z'-factor score was calculated prior to the start of each HTS due to the use of different control inhibitors for each screen. A Z'-factor between 0.5 and 1.0 indicates an excellent assay to distinguish differences in activity from control reactions, i.e. determine activators and inhibitors. The Z'-factor for Screen 1 comparing ALDH2 activity with/without inhibitor (100 μ M Daidzin) was 0.60 (**Figure 10**). During the course of Screen 1 a more potent ALDH2 inhibitor was discovered and used as the control inhibitor for Screen 2. The Z'-factor for Screen 2 comparing ALDH2 activity with/without

inhibitor (1 μ M 2P3) was 0.50 (**Figure 11**). The better inhibitor did not improve the Z' -factor. For Screen 2 a Z' -factor comparing ALDH2 activity with/without activator (1 mM NAD) was also calculated and found to be 0.46 (**Figure 11**). Based off the Z' -factor both screens were excellent at discovering inhibitors of ALDH2 esterase activity. The Z' -factor for Screen 2 for determination of activation was nearly excellent as well. Although increasing the amount of enzyme could have made it easier to distinguish activators, it also would have made it more likely that any activator would not follow a linear rate for the duration of the screen. The lower Z' -factor for Screen 2 may be due to higher background due to the use of twice as much substrate.

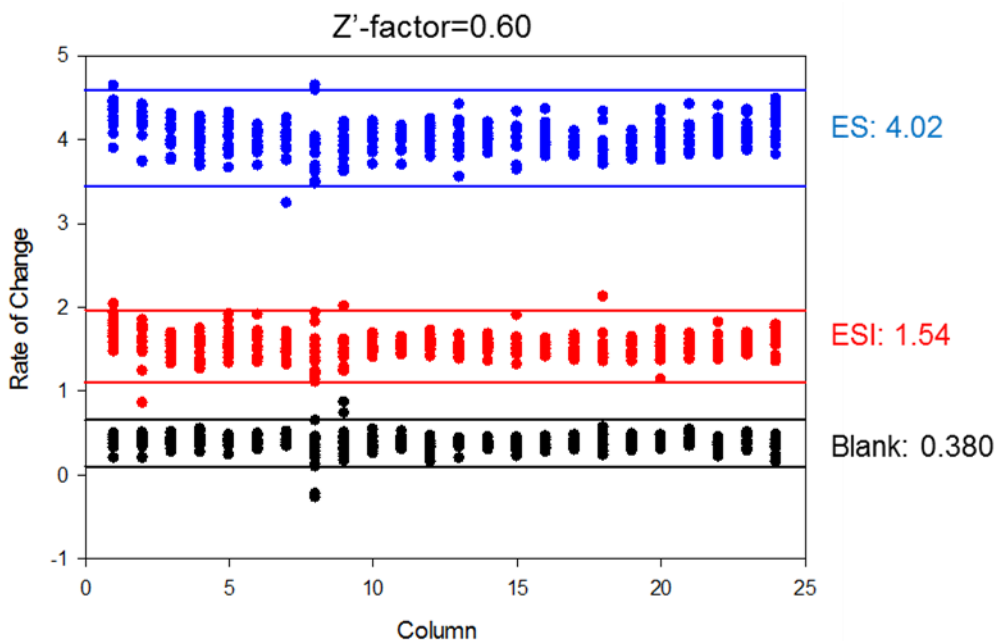


Figure 10 Z' -factor determination for Screen 1.

Each point represents the rate of change in absorbance at 405 nm of a reaction. The x-axis is the column (1-24) on the 384-well plate. The blue data points correspond to the enzyme + substrate (ES) control (mean=4.02); the red is enzyme + substrate + inhibitor (ESI) (mean=1.54); the black is the no enzyme blank control (mean=0.380). The lines represent 3x standard deviation from ES mean (blue), ESI mean (red), and blank (black). Each condition performed on a separate plate with n=384.

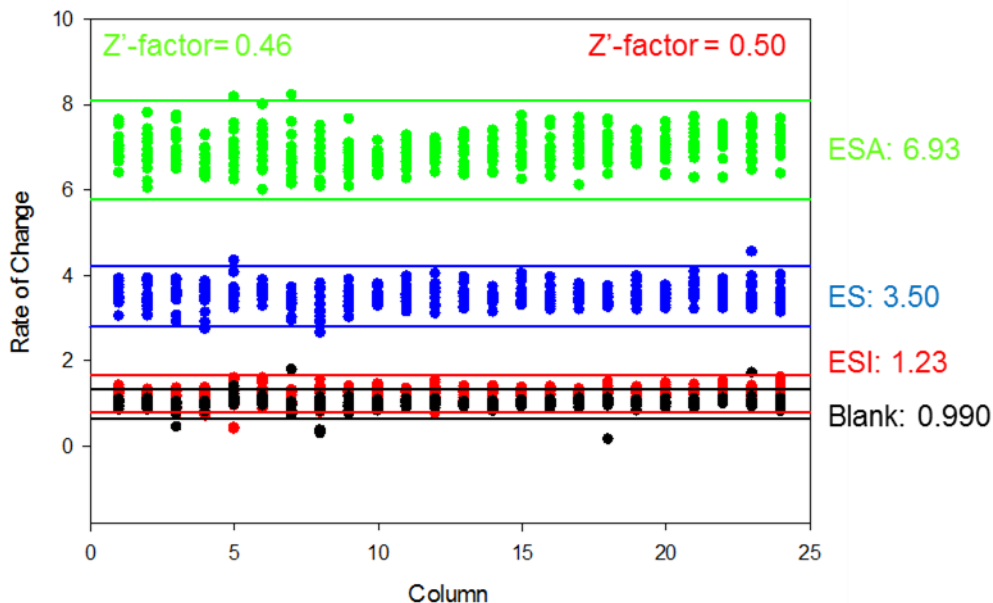


Figure 11 Z'-factor determination for Screen 2.

Each point represents the rate of change in absorbance at 405 nm of a reaction. The x-axis is the column (1-24) on the 384-well plate. The blue data points represent the enzyme + substrate (ES) control (mean=3.50); the red is enzyme + substrate + inhibitor (ESI) (mean=1.23); the green in enzyme + substrate + activator (ESA); the black in no enzyme blank control (mean=0.990). The lines represent 3x standard deviation from ES mean (blue), ESI mean (red), ESA mean (green) and blank (black). Z'-factor for ESA vs ES shown in green and for ESI vs ES shown in red. Each condition performed on a separate plate with n=384.

2. High-Throughput Screen Results

The two libraries totaling over 110,000 compounds from ChemDiv and ChemBridge were screened using the esterase assay. Plates were acquired from the Indiana University Chemical Genomics Core with 20 μ L of 25 μ M of each compound, which was already present in the first 22 columns of each 384-well plate. Each plate also contained a control column with enzyme and substrate (ES control). The average of intra-plate ES control served as the basis to determine whether a compound modulated esterase activity. Each plate also contained an additional control column with enzyme and substrate and inhibitor to ensure significant inhibition could be measured on each plate. A representative plate is

shown in **Figure 12**. Selection criteria were initially set at either greater than 2-fold activation or less than 60% activity. Due to the lack of activators obtained from Screen 1, the selection threshold was lessened to 1.25-fold activation for only Screen 1. The primary screen of Screen 1 yielded a total of 1395 compounds and that of Screen 2 yielded 536 compounds that were activators or inhibitors of ALDH2's esterase activity. These 1931 compounds were then rescreened using the same assay parameters. Only 53 compounds from Screen 1 and 14 compounds from Screen 2 met the threshold criteria in the secondary screen, meaning that over 95% of compounds did not meet the selection criteria a second time. Of the 67 compounds identified through the high-throughput screens, 59 were commercially available and purchased for further study.

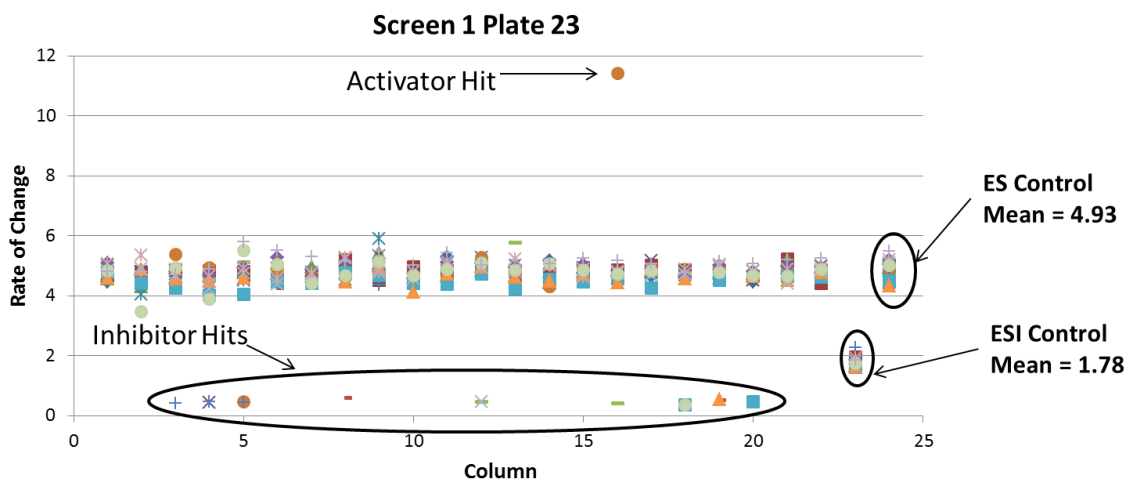


Figure 12 Example plate from Screen 1 for compounds that modify ALDH activity. Each point represent one well, with the x axis the column (1-24) on the plate and the y axis the rate of change in absorbance measured at $\lambda=405$ nm. Column 23 is the ESI control with a mean value of 1.78 (n=16). Column is the ES control with a mean value of 4.93 (n=16). On this plate we identified one activator and fifteen inhibitors.

B. Hit Compound Validation and Initial Determination of Selectivity

We were able to obtain 59 of the 67 compounds identified through the high-throughput screen. At this point we switched from monitoring the esterase function of aldehyde dehydrogenase to the aldehyde oxidation function in part to better evaluate how the compounds will modulate the complete catalytic mechanism of ALDHs. The effect of the hit compounds on the activity of ALDH1A1, ALDH2, and ALDH3A1 was tested as an initial determination of selectivity and potency. Of the 59 compounds examined at 10 μ M concentration, 45 did not modulate the activity of ALDH2 more than 20% in either direction relative to control. Several of the 45 compounds which did not modulate ALDH2 activity influenced the activity of one or both of the ALDH1A1 and ALDH3A1 enzymes by more than 20% (2CD12, 2BS2, 2BS6, 2P5, 2P7, 2P9, 2P11, 2P12, 2LC1, 2F3, 2F8, 2F10, 2F11, and 2F12). Of the 14 compounds that did modulate ALDH2 activity, several were determined to have low potency and/or selectivity based off the measurements at 10 μ M concentration. 2C1 activated each enzyme \sim 1.2 fold at 10 μ M concentration. 2CB4 inhibited all three isoenzymes greater than 80% and 2F13 inhibited all three around 50%. 2C2 inhibited ALDH1A1 activity much greater than ALDH2 activity. Although 2CD4 inhibited the activity of ALDH2, the compound showed activation of ALDH1A1. 2CD5 showed some selectivity towards ALDH2, though the potency was low compared to other hit compounds. 2CB5, 2P2, and 2P4 were selected for further analysis due to their high potency towards ALDH2 (\geq 80% inhibition) and relative selectivity against ALDH1A1 and ALDH3A1 (**Figure 13**). However, additional batches of 2P2 ordered to continue enzymatic studies no longer inhibited ALDH2 at this concentration. The first batch of 2P2 may have had an additional contaminant leftover

from synthesis of the compound which enhanced ALDH2 inhibition; however, this could not be verified due to the exhausted supply of the initial stock. As a consequence, 2CB5 and 2P4 were the two most promising remaining hit compounds. Both 2BS4 and 2LC2 showed selectivity towards ALDH2 but contain a terminal methyl ester group; these potential esterase substrates were initially avoided, as inhibition could be lost or diminished after ester hydrolysis. 2BS4 was eventually included again due to its structural similarity to 2P4 and 2CB5. 2P3, which did not show the same level of selectivity towards ALDH2 as 2P4 and 2CB5 but had the highest potency, was also included due to the structural similarity.

.

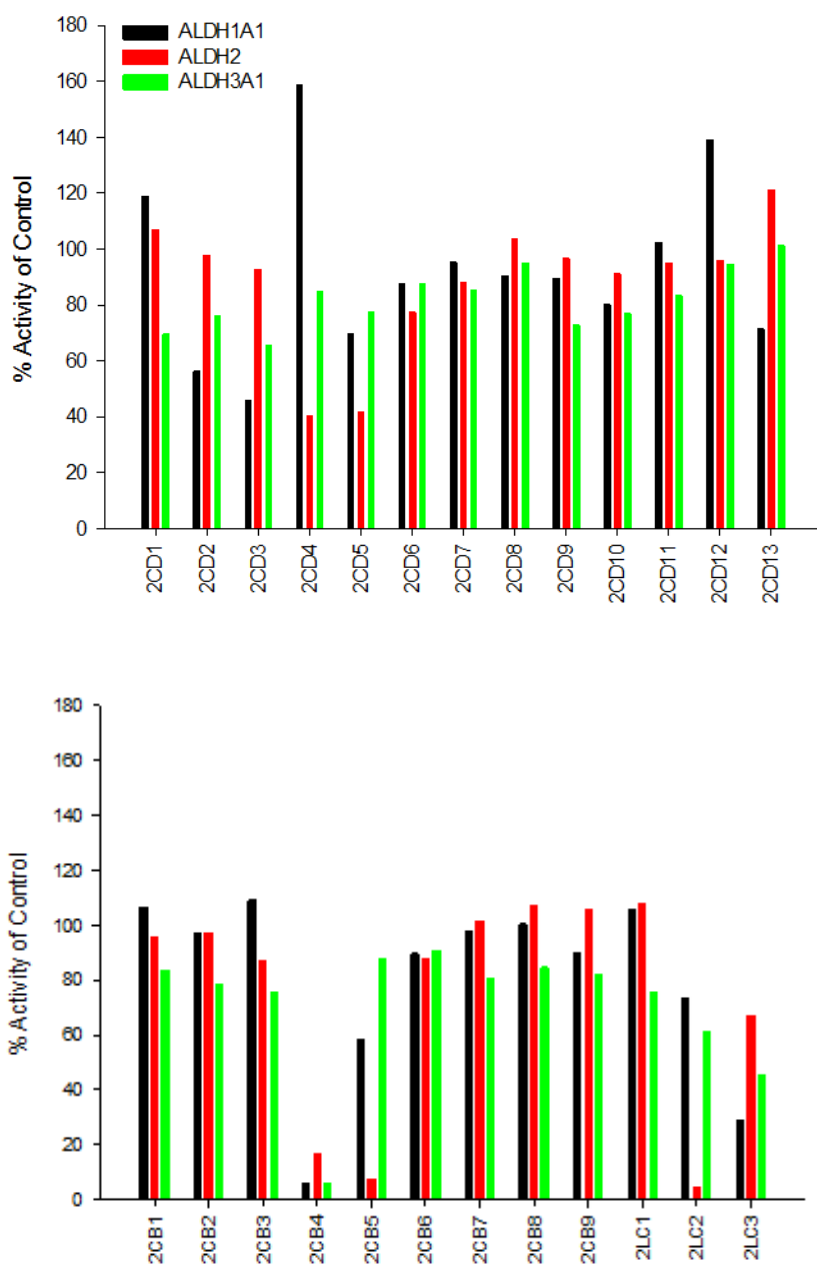


Figure 13 Effect on aldehyde oxidation of hit compounds from HTS. The activity of 59 compounds (10 μ M) identified via HTS was tested on three ALDH isoenzymes. Average of at least two ($n \geq 2$) independent trials.

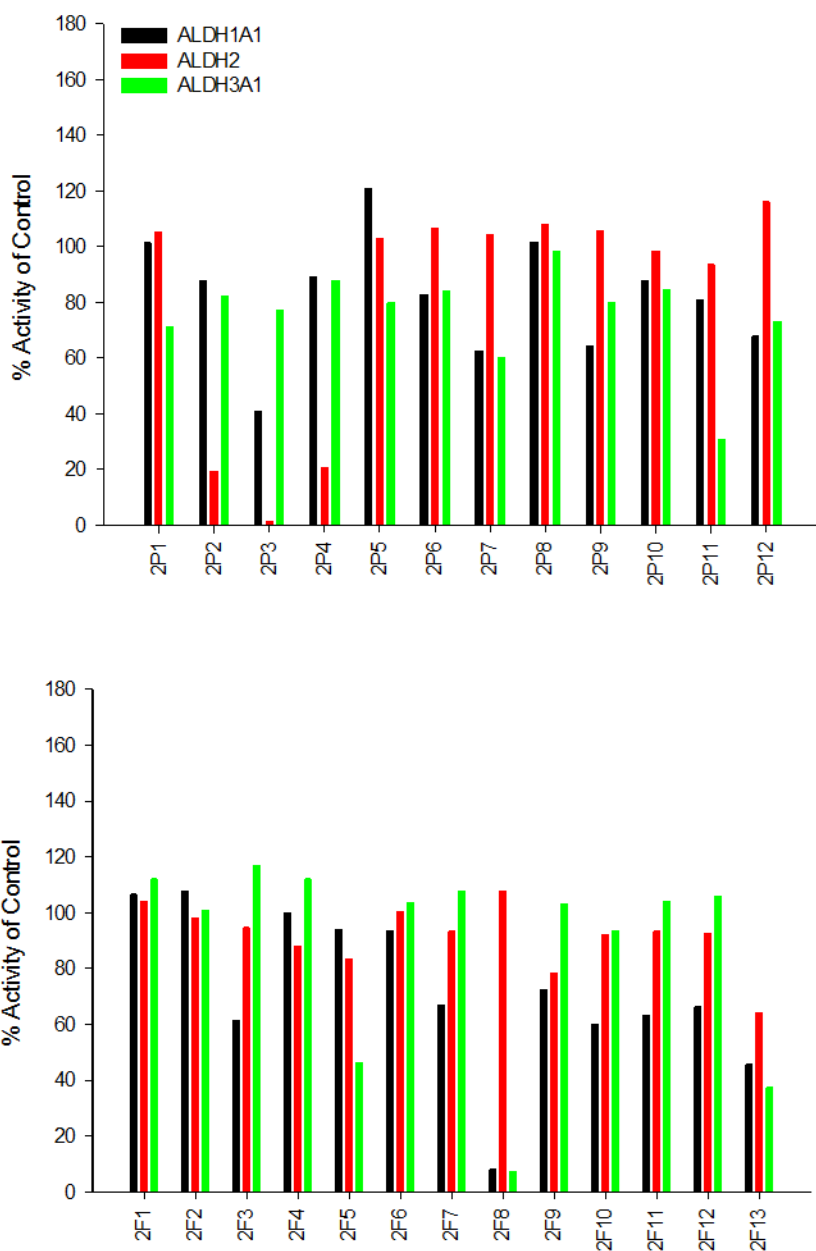


Figure 13 Continued Effect on aldehyde oxidation of hit compounds from HTS. The activity of 59 compounds (10 μ M) identified via HTS was tested on three ALDH isoenzymes. Average of at least two ($n \geq 2$) independent trials.

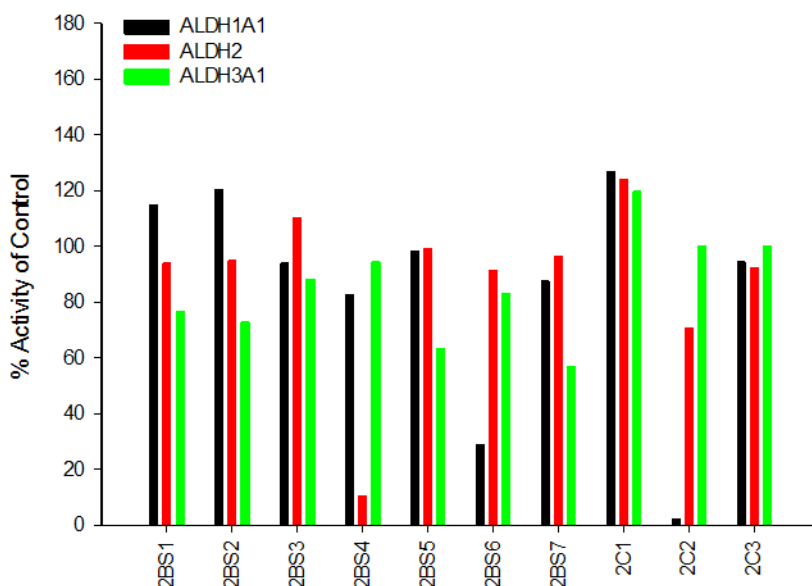


Figure 13 Continued Effect on aldehyde oxidation of hit compounds from HTS. The activity of 59 compounds (10 μ M) identified via HTS was tested on three ALDH isoenzymes. Average of at least two ($n \geq 2$) independent trials.

The effect of the four compounds (2BS4, 2P3, 2P4, and 2CB5) on other ALDH isoenzymes was tested to generate a broader view of the compounds' selectivity towards ALDH2 (**Figure 14**). The effect of 10 μ M of each compound on the dehydrogenase activity of the other three ALDH1A/2 family members (ALDH1A2, ALDH1A3, and ALDH1B1) was determined, in parallel with assays of ALDH4A1, ALDH5A1, and ALDH1L1 (rat). Inhibition of the isoenzymes by the four compounds was limited to the ALDH1/2 family as the compounds did not modulate the activity of ALDH3A1, ALDH4A1, ALDH5A1, or ALDH1L1 (rat). Each compound showed the greatest amount of inhibition towards ALDH2 of the isoenzymes tested. For any particular ALDH1/2

enzyme, 2P3 inhibited the most, followed by 2CB5, then 2P4 at 10 μM . The inhibition profile for the four compounds was very similar between ALDH1A2, ALDH1A3, and ALDH1B1. 2BS4 only showed inhibition towards ALDH2 at this single concentration of compound.

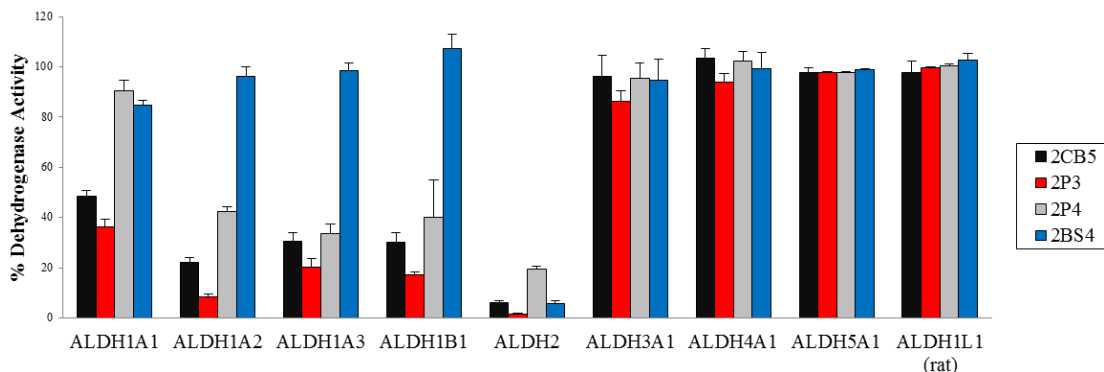


Figure 14 Effects of four aromatic lactones on activity of nine ALDH isoenzymes. Percent dehydrogenase activity for nine ALDH isoenzymes in the presence of 10 μM compound compared to control reaction with no compound present. Value is the average of at least three independent trials ($n \geq 3$) with standard error, except for the measurement of ALDH1B1 activity with 2P4 and ALDH1L1 activity with each compound ($n=2$).

C. EC_{50} Determination of Hit Compounds

1. Alda-1 Mimics

Although no compounds from the HTS activated ALDH2's oxidation of propionaldehyde by more than 20% at 10 μM concentration, three compounds (2CD11, 2CB8, and 2CB9) identified in the HTS were structurally similar to Alda-1 and thus were examined further (**Figure 15**). Each share the benzodioxol group that in Alda-1 is bound within the substrate tunnel oriented towards Cys302. The three compounds were found to activate the oxidation of propionaldehyde by ALDH2 while having no effect on the activity of ALDH1B1, ALDH1A1, ALDH1A2, ALDH1A3, or ALDH3A1. Each of the compounds

had an AC_{50} equal to approximately 50-60 μM and activated the oxidation of propionaldehyde by at most 2-fold (**Table 3**). Each compound became insoluble in the assay solution between 200 and 500 μM ; therefore solubility limits prevented a more accurate measurement of the AC_{50} for propionaldehyde oxidation by ALDH2. For 2CB8, full dose-response analysis could not be completed. The AC_{50} of ~ 60 μM is based off the assumption that the maximum activity would be near 2-fold if the curve could be completed.

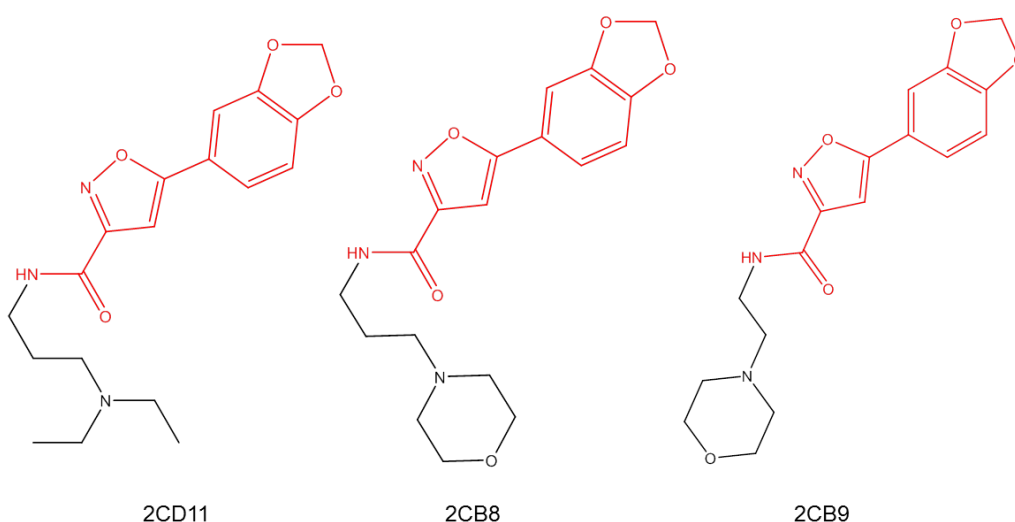


Figure 15 Three Alda-1 mimics identified via the HTS. Compounds share a benzodioxol group linked to a carboxamide through an isoxazole linker (shown in red).

Since Alda-1 activated the oxidation of smaller substrates more effectively, we also tested the effect the three activators had on the oxidation of acetaldehyde by ALDH2. The three compounds had varying effects on acetaldehyde oxidation. 2CB9 was the most potent ($AC_{50} = 9.6 \pm 2.2$ μM) but increased the maximum acetaldehyde oxidation activity the least ($160 \pm 4\%$). 2CD11 was the least potent ($AC_{50} = 28 \pm 5$ μM) but increased the maximum acetaldehyde oxidation activity of ALDH2 the most ($210 \pm 9\%$) (**Table 3**).

The AC₅₀ values for propionaldehyde and acetaldehyde oxidation with each compound are higher than those seen with Alda-1.⁵⁵ For this reason, along with the solubility issues, these compounds were not further studied.

Table 3 AC₅₀ determination of Alda-1 mimics with ALDH2.

Values are the mean of a single experiment of three independent measurements (n=3). Values for 2CB8 for propionaldehyde oxidation are approximated based off an incomplete curve using the assumption that binding behavior is consistent with the other compounds.

Compound	Aldehyde Substrate			
	Acetaldehyde		Propionaldehyde	
	Max Activity	AC ₅₀ (μM)	Max Activity	AC ₅₀ (μM)
2CD11	210 ± 9%	28 ± 5	180 ± 11%	50 ± 16
2CB8	200 ± 10%	14 ± 4	~200%	~60
2CB9	160 ± 4%	9.6 ± 2.2	200 ± 19%	61 ± 29

2. Coumarin and Psoralen Derivatives, in Comparison to Daidzin

The four compounds (2BS4, 2P3, 2P4, and 2CB5) are aromatic lactones (**Figure 16**). 2P3, 2P4 and 2CB5 are psoralen derivatives and 2BS4 is a coumarin derivative. The differences between 2P3, 2P4, and 2CB5 lie in the presence and length of the various alkyl substituents attached to the aromatic substructure. 2BS4 contains an alkyl chain with a terminal methyl ester group bound to the psoralen substructure via an ether linkage. The ether oxygen is in the same relative position as the furan oxygen of 2P3, 2P4, and 2CB5.

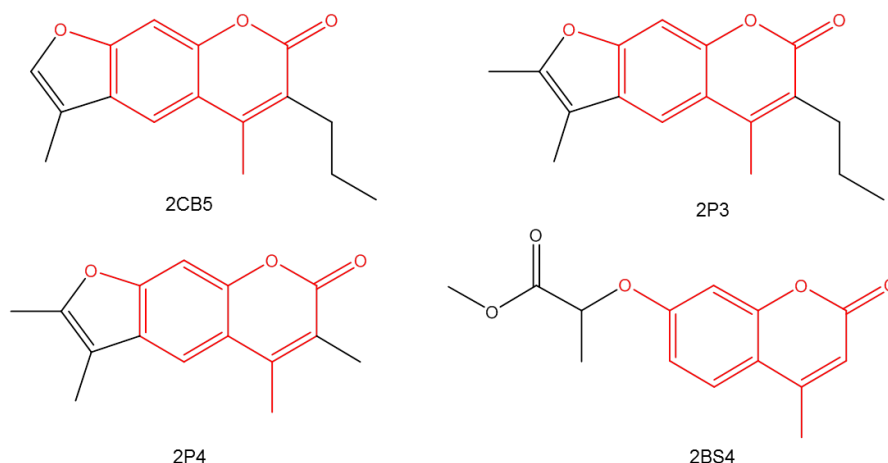


Figure 16 Four aromatic lactone inhibitors identified via the HTS. Compounds each share a coumarin aromatic structure with an oxygen atom bound to the benzyl ring. For 2CB5, 2P3, and 2P4; this takes the form of a psoralen aromatic structure.

The IC_{50} values for daidzin for the ALDH1/2 family were measured to compare our results to compounds (including CVT-10216) already described in the literature as ALDH2-selective inhibitors.^{201, 204} Consistent with prior work, daidzin was found to be about 100-fold more potent toward ALDH2 than ALDH1A1 (**Table 4**). However our IC_{50} values are 10-fold higher than prior values, likely due to differing substrate concentrations in the assays. In regards to the other ALDH1/2 enzymes, we found daidzin to inhibit ALDH1B1 ($IC_{50} = 5.1 \pm 0.5 \mu M$) and ALDH1A2 ($IC_{50} = 4.5 \pm 0.6 \mu M$) with similar potencies to ALDH2 ($IC_{50} = 3.5 \pm 0.1 \mu M$), while being less potent against ALDH1A1 and ALDH1A3. Inhibition of ALDH1A1 and ALDH1A2 by daidzin was observed, but compound solubility issues in the assay prevented full dose-response analyses.

The IC_{50} values of the four aromatic lactones were then determined for nine ALDH isoenzymes (**Table 4**) in order to better characterize the selectivity of the compounds

towards individual members of the ALDH1/2 family of isoenzymes and against other ALDH isoenzymes. None of the four compounds inhibited the activity of ALDH1L1 (rat), ALDH3A1, ALDH4A1, or ALDH5A1 when present in the reaction mixtures up to 100 μ M. 2BS4 showed selectivity towards ALDH2 versus the other eight isoenzymes tested with an IC_{50} value of $1.5 \pm 0.3 \mu$ M. The other three compounds inhibited ALDH2 more strongly, though they also inhibited the majority of the other ALDH1/2 isoenzymes at sub-micromolar concentrations. The lowest IC_{50} measured was that of 2P3 with ALDH (0.11 \pm 0.02 μ M), 30 times as potent as daidzin. 2P3 inhibited each of the five ALDH1/2 isoenzymes the strongest and was the only compound which completely inhibited each of the five isoenzymes.

Table 4 IC_{50} values for four aromatic lactones with nine ALDH isoenzymes. Values are the mean/SEM of three independent experiments, each n=3.

Inhibitor	IC_{50} (μ M)				
	ALDH2	ALDH1B1	ALDH1A1	ALDH1A2	ALDH1A3
Daidzin	3.5 ± 0.1	5.1 ± 0.5	>200	4.5 ± 0.6	>200
2CB5	0.34 ± 0.05	0.88 ± 0.28	$0.34 \pm 0.05^{\#}$	0.76 ± 0.07	1.1 ± 0.1
2P3	0.11 ± 0.02	0.36 ± 0.12	0.22 ± 0.05	0.30 ± 0.04	0.40 ± 0.06
2P4	0.19 ± 0.01	$0.31 \pm 0.07^{\#}$	NI	$0.33 \pm 0.04^{\#}$	0.27 ± 0.05
2BS4	1.5 ± 0.3	NI	NI	NI	NI

Inhibitor	IC_{50} (μ M)			
	ALDH1L1 (rat)	ALDH3A1	ALDH4A1	ALDH5A1
Daidzin	NI	NI	NI	NI
2CB5	NI	NI	NI	NI
2P3	NI	NI	NI	NI
2P4	NI	NI	NI	NI
2BS4	NI	NI	NI	NI

[#]Compounds had ~60% maximum inhibition NI=No Inhibition

2P4 has a similar IC_{50} value for ALDH2 ($0.19 \pm 0.01 \mu\text{M}$) and ALDH1A3 as 2P3, but only partially inhibits ALDH1B1 and ALDH1A2 and does not inhibit ALDH1A1. 2CB5 has the highest IC_{50} values for the five ALDH1A/2 isoenzymes and only partially inhibited ALDH1A1. The number and length of alkyl substitutions on the aromatic lactone appears to correlate with the potency of inhibition towards the isoenzymes. This correlation is best seen in terms of ALDH1A1 inhibition. 2P3 and 2CB5 have a propyl chain proximal to the lactone carbonyl and inhibit ALDH1A1, whereas 2P4 has a methyl chain in the same position and does not inhibit ALDH1A1. Additionally, 2CB5 lacks the methyl chain proximal to the furan oxygen seen in 2P3 and does not inhibit ALDH1A1 as strongly as 2P3.

D. Characterization of Interaction of Aromatic Lactones with ALDH2

1. Kinetic Characterization of 2P4 in ALDH2 Assays

Covariation experiments were completed with 2P4 to better understand the mechanisms by which this compound inhibits ALDH2. 2P4 was chosen as a representative of the psoralen derivatives as 2P4 showed the most selectivity for inhibition of this enzyme. Due to the low K_m of ALDH2 for propionaldehyde ($<1 \mu\text{M}$), the production of NADH by ALDH2 was measured via fluorescence when varying aldehyde substrate.²²³ A standard curve for the fluorescence of NADH was generated to convert the arbitrary fluorescence units to nanomoles of NADH produced (**Figure 17**). The K_m for propionaldehyde was $49 \pm 9 \text{ nM}$ and the K_m for NAD^+ was $31 \pm 4 \mu\text{M}$ using the fluorescence assay (**Figure 18**). 2P4 was found to non-competitively inhibit (mixed-type) the binding of aldehyde substrate to ALDH2 with a $K_i = 31 \pm 3 \text{ nM}$ (**Figure 19A**). Covariation experiments

varying the amount of NAD^+ were able to be completed using the absorbance assay. 2P4 was found to competitively inhibit the binding of NAD^+ to ALDH2 with a $K_i = 87 \pm 8 \text{ nM}$ (Figure 19B).

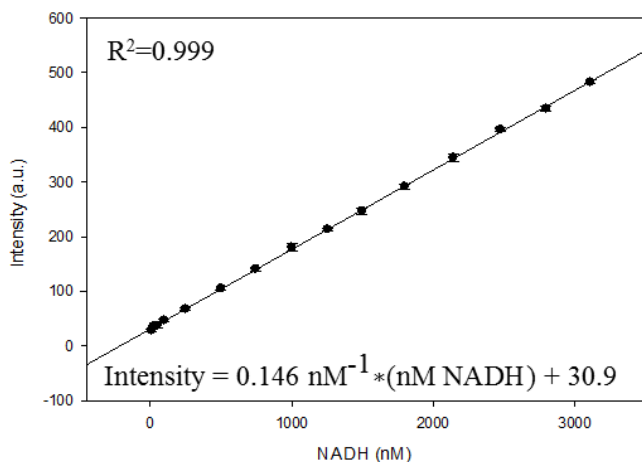


Figure 17 Standard curve for fluorescence of NADH. Each point represents the mean/SEM of two separate experiments of three replicates each ($n=6$).

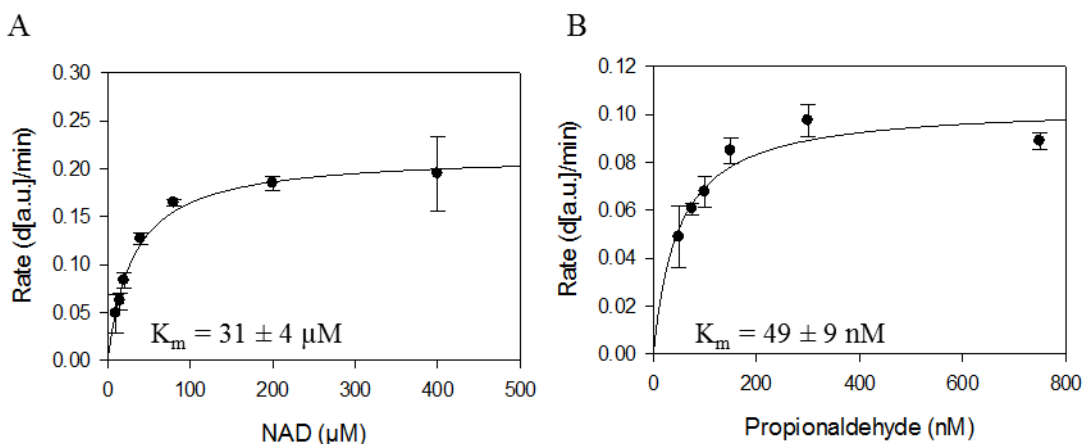


Figure 18 Substrate K_m determination using fluorescence assay. The K_m for (A) NAD and (B) propionaldehyde using fluorescence assay was measured. Each point represents the mean/SEM of one experiment consisting of three replicates ($n=3$).

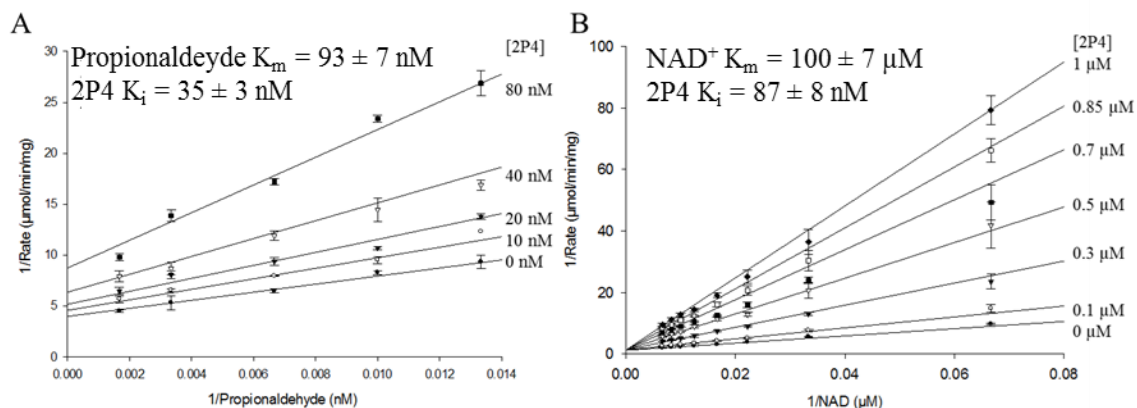


Figure 19 Steady-state kinetic characterization of inhibition of ALDH2 by 2P4. (A) Lineweaver-Burk representation of (mixed-type) non-competitive inhibition of 2P4 versus varied propionaldehyde with ALDH at fixed concentration of NAD^+ (400 μM) measured via fluorescence. Values are the mean/SEM of four independent experiments, each $n=2$. (B) Lineweaver-Burk representation of competitive inhibition of 2P4 versus varied NAD^+ with ALDH2 at fixed concentration of propionaldehyde (1 mM) measured via absorbance. Values are the mean/SEM of three independent experiments, each $n=3$.

2. 2P3-ALDH2 Crystal Structure

We wished to solve the structure of an enzyme-compound complex to understand where the aromatic lactone binds to the enzyme and what residues and interactions lead to selectivity. 2P3 was used for crystallographic studies as it was the most potent for ALDH2 among the compounds. The structure of the 2P3-ALDH2 complex was solved to a resolution of 2.40Å (Table 5).

Table 5 Collection and refinement statistics for the 2P3-ALDH2 complex.

PDB Code	5L13
Collection	
Space Group	P2 ₁ 2 ₁ 2 ₁
Cell Dimensions	
a,b,c (Å)	99,127,295
α,β,γ (deg)	90,90,90
Resolution (Å)	50.0-2.40
Rmerge	0.093 (0.280)*
I/ σ	16.2 (5.0)
Completeness (%)	94.2 (85.7)
Redundancy	5.0 (4.8)
Refinement	
No. of reflections	131537
Rwork/Rfree	0.16/0.21
RMSD	
Bond Length (Å)	0.009
Bond Angle (deg)	1.324

*Values in parentheses are for data in the highest resolution shell (2.44 to 2.40 Å)

2P3 was found to bind in the substrate binding site of ALDH2 (**Figure 20A**). The binding site is formed in part by the side chains of four phenylalanine residues (170, 296, 459, and 465). The side chain of the catalytic Cys302 rotates toward the NAD⁺ binding site to accommodate the binding of 2P3. The propyl chain proximal to the lactone extends into a pocket formed in part by Glu268, Glu476, Trp177, and Thr244, while the alkyl chains on the furan ring are oriented towards the solvent exposed surface. The carbonyl of 2P3 mimics the position of a potential aldehyde substrate engaging the oxyanion hole during aldehyde oxidation and hydrogen bonds with the peptide nitrogen of Cys302 (**Figure 20B**). The hydrophobic interactions and this single hydrogen bond orient the compound in the substrate binding site.

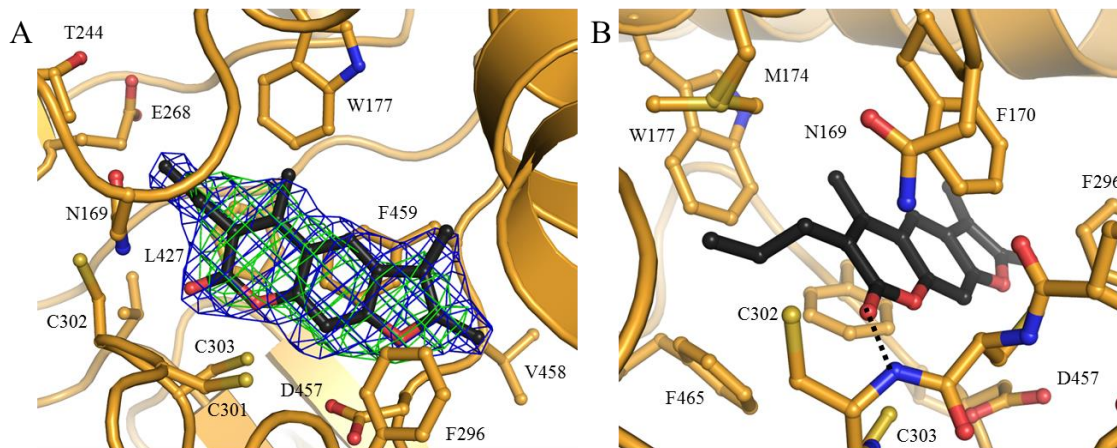


Figure 20 Crystal structure of 2P3-ALDH2 complex

(A) Representative electron density map of 2P3 bound to ALDH2 with the original F_o-F_c map in green contoured at 3.0 standard deviations and the final $2F_o-F_c$ map in blue contoured at 1.0 standard deviation. (B) Alternative viewing angle of 2P3 binding site. A hydrogen bond between lactone carbonyl and peptide nitrogen of Cys302 is shown as black dashed line.

3. Kinetic Characterization of 2BS4

Covariation experiments were also completed with 2BS4 for ALDH2 as 2BS4 had a slightly different aromatic structure, which could possibly change the inhibition profile. 2BS4 was found to competitively inhibit the binding of NAD^+ to ALDH2 with a $K_i = 310 \pm 36$ nM (**Figure 21**). Due to the possibility that the inhibitory actions of 2BS4 are a result of being a competitive esterase substrate, an incubation experiment was performed. ALDH2 was incubated with either 3 μ M or 15 μ M 2BS4, or $\sim 2x$ and $\sim 10x$ the IC_{50} value, for up to 72 hours (**Figure 22**). ALDH2 incubated with 15 μ M 2BS4 did not recover any activity upon dilution for up to 72 hours. ALDH2 incubated with 3 μ M 2BS4 exhibited a slightly different pattern after dilution. The enzyme was not completely inhibited at first, which was consistent with the IC_{50} measurement. After one hour incubation, the 3 μ M

2BS4/ALDH2 mixture was completely inhibited after dilution. However, the 3 μM 2BS4/ALDH2 mixture slowly regained activity starting after one day. This would suggest that 2BS4 is losing the ability to inhibit ALDH2 over time, possibly through hydrolysis of the ester.

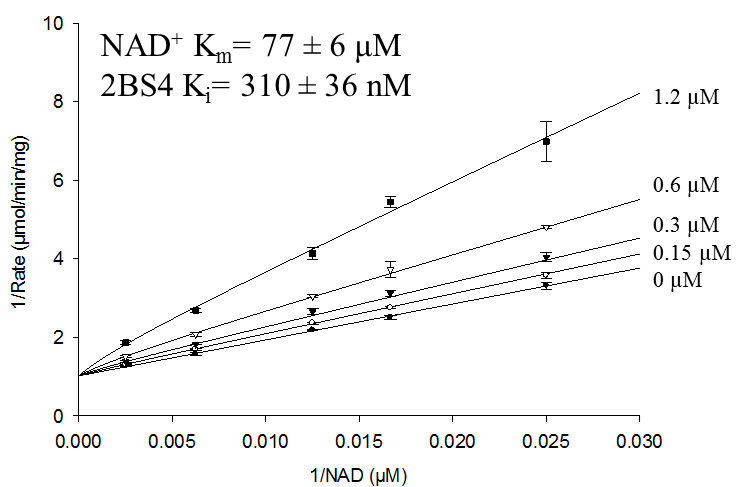


Figure 21 Steady-state kinetic characterization of inhibition of ALDH2 by 2BS4. Lineweaver-Burk representation of competitive inhibition for 2BS4 versus varied NAD^+ with ALDH2 at fixed concentration of propionaldehyde (1 mM). Values are the mean/SEM of four independent experiments ($n=4$).

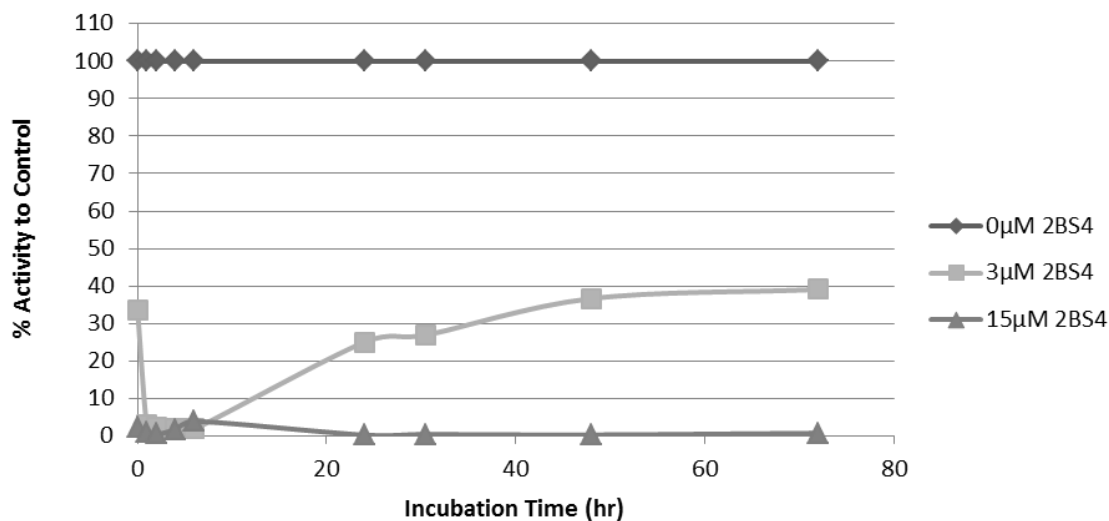


Figure 22 Incubation of ALDH2 with 2BS4. Dehydrogenase activity of ALDH2 after incubation with either 0 μM , 3 μM , or 15 μM 2BS4. Each data point represents the mean of duplicate assays ($n=2$).

The complete inhibition of ALDH2 by 2BS4 after dilution could be consistent with a covalent mechanism of inhibition. For this reason, IC_{50} curves for 2BS4 with ALDH2 were measured using different incubation times (**Figure 23**). No time dependence was seen for the inhibition phase. 2BS4 exhibited approximately the same IC_{50} value after zero, two, or ten minutes of pre-incubation of compound and enzyme.

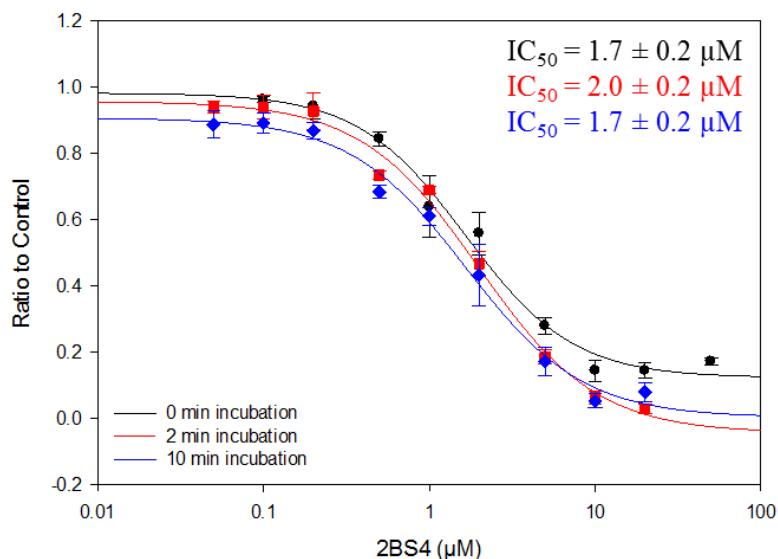


Figure 23 IC_{50} values for BUC22 with ALDH2 after different incubation periods. IC_{50} curves for the inhibition of ALDH2 by 2BS4 after various incubation times (0, 2, and 10 minutes). Values represent the mean/SEM of three individual measurements ($n=3$).

E. Characterization of Additional Psoralen and Coumarin Analogs

1. Single Concentration Selectivity for Structure-Activity Relationships

Psoralen- and coumarin-derived analogs were purchased and characterized to develop structure activity relationships for this compound class to improve upon the selective selectivity of the psoralen analogs for ALDH2. Because 2BS4 selectively inhibited ALDH2 before subsequent hydrolysis, it was hypothesized that similar compounds without the ester group could reversibly inhibit ALDH2 while maintaining selectivity. A total of 35 compounds were ordered from ChemBridge Company (San Diego, CA) and ChemDiv Company (San Diego, CA) as a representative sample of available compounds using the binding location of 2P3 to ALDH2 as a guide. Twelve compounds share the psoralen sub-structure of 2P3, 2P4, and 2CB5 (Scaffold I) and twenty-three compounds share the coumarin sub-structure of 2BS4 (Scaffold II) (**Figure 24**).

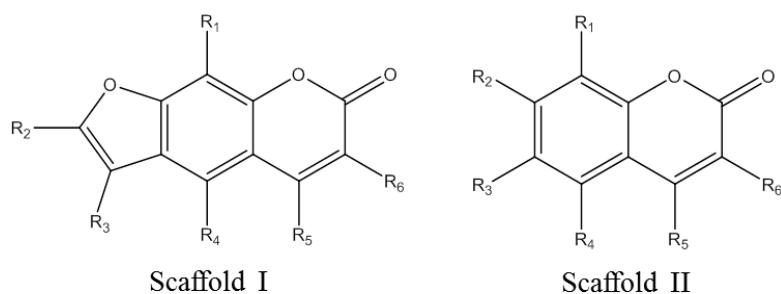


Figure 24 Compound scaffolds of psoralen- and coumarin-derived analogs. Depiction of scaffolds for psoralen- (Scaffold I) and coumarin-derived (Scaffold II) analogs with locations for potential substituents labeled R₁ – R₆.

The effect of 10 μ M compound on the activity of ALDH1A1, ALDH2, and ALDH3A1 was measured as an initial estimate for selectivity amongst ALDHs (**Tables 6 & 7**). Scaffold I consists of compounds BUC1-12 in addition to 2P3, 2P4, and 2CB5. Some analogs had additional alkyl chains added to Scaffold I. The addition of a t-butyl group at R₃ (BUC1) lowered the inhibition towards ALDH2. The addition of a methyl group to R₁ (BUC2) nearly eliminated inhibition towards ALDH2. Lengthening the alkyl chain at R₅ to three carbons (BUC3) maintained inhibition towards ALDH2. Other analogs increased the size of the ring structure of Scaffold I. The addition of a cyclohexane to the furan ring (BUC4) weakened inhibition towards ALDH2. The addition of a benzyl (BUC5), cyclohexyl (BUC6), or cyclopentyl (BUC7) ring proximal to the lactone carbonyl maintained inhibition towards ALDH2 while showing some selectivity towards ALDH1A1 and ALDH2. The addition of a benzyl group at either R₅ (BUC10) or R₆ (BUC8) led to moderate inhibition of ALDH1A1 with little to no inhibition of ALDH2. BUC11 and BUC12 have either a 1-(piperidin-1-yl)propan-1-one (BUC11) or N-benzylpropionamide (BUC12) group at R₆. The 1-(piperidin-1-yl)propan-1-one linker is tolerated as BUC11 inhibits both ALDH1A1 and ALDH2 >90% at 10 μ M. BUC12 was the only compound within Scaffold I which showed inhibition towards ALDH3A1.

Table 6 Structure activity relationships for psoralen derivatives.

Percent activity compared to control was measured at 10 μ M compound with ALDH1A1, ALDH2, and ALDH3A1. Compounds picked for further study highlighted in gray. Mean value from at least three trials ($n \geq 3$).

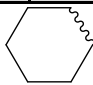

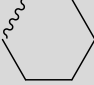

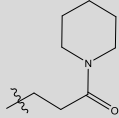
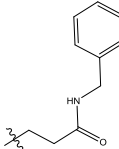
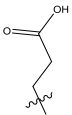
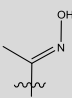
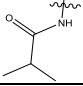
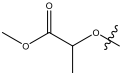
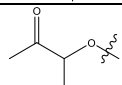
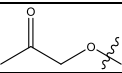
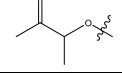
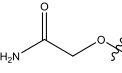
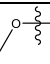
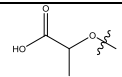
Cmpd	Scaffold I Position						LogP	% Activity		
	R1	R2	R3	R4	R5	R6		ALDH 1A1	ALDH 2	ALDH 3A1
2CB5	H	H	Me	H	Me	propyl	4.47	48.6	6.25	96.1
2P3	H	Me	Me	H	Me	propyl	4.92	36.3	1.61	86.3
2P4	H	Me	Me	H	Me	Me	4.39	90.5	19.5	95.3
BUC1	H	H	<i>t</i> -Bu	H	Me	Me	3.94	94.5	69.7	87.0
BUC2	Me	Me	Me	H	Me	Me	4.36	78.4	87.2	102
BUC3	H	Me	Me	H	propyl	H	4.47	74.1	23.8	80.4
BUC4	H			H	Me	Me	4.48	64.3	61.3	96.1
BUC5	H	Me	Me	H			3.89	82.4	42.2	93.4
BUC6	H	Me	Me	H			4.27	56.3	16.3	94.1
BUC7	H	Me	Me	H			4.26	50.8	8.25	87.1
BUC8	H	H	Me	H	Me	benzyl	4.98	58.5	83.6	90.3
BUC9	H	H	phenyl	H	Me	Me	4.80	87.4	92.8	88.9
BUC10	H	Me	Me	H	benzyl	H	4.80	57.0	73.7	81.6
BUC11	H	Me	Me	H	Me		4.06	8.69	3.80	105
BUC12	H	Me	Me	H	Me		4.52	93.6	69.8	68.3

Table 7 Structure activity relationships for coumarin derivatives. Percent activity compared to control was measured at 10 μ M compound with ALDH1A1, ALDH2, and ALDH3A1. Compounds picked for further study highlighted in gray. Mean value from at least three trials ($n \geq 3$).

Cmpd	Scaffold II Position						LogP	% Activity		
	R1	R2	R3	R4	R5	R6		ALDH 1A1	ALDH 2	ALDH 3A1
BUC13	H	Me			Me	Me	3.92	71.5	46.4	98.1
BUC14			H	H	H	H	1.77	61.0	95.2	28.3
BUC15	Me			H	Me	Me	2.10	67.4	80.2	79.2
BUC16	H			H	Me	H	2.11	65.2	25.5	53.6
BUC17	H		H	H	Me	H	3.01	35.5	94.6	9.46
BUC18	H		H	H	Me	H	3.94	37.3	93.3	23.7
BUC19	H		H	H	Me	H	3.19	29.0	97.8	67.1
BUC20	H		H	H	Me	H	1.22	35.7	41.3	20.4
BUC21	H		H	H	Me	H	2.85	49.6	95.0	95.5
BUC22	H		H	H	Me	H	3.63	14.3	71.7	109
BUC23	H		H	H	Me	H	3.92	8.80	101	41.5
BUC24	H		H	H			2.64	58.7	64.4	103
BUC25	H		H	H	Me	benzyl	3.44	24.6	99.7	86.9

Table 7, continued Structure activity relationships for coumarin derivatives. Percent activity compared to control was measured at 10 μ M compound with ALDH1A1, ALDH2, and ALDH3A1. Compounds picked for further study highlighted in gray. Mean value from at least three trials ($n \geq 3$).

Cmpd	Scaffold II Position						LogP	% Activity		
	R1	R2	R3	R4	R5	R6		ALDH 1A1	ALDH 2	ALDH 3A1
BUC26	H	OH	H	H	Me		1.82	96.6	101	105
BUC27	H	H	Br	H	H		2.10	96.0	48.2	91.7
BUC28	H	Me		H	Me	H	2.05	59.8	96.3	105
2BS4	H		H	H	Me	H	1.90	84.8	5.72	94.5
2BS4A	H		H	H	Me	H	1.90	68.7	94.4	101
2BS4B	H		H	H	Me	H	1.72	52.2	99.1	64.1
2BS4C	H		H	H	Me	H	1.37	91.4	93.3	106
2BS4D	H		H	H	Me	H	1.71	28.5	89.5	67.1
2P14	H		H	H	Me	H	2.46	80.2	94.8	36.4
2P15	H		H	H	Me	H	1.63	97.5	99.3	93.9

Scaffold II compounds are variations of 2BS4, but all lack the ester group of 2BS4. Three different methyl ketones (2BS4A-C) similar to 2BS4 did not inhibit ALDH2. 2BS4A and 2BS4B also inhibited ALDH1A1 and/or ALDH3A1 while 2BS4C did not inhibit any of the three isoenzymes. An amide (2BS4D) similar to 2BS4 only inhibited ALDH1A1 activity. Shorting the side chain of 2BS4 to the methyl ether (2P14) led to inhibition of ALDH3A1; while the free acid form of 2BS4 (2P15) did not inhibit any of the three isoenzymes.

More diverse additions to Scaffold II were also examined (BUC13-28). The addition of oxygen-containing rings had varied results. A 3-methylfuran ring at R₃ and R₄ (BUC13) led to partial inhibition of ALDH2 while addition of a furan ring at R₁ and R₂ (BUC14) led to strong inhibition of ALDH3A1 with no inhibition of ALDH2. The addition of 4H-pyran-4-one at R₂ and R₃ (BUC15) led to slight inhibition of ALDH1A1. The addition of δ -valerolactone at R₂ and R₃ (BUC16) led to inhibition of ALDH2 with lesser inhibition of ALDH1A1 and ALDH3A1. Compounds BUC17-BUC23 changed the methyl 2-methoxypropanoate group at R₂ in 2BS4 to more diverse structural groups. BUC17 and BUC18 contain unsaturated alkyl chains at R₂ and inhibit ALDH1A1 and ALDH3A1. BUC19 has a 2-oxo-2-phenylethoxy group and inhibits ALDH1A1 with moderate inhibition of ALDH3A1. BUC20 has a terminal nitrile and inhibits ALDH1A1, ALDH2, and ALDH3A1 at similar levels. BUC21 and BUC22 both appear to selectively inhibit ALDH1A1, though BUC21 only inhibits 50% at 10 μ M mostly due to the large N-phenylacetamide group at R₂. BUC22 contains a diethylamine in the same position and inhibits ALDH1A1 ~85% at 10 μ M. BUC23, which substituted a 1,4-

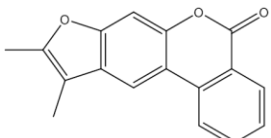
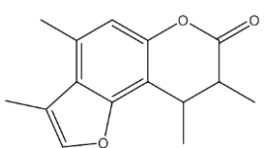
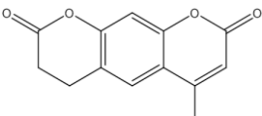
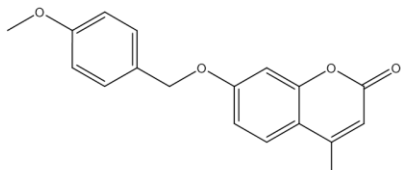
bis(methoxymethyl)benzene at R₂, strongly inhibited ALDH1A1 with partial inhibition towards ALDH3A1. Compounds BUC24-28 have changes at multiple positions compared to 2BS4. BUC24 has a (3-oxobutan-2-yl)oxy group at R₂ and benzyl ring attached at R₅ and R₆ which led to moderate inhibition of ALDH1A1 and ALDH2. BUC26 has a hydroxyl group at R₂ and propionic acid group at R₆ and did not inhibit any of the three isoenzymes. The other three compounds showed some level of selectivity for either ALDH1A1 or ALDH2. BUC25, which added a methane sulfonyl group at R₂ and a benzyl group at R₆, and BUC28, which added isobutyramide at R₃, selectively inhibited ALDH1A1 and BUC27, which has only hydrogen at R₂ and added a bromine at R₃ and ketoxime at R₆, selectively inhibited ALDH2. Of the 35 additional analogs tested, seven showed potential selectivity for ALDH2 based off activity at 10 μM compound (BUC3, BUC5-BUC7, BUC13, BUC16, and BUC27). Three compounds showed potential selectivity towards ALDH1A1 (BUC22, BUC23, and BUC25). These ten compounds and BUC11, which inhibited both ALDH1A1 and ALDH2 >90% at 10 μM compound, were selected for further analysis.

Due to the hydrophobic nature of the substrate binding site within the free enzyme species of ALDH2, the logP values for the 35 analogs in addition to the initial four hits were examined (**Table 4**). No direct correlation between logP values and inhibition of ALDH2 could be developed. For example, BUC3 and BUC16 both inhibit ALDH2 with the same potency at 10 μM compound and have vastly different logP values. Although BUC3 has a logP value of 4.47 and BUC16 has a logP value of 2.11, both compounds inhibit ALDH2 ~75% at 10 μM compound.

2. EC₅₀ Determination

EC₅₀ values were measured in regards to ALDH1A1, ALDH2, and ALDH3A1 for the eleven selected compounds as a better measure of selectivity and potency. Four compounds did not show selectivity or full inhibition for ALDH1A1 or ALDH2 (**Table 8**). We sought complete inhibitors of the isoenzymes, so BUC5 and BUC13 were not examined further as they only partially inhibited ALDH2. BUC16 and BUC23 had sub-micromolar IC₅₀'s for ALDH2 and ALDH1A1 respectively; however, both partially inhibited ALDH3A1. As these compounds were no longer selective for the ALDH1/2 family, these compounds were also not examined further.

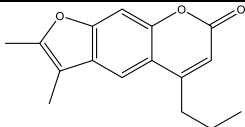
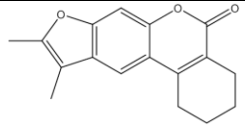
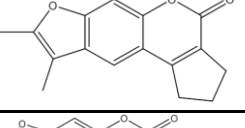
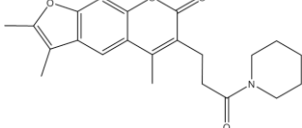
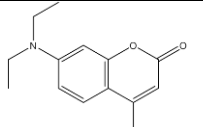
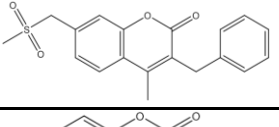
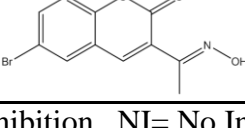
Table 8 IC₅₀ values for four analogs with ALDH1A1, ALDH2, and ALDH3A1. Values are the mean/SEM of three independent experiments (n=3).

Compound	Structure	IC ₅₀ (μM)		
		ALDH1A1	ALDH2	ALDH3A1
BUC5		NI	0.15 ± 0.01 [#]	NI
BUC13		NI	0.15 ± 0.01 [#]	NI
BUC16		NI	0.47 ± 0.02	5.4 ± 1.0 [#]
BUC23		0.17 ± 0.01	NI	0.50 ± 0.05 [#]

[#]50-60% max inhibition NI= No inhibition

The other seven compounds did not inhibit ALDH3A1 and fully inhibited ALDH1A1 and/or ALDH2. EC₅₀ values for ALDH1B1, ALDH1A2, and ALDH1A3 were also measured in addition to those for ALDH1A1, ALDH2, and ALDH3A1 for these seven compounds (**Table 9**). Compounds BUC3, BUC6, and BUC7 inhibit the majority of the ALDH1/2 family with sub-micromolar IC₅₀ values but exhibit little selectivity within the family. Each one of the three compounds fully inhibits ALDH2, ALDH1B1, and ALDH1A2 and does not inhibit ALDH3A1. The three compounds have differing effects towards ALDH1A1 and ALDH1A3. BUC3 does not inhibit ALDH1A1 and activates ALDH1A3 ~2-fold with an AC₅₀ value of $0.87 \pm 0.09 \mu\text{M}$. BUC6 partially inhibits ALDH1A1 and does not inhibit ALDH1A3. BUC7 partially inhibits both ALDH1A1 and ALDH1A3. BUC11 also does not show selectivity within the ALDH1/2 family, though it does show ~10-fold preference towards inhibiting ALDH1A1 (IC₅₀ = $0.13 \pm 0.01 \mu\text{M}$) versus the other four ALDH1/2 isoenzymes. BUC22 was found to selectively inhibit ALDH1A1 (IC₅₀ = $0.76 \pm 0.07 \mu\text{M}$) with only minor effects on ALDH1A2. BUC25 showed a preference towards ALDH1A1 (IC₅₀ = $2.8 \pm 0.1 \mu\text{M}$) while not inhibiting ALDH2. BUC27 selectively inhibited ALDH2 (IC₅₀ = $4.6 \pm 0.5 \mu\text{M}$) while also exhibiting two-fold activation of ALDH1A3 (AC₅₀ = $35 \pm 3 \mu\text{M}$).

Table 9 EC₅₀ values for seven analogs with the ALDH1/2 family and ALDH3A1. The coumarin derivatives are more potent, while the psoralen derivatives are more selective. AC₅₀ curves had a maximum activity of ~200% control. Values are the mean/SEM of three independent experiments (n=3).

Compound	Structure	IC ₅₀ (μM)					
		ALDH 2	ALDH 1B1	ALDH 1A1	ALDH 1A2	ALDH 1A3	ALDH 3A1
BUC3		0.36 ± 0.03	0.086 ± 0.002	NI	0.069 ± 0.009	AC ₅₀ 0.87 ± 0.09	NI
BUC6		0.067 ± 0.006	0.095 ± 0.015	0.13 ± 0.01 [#]	0.065 ± 0.004	NI	NI
BUC7		0.067 ± 0.003	0.16 ± 0.01	0.17 ± 0.02 [#]	0.13 ± 0.01	0.17 ± 0.02 [#]	NI
BUC11		2.0 ± 0.2	2.6 ± 0.3	0.13 ± 0.01	1.6 ± 0.1	14 ± 1	NI
BUC22		NI	NI	0.76 ± 0.07	>10	NI	NI
BUC25		NI	13 ± 1	2.8 ± 0.1	11 ± 1	10 ± 1	NI
BUC27		4.6 ± 0.6	NI	NI	NI	AC ₅₀ 35 ± 3	NI

[#]50-60% max inhibition NI= No Inhibition

3. Characterization of BUC11's Interaction with ALDH1A1 and ALDH2

The interaction of BUC11 with ALDH1A1 and ALDH2 was investigated further through the use of X-ray crystallography and kinetic studies. The structure of BUC11 bound to ALDH1A1 in the absence of coenzyme was solved to a resolution of 1.70Å (**Table 10**).

Table 10 Collection and refinement statistics for the BUC11-ALDH1A1 complex.

PDB Code	5L2M
Collection	
Space Group	P422
Cell Dimensions	
a,b,c (Å)	109,109,83
α,β,γ (deg)	90,90,90
Resolution (Å)	50.0-1.70
Rmerge	0.119 (0.526)*
I/ σ	17.2 (5.5)
Completeness (%)	98.4 (97.6)
Redundancy	12.6 (12.2)
Refinement	
No. of reflections	52110
Rwork/Rfree	0.23/0.26
RMSD	
Bond Length (Å)	0.011
Bond Angle (deg)	1.500

* Values in parentheses are for data in the highest resolution shell (1.73 to 1.70Å)

BUC11 was found to bind within the substrate binding site of ALDH1A1 (**Figure 25A**) with the psoralen backbone oriented between Tyr297, Gly458, His293, and Phe290. The piperidine ring of BUC11 is oriented towards the catalytic cysteine rather than the carbonyl of the lactone as seen with 2P3 bound to ALDH2. The piperidine ring in this position does not approach the NAD(H) binding site (**Figure 25B**). Covariation experiments were used to evaluate if the change in binding site changed the enzymatic mechanism of inhibition. BUC11 was found to exhibit uncompetitive inhibition ($K_i = 170 \pm 13$ nM) versus varied NAD⁺ for ALDH1A1 (**Figure 26A**). However, BUC11 was found to exhibit competitive inhibition ($K_i = 1.1 \pm 0.1$ μ M) versus varied NAD⁺ for ALDH2 (**Figure 26B**).

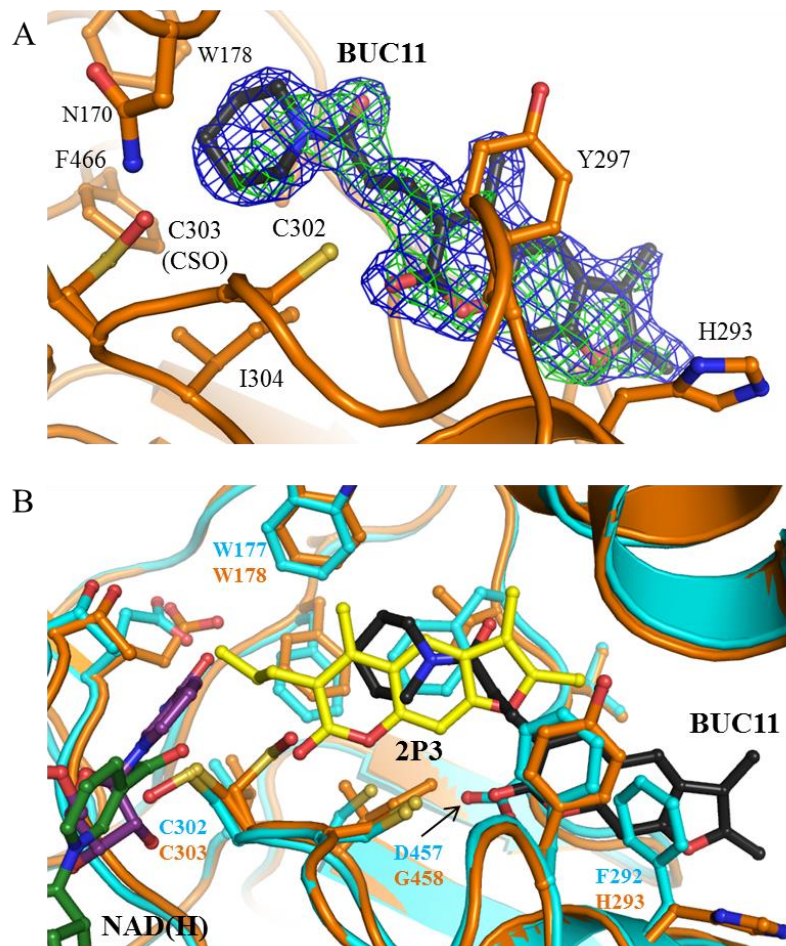


Figure 25 Crystal structure of BUC11-ALDH1A1 complex. (A) Electron density map of BUC11 bound to ALDH2 with the original F_o-F_c map in green contoured at 2.5 standard deviations and the final $2F_o-F_c$ map in blue contoured at 1.0 standard deviation. (B) Comparison of binding modes of BUC11 (black) bound to ALDH1A1 (orange) and 2P3 (yellow), NADH (green), and NAD⁺ (purple) bound to ALDH2. NAD⁺/NADH binding positions obtained from PDB1O02 and 1O04.

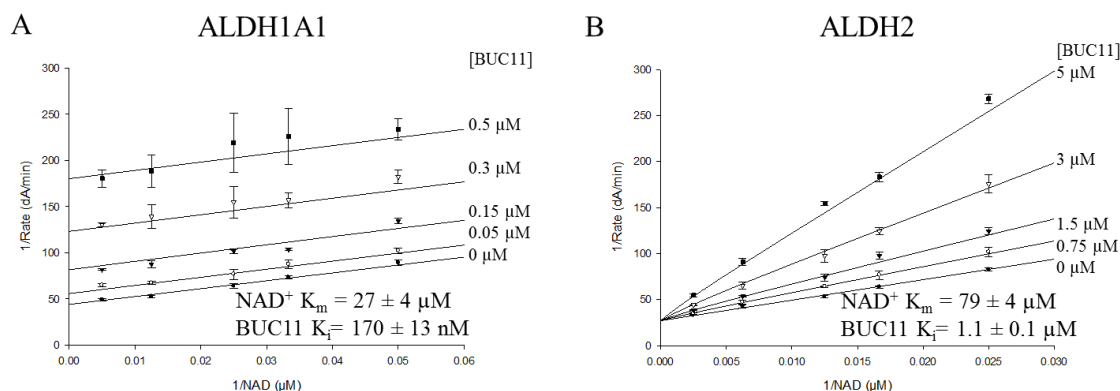


Figure 26 Steady state kinetic characterization of BUC11 with ALDH enzymes. (A) Lineweaver-Burk representation of uncompetitive inhibition for BUC11 versus varied NAD^+ with ALDH1A1 at fixed concentration of propionaldehyde (1 mM). (B) Lineweaver-Burk representation of competitive inhibition for BUC11 versus varied NAD^+ with ALDH2 at fixed concentration of propionaldehyde (1 mM). Values are mean/SEM of three independent experiments ($n=3$).

4. Characterization of BUC25's Interaction with ALDH1A1

The interaction of BUC25 with ALDH1A1 was investigated further by solving the crystal structure of BUC25 bound to ALDH1A1 to a resolution of 1.70 Å (**Table 10**). BUC25 binds in the substrate binding site (**Figure 27A**) and the lactone carbonyl is oriented towards the catalytic cysteine though not as close as 2P3 bound to ALDH2 (**Figure 27B**). The additional benzyl group would appear to prevent the compound from approaching the catalytic cysteine. Although the electron density for the benzyl group of BUC25 was not as strong as the remainder of the compound, its position and movement of Trp178 was reminiscent of the interaction between CM037 and ALDH1A1 in the same region which has similar weak density near Trp178.²¹⁶

Table 11 Collection and refinement statistics for the BUC25-ALDH1A1 complex.

PDB Code	5L2N
Collection	
Space Group	P422
Cell Dimensions	
a,b,c (Å)	109,109,83
α,β,γ (deg)	90,90,90
Resolution (Å)	50.0-1.70
Rmerge	0.094 (0.639)*
I/ σ	16.9 (3.3)
Completeness (%)	100 (100)
Redundancy	8.4 (8.2)
Refinement	
No. of reflections	52587
Rwork/Rfree	0.23/0.26
RMSD	
Bond Length (Å)	0.012
Bond Angle (deg)	1.538

*Values in parentheses are for data in the highest resolution shell (1.73 to 1.70Å)

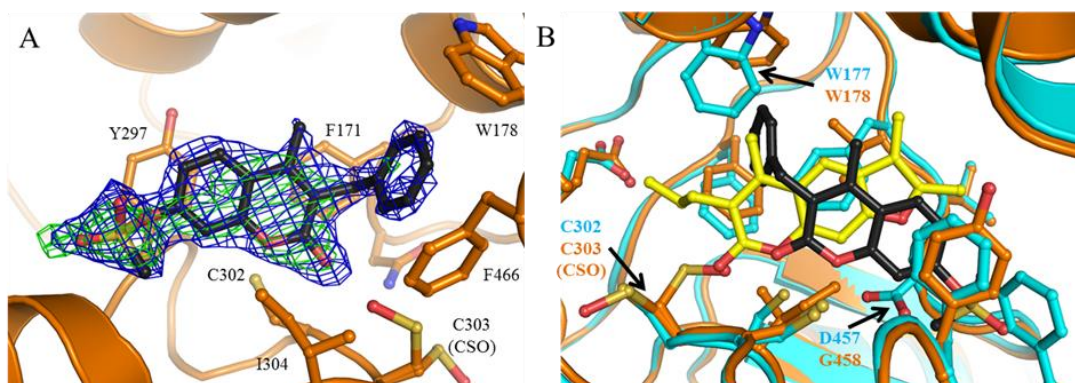


Figure 27 Crystal structure of BUC25-ALDH1A1 complex.

(A) Electron density map of BUC25 bound to ALDH1A1 with the original F_0-F_c map in green contoured at 2.5 standard deviations and the final $2F_o-F_c$ map in blue contoured at 1.0 standard deviation. (B) Overlay of BUC25 (black) bound to ALDH1A1 (orange) and 2P3 (yellow) bound to ALDH2 (cyan).

5. Characterization of BUC22's Interaction with ALDH1A1

The interaction of BUC22 with ALDH1A1 was examined by X-ray crystallographic and enzyme kinetic studies. The structure of the BUC22-ALDH1A1 complex was solved to a resolution of 2.05Å in the P1 space group (**Table 12**).

Table 12 Collection and refinement statistics for the BUC22-ALDH1A1 complex.

PDB Code	5L2O
Collection	
Space Group	P1
Cell Dimensions	
a,b,c (Å)	91,98,127
α,β,γ (deg)	81,86,64
Resolution (Å)	50.0-2.05
Rmerge	0.069 (0.280)*
I/ σ	10.7 (2.7)
Completeness (%)	90.8 (91.7)
Redundancy	2.1 (2.1)
Refinement	
No. of reflections	211433
Rwork/Rfree	0.17/0.20
RMSD	
Bond Length (Å)	0.011
Bond Angle (deg)	1.397

*Values in parentheses are for data in the highest resolution shell (2.09 to 2.05Å)

This space group was different than those of the BUC11-ALDH1A1 and BUC25-ALDH1A1 complexes and consisted of two tetramers in the asymmetric unit as opposed to a single monomer. BUC22 binds in the coenzyme binding site of ALDH1A1 (**Figure 28A**) near Pro227 and Val250 similar to the adenine of NAD⁺. The aromatic ring structure of BUC22 is rotated slightly from that of adenine in this position (**Figure 28B**). The binding site of BUC22 is removed from that of 2P3 in ALDH2 and BUC11 and BUC25 in ALDH1A1. Covariation experiments were completed to further characterize

BUC22's interaction with ALDH1A1. BUC22 was found to exhibit non-competitive inhibition versus varied NAD^+ for ALDH1A1 (**Figure 29A**) with $K_i = 1.2 \pm 0.1 \mu\text{M}$. This mode of inhibition is different from that of 2P3 in ALDH2 and BUC11 and BUC25 in ALDH1A1. A compound similar to BUC22 was used to further support the kinetic data of BUC22. BUC20 replaces the diethylamine of BUC22 with a terminal cyano group and inhibits both ALDH1A1 and ALDH2. BUC20 was found to exhibit noncompetitive inhibition versus varied NAD^+ for ALDH1A1 (**Figure 29B**) and noncompetitive (mixed-type) inhibition versus varied NAD^+ for ALDH2 (**Figure 29C**).

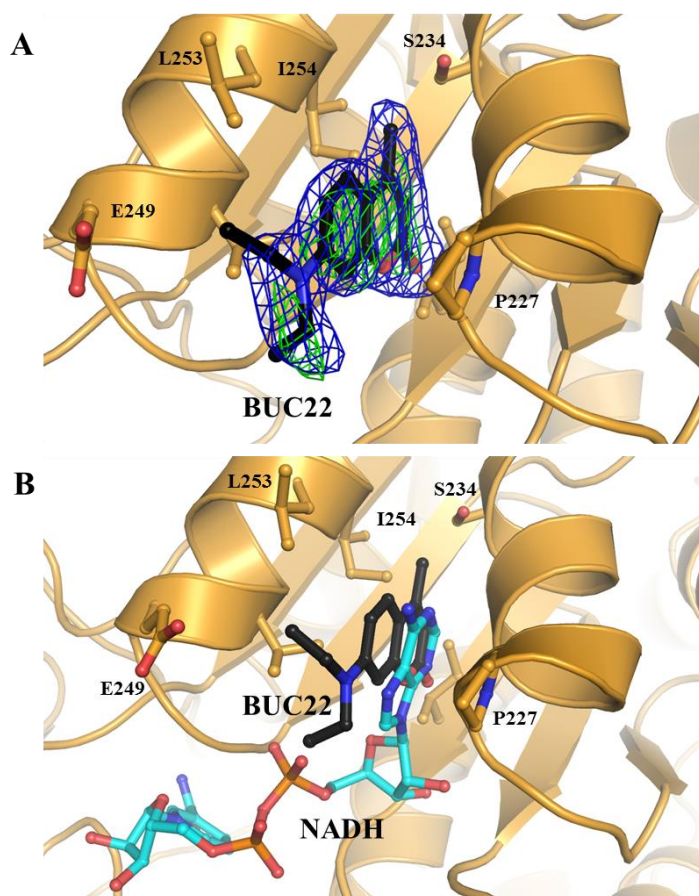


Figure 28 Crystal structure of BUC22-ALDH1A1 complex.

(A) Representative electron density map of BUC22 bound to ALDH1A1 with the original $F_o - F_c$ map in green contoured at 2.5 standard deviations and the original $2F_o - F_c$ map in blue contoured at 1.0 standard deviation. (B) Overlay of BUC22 and NADH (PDB 4WB9) bound to ALDH1A1.

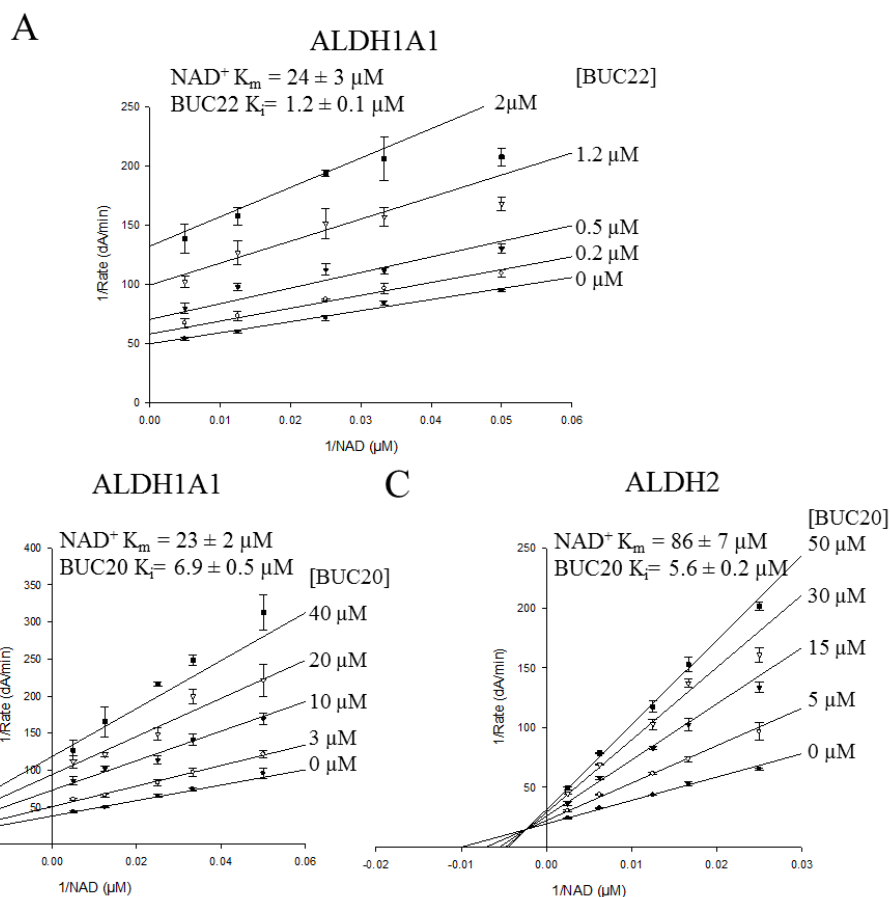


Figure 29 Steady-state kinetic characterization of inhibition by BUC22 and BUC20. (A) Lineweaver-Burk representation of noncompetitive inhibition for BUC22 versus varied NAD^+ with ALDH1A1. (B) Lineweaver- Burk representation of noncompetitive inhibition for BUC20 versus varied NAD^+ with ALDH1A1. (C) Lineweaver-Burk representation of noncompetitive inhibition (mixed-type) inhibition for BUC20 with varied NAD^+ with ALDH2. All experiments completed at fixed concentration of propionaldehyde (1 mM). Values are the mean/SEM of three independent experiments (n=3).

6. Characterization of BUC27's Interaction with ALDH2

BUC27 was the lone ALDH2-selective compound that was not an ester discovered in this study. Covariation experiments were performed to determine how BUC27 inhibits ALDH2. BUC27 was found to competitively inhibit the binding of NAD^+ to ALDH2 with a $K_i = 2.4 \pm 0.1 \mu\text{M}$ (Figure 30).

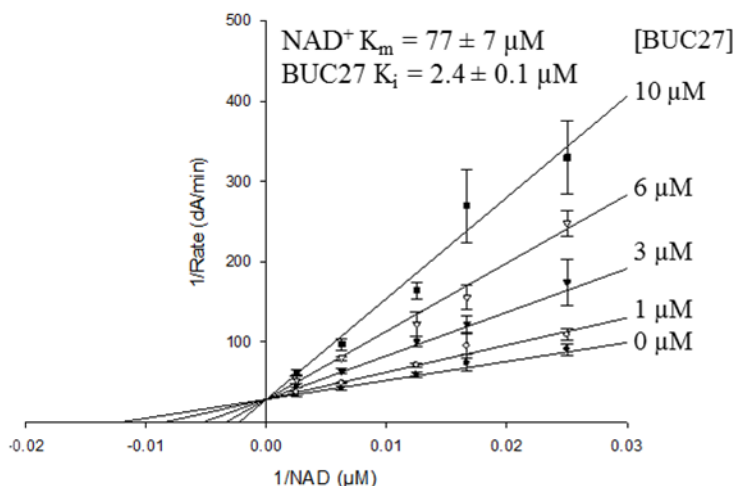


Figure 30 Steady-state kinetic characterization of inhibition of ALDH2 by BUC27. Lineweaver-Burk representation of competitive inhibition for BUC27 versus varied NAD^+ with ALDH2 at fixed concentration of propionaldehyde (1 mM). Values are the mean/SEM of three independent experiments ($n=3$).

F. Effect of BUC22 on Viability of Breast Cancer Cells in 3D Culture

The cellular effects of BUC22 were examined by treating MDA-MB-468 cells over the course of five days. Results were compared to the effect of 30 μM CM39, which had previously been shown to inhibit the proliferation of MDA-MB-468 cells by Brandon Lane (IUSM) and has been used in collaborative studies with the University of Michigan in A2780DK ovarian cancer cells to achieve similar results. High concentrations of BUC22 decreased cell proliferation as measured by the MTT assay. Treatment of 100 μM BUC22 over a period of five days led to a ~2-fold decrease in mitochondrial function (**Figure 31**). This was close to the same effect that 30 μM CM39 had on the same cell line.

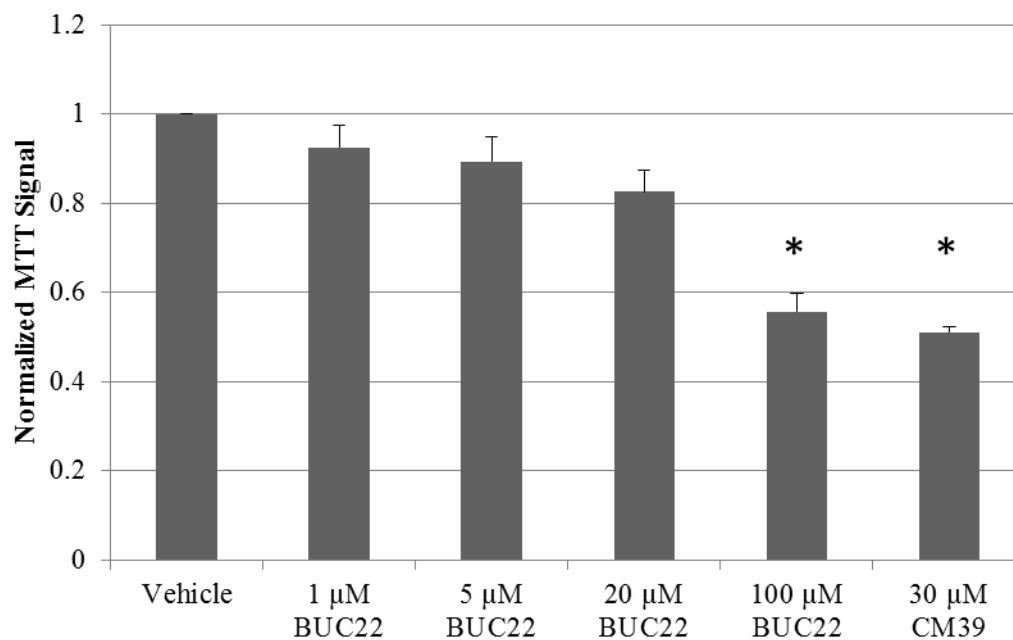


Figure 31 Effect of BUC22 treatment on proliferation of breast cancer cells
 MTT assay was performed on MDA-MB-468 cells after treatment with BUC22 for five days. CM39 was included as a positive control for inhibition. Values are the mean/SEM of three independent experiments relative to vehicle control, each n=3. *p<0.01 versus vehicle

IV. Discussion

The ALDH1/2 family plays a major role in many physiological processes and pathologies. Five members of the family share approximately 70% protein sequence identity and demonstrate significant overlap in their substrate specificity. Consequently, selective inhibitors of these enzymes would help better delineate their individual function. Although the cofactor binding site is highly conserved amongst ALDH isoenzymes, there are distinct differences within the substrate binding sites that support the discovery of compounds which could selectively target individual isoenzymes. For example, the substrate binding site of ALDH2 is the narrowest and most hydrophobic. Although inhibition of ALDH2 has been utilized as an approach for the treatment of alcohol abuse for over 60 years, selective inhibitors of ALDH2 remain elusive.²¹⁹ Based on prior success in finding selective modulators for ALDH1A1 and ALDH3A1 by high-throughput screening, we performed a high-throughput screen to identify potential inhibitors and activators of ALDH2.^{214, 220}

Our high-throughput screen encompassed over 110,000 compounds. The primary screens identified 1931 compounds that met our selection criteria; of these, 67 compounds (<5%) rose to the same selection criteria during retest of the hits. HTS are inherently noisy and produce many false positives. For example, outliers were found in the Z' -factor determination (**Figures 10 & 11**) from identical reactions run simultaneously on the same plate. False positives can occur due to spectral interference from compounds, robot pipetting errors, debris or bubbles in the well, misalignment of the plate during plate reading, or inaccuracies in compound concentration. For instance, during Screen 2 the

robot failed to pipet substrate to a subset of wells on several plates; these compounds were included in the secondary screen for evaluation to ensure complete library coverage. The secondary screen was designed to remove false positives from further consideration, saving time and resources.

The effect of 59 of the 67 compounds identified via the esterase HTS on the dehydrogenase activity of ALDH1A1, ALDH2, and ALDH3A1 was examined as an initial determination of selectivity. Only 9 of the 59 compounds modulated the dehydrogenase activity of ALDH2 by more than 20% at 10 μ M concentration, the same concentration tested in the HTS. Switching to the dehydrogenase assay eliminates more false positives as the assay is not dependent on the same readout. Additionally, compound concentration in the HTS is determined by the average mass of the compounds in the entire library. After purchase of compounds, the concentrations tested in the dehydrogenase assay are most likely not identical. This may eliminate compounds which were near the selection threshold, but whose concentration was underestimated with the assumptions made in the HTS.

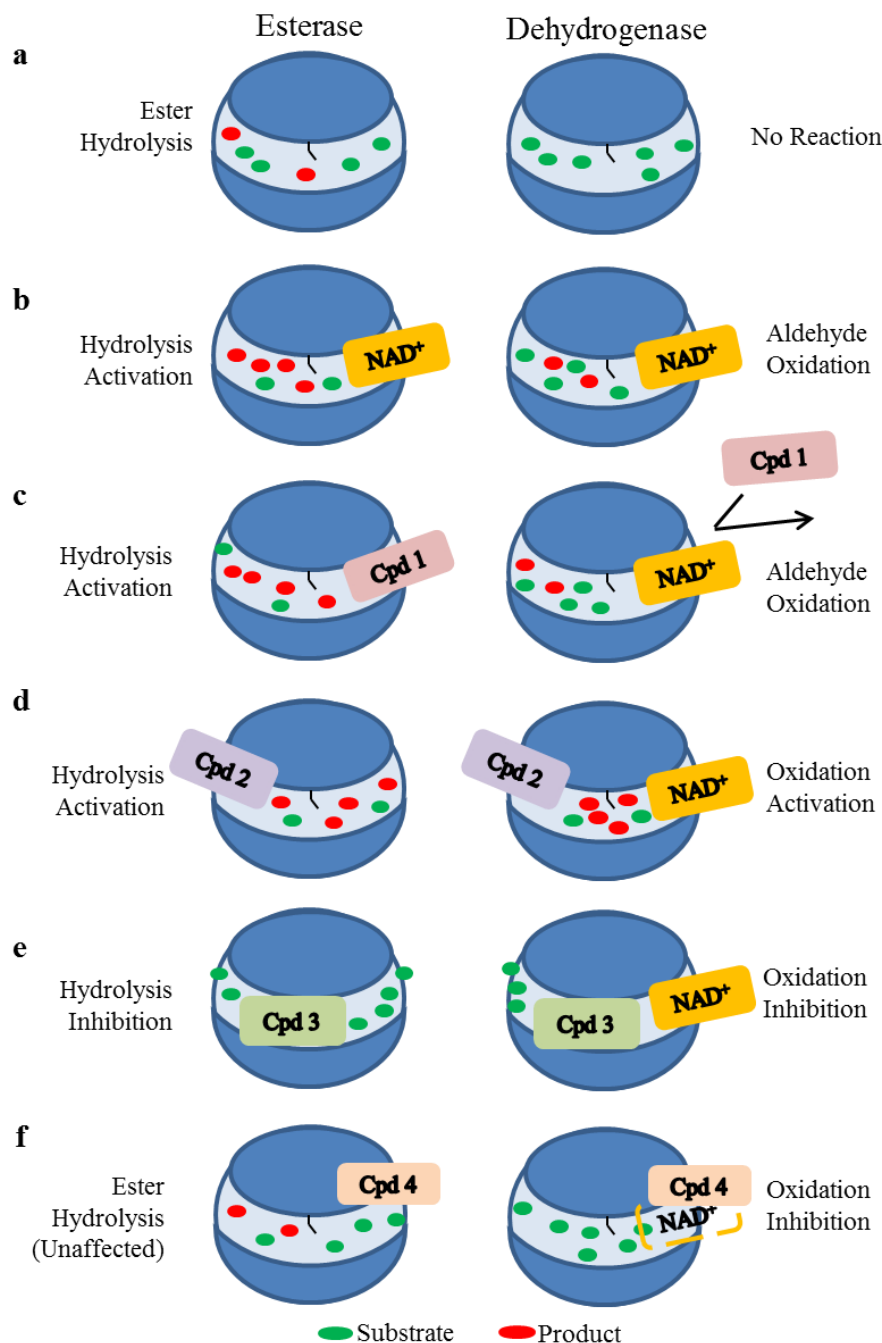


Figure 32 Effect of different compounds on esterase and dehydrogenase assays. In the absence of NAD⁺ (a), only ester hydrolysis will occur. NAD⁺ (b) or compounds 1(c) or 2 (d), which block one end of the tunnel, will activate esterase activity. Compound 1 will not inhibit dehydrogenase activity unless it can outcompete NAD⁺. Compound 2 could also activate oxidation provided the substrate can fit between the compound and the catalytic cysteine. Compound 3 (e), which blocks access to the catalytic cysteine, would inhibit both reactions. Compound 4 (f) would prevent NAD⁺ binding and inhibit aldehyde oxidation, but would have minimal effects on esterase activity.

The esterase screen may also identify compounds which activate the esterase reaction in a similar fashion to NAD⁺ by binding in the coenzyme binding site closing one end of the catalytic tunnel resulting in more productive encounters between the ester substrate and the catalytic cysteine (**Figure 32-c**).⁵⁵ These compounds may not be able to bind to the enzyme in the presence of NAD⁺, minimizing their effect on dehydrogenase activity. Other compounds which bind in the coenzyme binding site but do not alter access to the tunnel would not be identified through the HTS (**Figure 32-f**). This limits the identification of compounds that bind in the NAD⁺-binding site, as many of these compounds would not be selective due to the high conservation of the site among ALDH enzymes.

Although initial characterization of the compounds interaction with ALDH2 did not identify any substantial activators of ALDH dehydrogenase activity, three compounds (2CD11, 2CB8, and 2CB9) shared the benzodioxol of Alda-1, the ALDH2 activator, and were examined further. Alda-1 binds to ALDH2 similar to compound 2 in **Figure 32-d** with the benzodioxol group in the substrate binding site oriented towards the catalytic cysteine. Alda-1 displays substrate-dependent effects due to the limited space between the compound and the catalytic cysteine in the substrate binding site. Like Alda-1, the three compounds also exhibit substrate-dependent activation of ALDH2. The three compounds most likely bind in a similar position in ALDH2 as the activator Alda-1, where smaller substrates can still access the active cysteine. However, the three compounds are less potent activators than Alda-1.⁵⁵ These compounds and Alda-1 have

similar solubility issues, and the additional decreased potency of the compounds made it difficult to complete full dose-response curves.

The HTS identified a class of four aromatic lactones which selectively inhibit the ALDH1/2 family. The four compounds can be further divided by kinetic data and structure similarity into three psoralen derivatives and one coumarin derivative. The three psoralen derivatives inhibit most or all of the ALDH1/2 family with IC_{50} values between 0.1 – 1.0 μ M. The differences in alkyl substituents to the psoralen substructure have a measurable impact on the inhibition of the ALDH1/2 family. The additional methyl groups at positions R_2 and R_3 on the furan ring increase inhibition towards the ALDH1/2 family, most likely due to increased hydrophobic contacts (**Figure 33**).

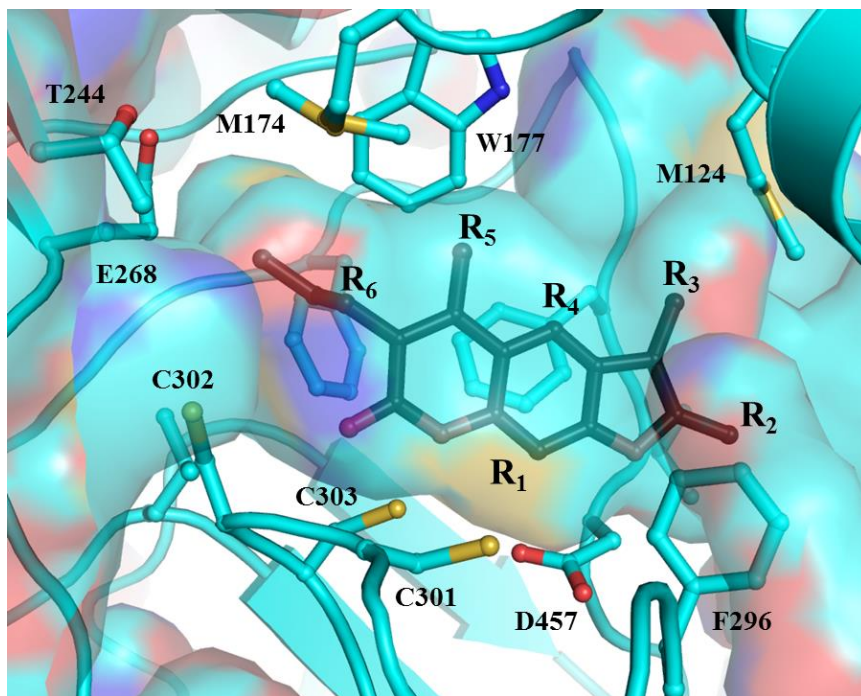


Figure 33 Orientation of 2P3 in catalytic tunnel of ALDH2. 2P3 is shown in its binding location in the catalytic site of ALDH2. Substituent positions are labeled.

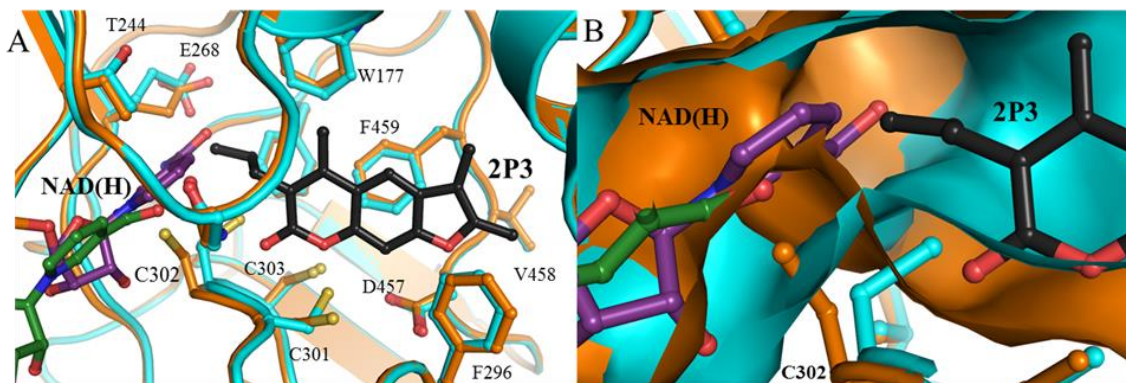


Figure 34 Comparison of NAD^+ and 2P3 binding to ALDH2. (A) Overlay of 2P3 (black) bound to ALDH2 (orange) and NAD^+ /NADH (purple/green) bound to ALDH2 (cyan). (B) Zoomed-in view of same overlay showing surface of ALDH2 for each binding partner. (PDB 1O00, 1O02, 1O04)

2P4 was found to be competitive with respect to varied NAD^+ and non-competitive (mixed-type) with respect to varied propionaldehyde; however, the closely related analog 2P3 was found to bind in the substrate binding site. Binding in the substrate binding site would normally be expected to exhibit competitive inhibition with respect to varied aldehyde. The binding of 2P3 causes Cys302 to rotate toward the NAD^+ binding site (**Figure 34**). When Cys302 resides in this shifted position, NAD^+ cannot be productively positioned to accept the hydride ion during the dehydrogenase reaction. The propyl chain at position R₆ of 2P3 may also hinder the positioning of the nicotinamide ring of NAD^+ . Similarly, 2P3 cannot bind to the free enzyme form of ALDH2 if Cys302 is not rotated away. Consequently, the binding of 2P3 prevents the productive binding of NAD^+ and vice versa. Although the majority of 2P3 binds within the substrate binding site, just enough of the compound overlaps with the NAD^+ binding site to generate the competitive inhibition towards varied NAD^+ seen with 2P4. NAD^+ will bind to the enzyme first and

can adopt multiple conformations (**Figure 5**) prior to assuming the productive conformation required for catalysis.^{43, 48} 2P3 could bind to one of the non-productively positioned complexes with NAD⁺. These off-pathway complexes would be consistent with the non-competitive (mixed-type) inhibition towards aldehyde substrate. Although NAD⁺ and 2P3/4 could be bound to ALDH2 simultaneously, 2P3/4 must dissociate before NAD⁺ can isomerize into a productive conformation for hydride transfer (**Figure 35**). Once NAD⁺ is in the correct position, substrate aldehyde will bind to the enzyme and the reaction proceeds. ALDH2 most likely follows an ordered bi-bi mechanism where NADH is released last.^{43, 48} 2P3 cannot bind to the enzyme alongside NADH (**Figure 34**), so NADH must be released before 2P3/4 can bind to the enzyme again to inhibit the reaction.

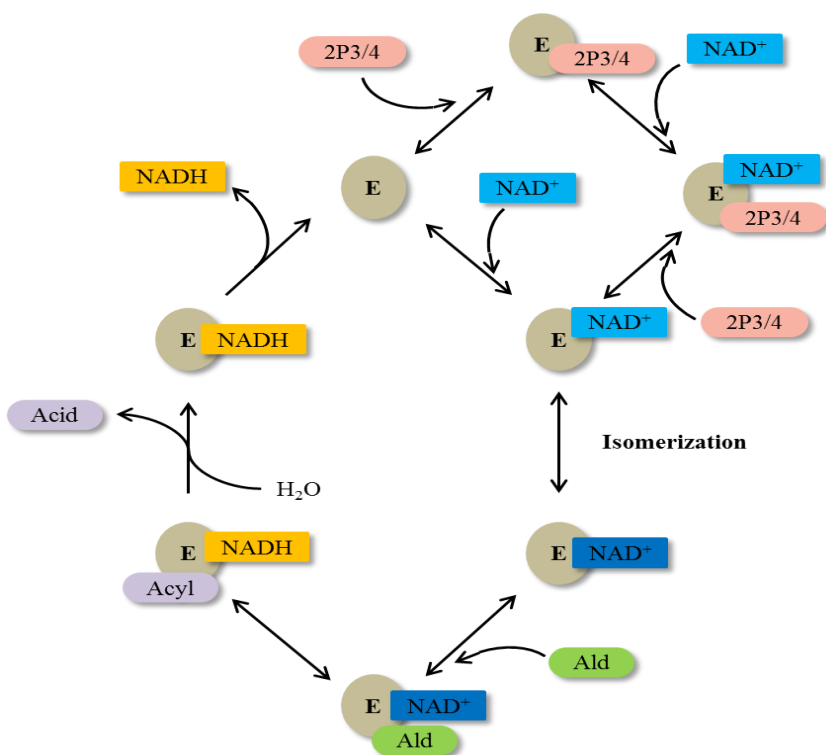


Figure 35 Schematic of 2P3/4 inhibition of ALDH2

2P4 exhibits competitive inhibition with respect to varied NAD⁺ and non-competitive (mixed-type) with respect to varied propionaldehyde. 2P3 can bind to the free enzyme, and it is possible and likely that 2P3 can also bind simultaneously with NAD⁺ in a non-productive conformation. Isomerization of NAD⁺, and subsequent aldehyde oxidation, can only occur once 2P3/4 dissociates from the enzyme.

Of the four initially identified lactones, 2BS4 has the most unique inhibition profile.

2BS4 is less potent than 2P3/4 but is selective for ALDH2 against all other tested ALDH isoenzymes. Although 2BS4 contains the aromatic lactone moiety which helps orient 2P3 in the substrate binding site, 2BS4 also contains a terminal ester group and could be a potential substrate for ALDH2. Either the lactone carbonyl or the terminal ester could be oriented towards the catalytic cysteine of ALDH2 based off the binding position of 2P3. Data shows that the ester of 2BS4 is slowly hydrolyzed over time, possibly through a

combination of ALDH2-catalyzed and non-catalyzed hydrolysis in solution. The relative contribution of each is unclear due to the timeframe (2-3 days). 2BS4 exhibits a time-dependence for inhibition, but the time-dependence was not observed for the inhibition phase, but is related to how long the enzyme remains inhibited after complex formation. 2BS4 behaves like a “slow off” inhibitor of ALDH2. The hydrolysis limits the use of 2BS4 as an ALDH2 inhibitor for *in vivo* studies, since the free acid form is not inhibitory (see below).

A total of 35 aromatic lactone analogs were purchased in an attempt to improve the selectivity of the three psoralen compounds for ALDH2, and to achieve the selectivity seen with the coumarin 2BS4, minus the ester group. Although the analogs were picked based off the binding position of 2P3 to ALDH2, many of the analogs do not inhibit ALDH2 activity. The narrow catalytic tunnel of ALDH2 limits the size of substituents that can be added to the structure of the scaffold (**Figure 33**). Several compounds were also ordered to confirm the binding mode of 2P3 since additions at certain positions to the compound should eliminate ALDH2 inhibition. For instance, BUC2 has a methyl group at position R₁ which no longer fits within the narrow binding tunnel and does not inhibit ALDH2. There are many other compounds that have larger additions at position R₁ that were not ordered; these compounds would also not inhibit ALDH2. Bulky side chains such as t-butyl and phenyl groups at position R₃ or benzyl groups at positions R₅ or R₆ also cause the compound to no longer fit as well in the narrow tunnel. The best additions amongst the psoralen compounds (Scaffold I) were increasing the size of the alkyl substitutions at positions R₅ and R₆ adjacent to the lactone carbonyl carbons,

including the addition of a fourth ring. The coumarin analogs which most closely resembled 2BS4 did not inhibit ALDH2, supporting the idea that 2BS4 inhibits the enzyme differently than the other compounds in the series. Carboxylates are generally poor inhibitors of the ALDH1/2 family, as in the case for the free acid of 2BS4 (2P15) and the inhibition of 2BS4 appears to be derived from the terminal ester. Several of the coumarin analogs inhibit the activity of ALDH3A1, suggesting the additional furan ring of the psoralen compounds helps select against ALDH3A1, though is not essential. After initial testing with ALDH1A1, ALDH2, and ALDH3A1, 11 of the additional analogs warranted further dose-response analysis.

The eleven compounds showed the same similar pattern at the four initial aromatic lactones; that is, the psoralen derivatives are more potent, but less selective, than the coumarin derivatives. BUC5, BUC6, and BUC7 add an additional ring structure at positions R₅ and R₆ proximal to the aromatic lactone (**Figure 33**). The additional cyclohexyl and cyclopentyl rings in BUC6 and BUC7 slightly increase the potency towards ALDH2 while lessening the total amount of inhibition towards ALDH1A1 and ALDH1A3. BUC3, which opens the cyclopentyl ring of BUC7 to form a propyl chain at position R₅, also does not inhibit ALDH1A1, though BUC3 does activate ALDH1A3 through a yet-unknown mechanism. BUC5, which increases the size of the aromatic ring structure by adding a benzyl ring, only partially inhibits ALDH2 while selecting against ALDH1A1 inhibition. The amount of inhibition towards ALDH1A1 and ALDH2 by these compounds with larger rings is most likely related to how well the larger compound fits in the active site. The ring additions at R₅ and R₆ must fit between Trp177 and

Met174 in ALDH2, which are both conserved throughout the ALDH1/2 family (**Figure 33**). The benzyl ring of BUC5 may not fit as well due to the constraints of maintaining aromaticity whereas the cyclopentyl and cyclohexyl rings do not have these restraints.

BUC11 represents a large number of available analogs which use a 1-acylpiperidine linker to connect the psoralen ring structure to a variety of other chemical moieties. These compounds also have variations in the amount of alkyl substituents on the psoralen scaffold, similar to 2P3, 2P4, and 2CB5. BUC11 exhibits different modes of inhibition towards varied NAD^+ for ALDH1A1 and ALDH2, suggesting that BUC11 inhibits these two enzymes through different mechanisms. BUC11 exhibits uncompetitive inhibition towards varied NAD^+ for ALDH1A1, which is consistent with the distance between the NAD^+ and BUC11 binding sites in ALDH1A1 (**Figure 25B**) and is expected for compounds that displace aldehyde substrates for ordered Bi Bi systems. The competitive inhibition towards varied NAD^+ for ALDH2 is similar to the mechanism exhibited by 2P4. This would suggest that BUC11 binds to ALDH2 in a similar position as 2P3 with the 1-acylpiperidine extending past Cys302 and posed toward the NAD^+ site, consistent with its competitive mode of inhibition. However, for ALDH1A1 the presence of Gly458 and its larger substrate pocket promotes a shift in binding mode and mechanism of inhibition for BUC11. The corresponding residue to Gly458 in the other four ALDH1/2 isoenzymes is either an asparagine or aspartate, which precludes the binding mode observed in ALDH1A1. The 1-acylpiperide may have more difficulty extending into the NAD^+ site for ALDH1A3, as the IC_{50} value is 10x larger than those for ALDH2, ALDH1B1, and ALDH1A2.

The coumarin derivative BUC25 also binds in the substrate binding site. The distance between the carbonyl lactone and catalytic cysteine suggests that binding of BUC25 does not prevent the productive binding of NAD⁺ to ALDH1A1, as the additional benzyl group of BUC25 prevents the compound from binding closer to the catalytic cysteine. BUC25 does not inhibit ALDH2 and the mode of binding provides insight into this selectivity. The methane sulfonyl group of BUC25 binds in the pocket formed by Gly458 in ALDH1A1. The corresponding aspartate/asparagine residues in the other ALDH1/2 isoenzymes would force the coumarin scaffold to adopt a position akin to 2P4 in ALDH2. However, unlike the more flexible linker in BUC11, the large benzyl ring cannot adopt a conformation to productively bind within the NAD⁺-binding cleft and the benzyl ring of BUC25 would encounter more steric hindrance from the conserved tryptophan (Trp177 in ALDH2) since the residues surrounding Trp177 are bulkier in ALDH2. The tryptophan may be able to slightly move in ALDH1B1, ALDH1A2, and ALDH1A3, though not as much as in ALDH1A1. This is evidenced by the compound being ~5x less potent for these three isoenzymes compared to ALDH1A1.

Surprisingly, unlike 2P3, BUC11, or BUC25, BUC22 was found to bind in the in coenzyme binding site of ALDH1A1. The difference in binding location, and the crystal forming in a unique space group (P1), raised the possibility that the binding site might be influenced by the crystal environment. However, there is a structural basis for the selectivity between ALDH2 and ALDH1A1 in this binding location which suggests that the binding within the coenzyme site may be more than an artifact of this particular crystal form (**Figure 36**). Ile249 in ALDH2 is replaced by Val250 in ALDH1A1 and

although it is the addition of a single methyl group, the substitution narrows this side of the site enough to impede binding of the diethylamino substituent in ALDH2.

Additionally, Val252 and Ala233 in ALDH2 versus Leu253 and Ser234 in ALDH1A1 may loosen the contacts between the enzyme and BUC22 enough that the binding energetics cannot overcome the steric clash with Ile249 through slightly shifting to the other side of the binding cleft.

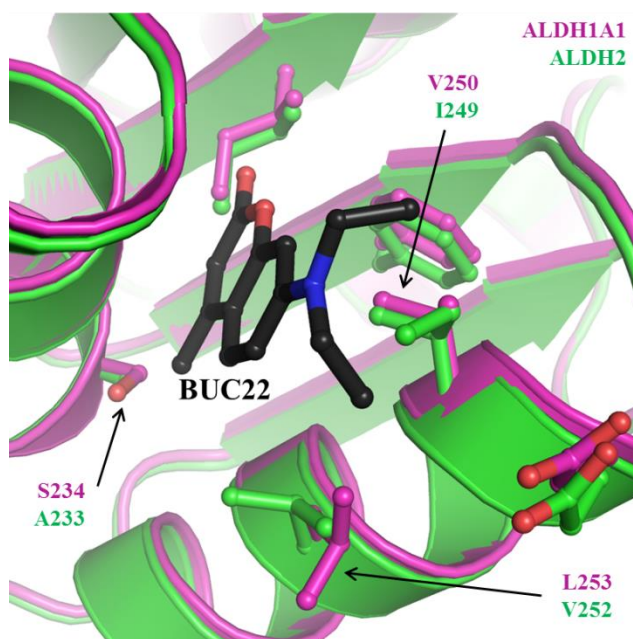


Figure 36 Comparison of BUC22 binding to ALDH1A1 versus ALDH2. BUC22 (black) binds to ALDH1A1 (purple) in the NAD⁺-binding site. Three amino acids in the vicinity of the binding location are not conserved between ALDH1A1 and ALDH2 (green) and may explain the selectivity seen between the two enzymes.

The kinetic data of BUC22, however, is not completely consistent with this binding location. Compounds which bind in the adenine binding site should exhibit competitive inhibition towards varied NAD⁺, but BUC22 exhibits noncompetitive inhibition. Though

inconsistent with binding in the adenine binding site, it is also a different mode of inhibition from compounds determined to bind in the substrate binding site, 2P4 (competitive) and BUC11 (uncompetitive), which suggests BUC22 binds differently than these other analogs. BUC20, a related analog, also exhibits a noncompetitive mode of inhibition towards varied NAD^+ for ALDH1A1 and ALDH2. Due to its linear cyano group, BUC20 is not predicted to clash with Ile249 in ALDH2. Consequently BUC20 inhibits both ALDH1A1 and ALDH2. The reason behind the discrepancy between the kinetic data and structural data is unclear, though there is a possibility that BUC22 could bind to multiple sites and enzyme species. When NAD^+ is absent, the compound prefers to bind in the NAD^+ binding site (as in the case of the solved structure), but when NAD^+ is present, the compound may bind in another location giving rise to the observed kinetic pattern. This additional site could be the substrate binding site, such as where BUC25 binds.

BUC27 was the only compound that selectively inhibited ALDH2 in this study, other than the ester 2BS4. Both BUC27 and 2P4 exhibit competitive inhibition towards varied NAD^+ , suggesting that BUC27 likely alters the conformation of the catalytic cysteine to interfere with the productive binding of NAD^+ for catalysis, similar to 2P3. If BUC27 were to adopt a similar conformation to that of 2P3 bound to ALDH2, the ketoxime would occupy the same pocket as the propyl chain. The bromine would be oriented towards Met124 would could lead to favorable interaction between the halogen substituent and the sulfur side chain atom (**Figure 37**).

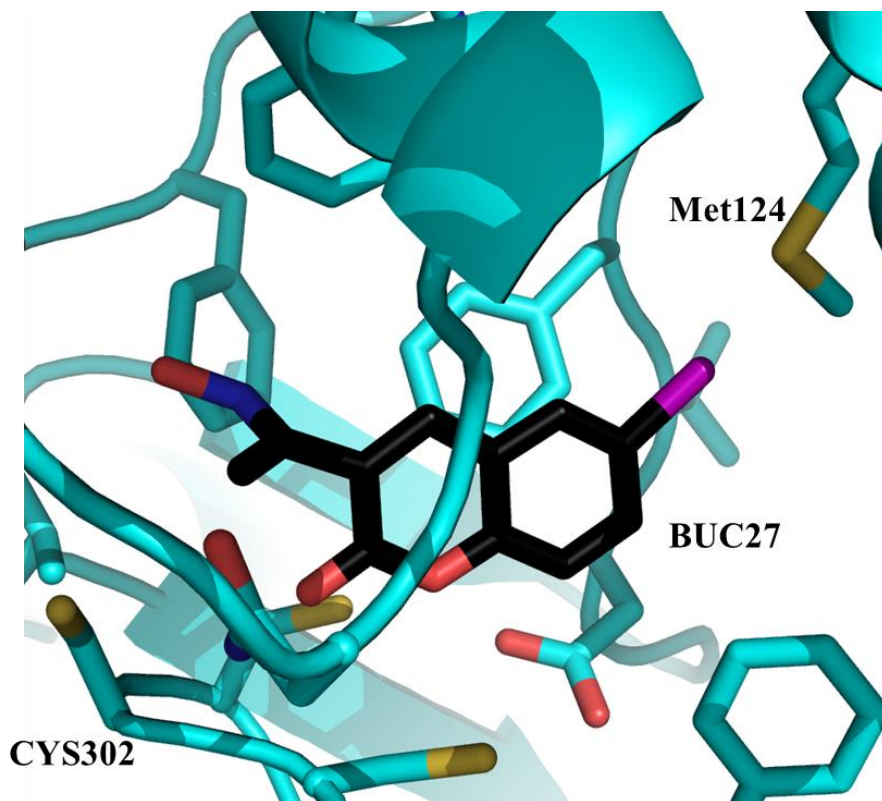


Figure 37 Docking of BUC27 in substrate binding site of ALDH2. BUC27 was docked in the substrate binding site of ALDH2 so that the aromatic lactone was in the same position as that of 2P3 bound to ALDH2. In this position the bromine could form a favorable interaction with Met124, which is unique to ALDH2. Future compounds could focus on promoting interaction between compound and Met124 to achieve selectivity for ALDH2.

This potential interaction is not possible for the three ALDH1A isoenzymes as a glycine occupies the equivalent position. However, it is unclear what effect the equivalent glutamate in ALDH1B1 would have on BUC27 binding. The glutamate of ALDH1B1 could provide additional contacts for BUC27 binding, thus the rationale for selectivity towards ALDH2 by BUC27 is still unclear. The mechanism behind BUC27's activation of ALDH1A3, and that behind BUC3's activation, is also not clear but may be similar to

that of Alda-1, where binding of Alda-1 in the outer portion of the substrate binding site increases the amount of productive encounters with the catalytic cysteine for smaller aldehydes.

The inhibition pattern of these compounds was compared to that of daidzin, and we found that these compounds are more potent than daidzin under our assay parameters.

Additionally, daidzin was discovered to be less selective than previously reported. Daidzin inhibited the activity of ALDH2, ALDH1A2, and ALDH1B1 with equal potency, while being 100-fold less potent against ALDH1A1 and ALDH1A3. This same pattern of inhibition was also found in the psoralen derivatives, where many compounds inhibit ALDH2, ALDH1B1 and ALDH1A2 with similar potency and are often less active against ALDH1A1 and ALDH1A3 at some level. Although IC₅₀ values may be similar, many of the psoralen derivatives only partially inhibited ALDH1A1 and ALDH1A3, or did not inhibit at all.

In order to correlate the different binding modes and inhibition patterns to underlying structural differences, we examined the binding sites and interactions in more detail.

Structural comparison of three compound-enzyme complexes revealed the presence of two distinct aromatic binding “boxes” or “zones” (**Figure 38**). In ALDH2 the aromatic binding region is located between four phenylalanine residues (170,296,459,465) near the catalytic cysteine which surround 2P3 when bound. The activator Alda-1 and the isoflavone of the ALDH2 inhibitor daidzin bind in this same aromatic site.^{55, 204} The aromatic binding region of ALDH1A1 is wider, extends farther from the catalytic

cysteine and is more surface exposed. In ALDH1A1, Phe459 is replaced by a valine and Phe296 is replaced by tyrosine. The aromatic binding region of ALDH1A1 has additional aromatic residues at His293 and Phe290. Although the histidine residue is a phenylalanine in ALDH2, the side chain of Asp457 in ALDH2 blocks any connection of the two regions and gives rise to the smaller site in ALDH2 compared to ALDH1A1, which has a glycine in an equivalent position.

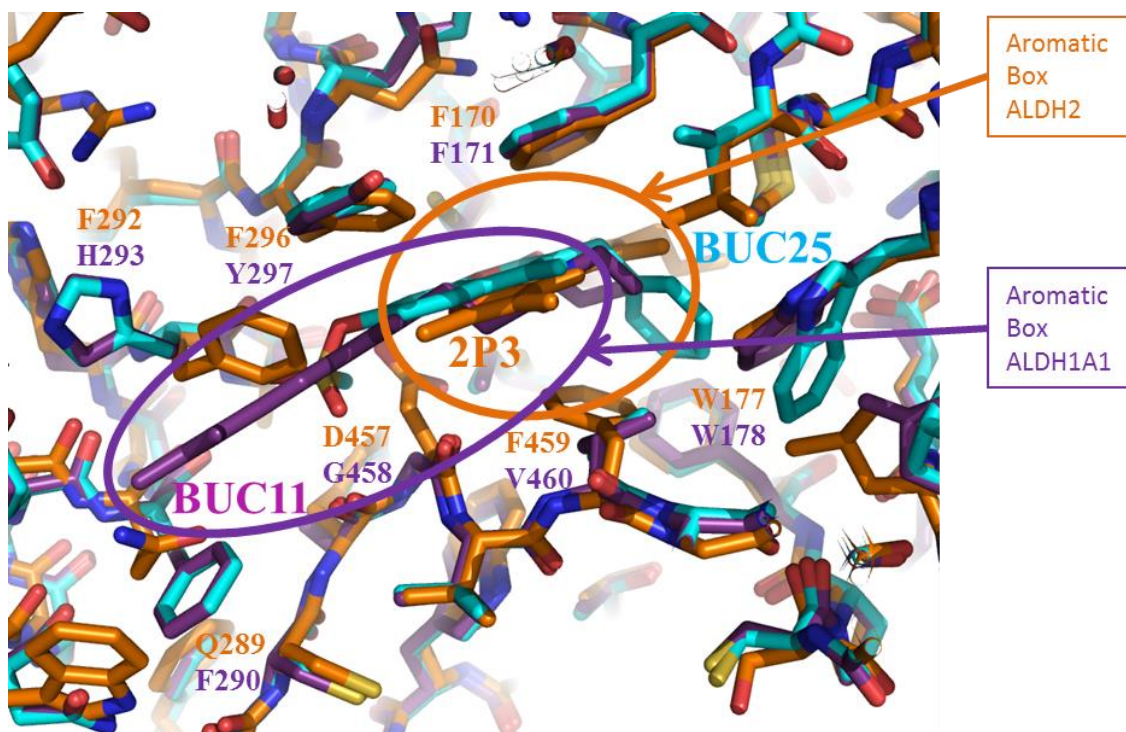


Figure 38 Alignment of three enzyme-inhibitor complexes. Alignment of 2P3 (orange) bound to ALDH2 and BUC11 (purple) and BUC25 (cyan) bound to ALDH1A1 shows an overlap of separate aromatic binding “boxes” or “zones”. D457 in ALDH2 limits the size of the zone in ALDH2, whereas G458 in ALDH1A1 provide a larger zone for the binding of aromatic compounds.

The aromatic lactones are able to shift positions to maximize contacts due to the hydrophobicity of the substrate binding site of ALDHs. Most enzymes rely on hydrogen bonding and/or ion interactions to align substrates in the substrate binding site; in contrast, the substrate binding site of ALDHs is highly hydrophobic with limited potential for hydrogen bonding. When substituents are added or removed from an activator/inhibitor that result in the compound no longer filling the available space, the compound can either not bind at all, or find another site where binding is also possible. The hydrophobicity of the tunnel, and lack of dependence on hydrogen bonding and ion interactions, provides more potential sites for compound binding in ALDHs.

The ability for the compounds to shift in the hydrophobic substrate binding site may help explain the difference in inhibition of ALDH1A1 between 2P3 and 2P4. The shortening of the alkyl chain at position R₅ from a propyl to a methyl group results in 2P4 not inhibiting ALDH1A1. Loss of contact between the scaffold and Val460 in ALDH1A1 (as compared to Phe459 in ALDH2) may require the longer propyl chain to “anchor” the compound near the catalytic cysteine. The methyl group may not create enough additional contacts which will cause the scaffold of 2P4 to shift to the location of BUC11 when bound to ALDH1A1 to increase the amount of contacts, which is possible due to the presence of Gly458. If bound in this location, 2P4 would not inhibit the enzyme as the compound would not impede access to the catalytic tunnel. 2P3, even with the longer propyl chain, would also not inhibit ALDH1A1 if bound similar to BUC11, which supports the idea that the longer alkyl chain enables 2P3 to bind closer to the catalytic cysteine to inhibit the enzyme. The additional contacts from the propyl chain may not be

needed with ALDH1A2, ALDH1A3, and ALDH1B1 (all of which replace Phe459 in ALDH2 with smaller aliphatic residues) as these three enzymes have an asparagine at the equivalent position of Gly458 and are each inhibited by 2P4. The additional side chain may provide enough binding surface that the smaller compound remains bound to the enzyme.

A second binding pocket exists in ALDH isoenzymes that can accommodate aromatic ring structures—the adenine binding cleft within the coenzyme binding site. When NAD⁺ is bound, the adenine ring is positioned between a conserved proline and a beta-branched amino acid (Pro226 and Ile249 in ALDH1A1). The crystal structure of BUC22 shows that at least one of the compounds can bind to the adenine site, though kinetic data supports the binding of BUC22 at an additional site, most likely the aromatic binding region in the substrate binding site.

The multiple aromatic binding sites within ALDH isoenzymes can help explain how the ALDH1A1-selective inhibitor BUC22 was discovered from a series of compounds identified through a screen targeting ALDH2. BUC22 was not one of the compounds found in the high-throughput screen, but a structural analog. Changing the substituents of the aromatic scaffold likely caused BUC22 to shift binding locations to the adenine binding site, which then provided selectivity against ALDH2. The alteration of substituents has been seen to change the selectivity of indole-2,3-diones for a particular ALDH isoenzyme.²²⁹ In that particular case, the compounds had different orientations

within the same binding site, while the coumarin and psoralen derivatives show a greater amount of movement with multiple binding sites.

An important factor for the use of any compound as a chemical probe is the ability to affect the activity of the target enzyme in a cellular context. Coumarins and psoralens can either be cell permeable or cell impermeable depending on the exact structure. Some psoralens are known to become trapped in cell membranes, with the most hydrophobic compounds predicted to be the most permeable.²³⁰ BUC22 was found to have a physiological effect on MDA-MB-468 breast cancer cells after five days of treatment. A significant two-fold decrease in the proliferative ability of the breast cancer cells was seen when treated with 100 μ M BUC22, 100-fold higher than the *in vitro* K_i (\sim 1 μ M), as measured by the MTT assay. The loss of potency could arise from a portion of BUC22 becoming trapped in the cell membrane, by the conversion of the compound into other, less potent derivatives upon entrance into the cell, or by export from the cell before inhibition occurs. As BUC22 is more hydrophobic than other permeable psoralens, a large portion of BUC22 should be able to enter the cell by predicted models. Additionally, this concentration is high enough that inhibition of ALDH1A2 by BUC22 may also contribute to the cell phenotype. Regardless, BUC22 is capable of causing a physiologic effect in cancer cells in 3D culture.

V. Conclusion and Future Directions

Members of the ALDH1/2 family are involved in retinoic acid signaling, the metabolism of dietary aldehydes, and the removal of toxic aldehydes from oxidative stress. ALDH1/2 enzymes have also been linked to the development of cancer, obesity, and neurological disease. Small molecule probes are needed to study the role of individual enzymes in both normal and disease states. The development of selective modulators has been difficult due to the structural similarity and overlapping substrate preferences within the ALDH1/2 family. At present, there are no commercially available compounds that selectively modulate ALDH2 activity compared to other ALDH isoenzymes.

Inhibitors targeting ALDH2, such as daidzin and its derivatives, have been used previously to study the function of ALDH2; however, daidzin is not as selective as previously reported. We found that daidzin inhibits ALDH2, ALDH1B1, and ALDH1A2 with equivalent potency. In light of these findings, the selectivity of daidzin derivatives including CVT-10216 should be examined further. Many of the aromatic lactones found during the course of this study have similar or better selectivity and/or potency than daidzin *in vitro*, suggesting the aromatic lactones, with further development, may be a better option for an ALDH2-selective inhibitor.

The aromatic lactones show the ability to bind throughout the aromatic “zones” in the catalytic site of ALDH1/2 enzymes. The aromatic “zone” in ALDH2 is smaller due to the presence of Asp457, limiting the potential orientations of the lactone within the catalytic site. The lactone can only be positioned with its carbonyl oriented directly toward the

catalytic cysteine (or rotated 180°). This allows for an easier interpretation of SAR data in regards to activity against ALDH2; for example, bulky substituents cause a loss of inhibition toward ALDH2 as the compound no longer fits in the narrow binding tunnel and any addition to R₆ next to the lactone carbonyl must likely fit into the coenzyme binding site to maintain binding and subsequent inhibition.

The interpretation for SAR data in regards to ALDH1A1 with these compounds is more challenging as multiple binding orientations are possible in the larger substrate binding site. The lactones can shift within the hydrophobic pocket to increase the amount of contacts while decreasing the amount of clashing based upon the substituents added to the scaffold. If a large substituent is placed at position R₆, the larger hydrophobic space provides an opportunity for the scaffold to shift away from the catalytic cysteine to provide room, as in the case for BUC11. Compounds are also likely to shift due to decreased contacts with the non-aromatic Val460. Smaller compounds, like 2P3, could bind in multiple locations within the catalytic site depending on the specific substituents on the aromatic scaffold. Although a crystal structure of 2P3 bound to ALDH1A1 would definitely answer where 2P3 binds, it may not help in determining the binding position and rationale behind the SAR of other smaller analogs with regards to ALDH1A1, as different substituents could shift the scaffold to a different location. If the compound is small enough the binding location could shift to the adenosine binding site, as in the case for BUC22 bound to ALDH1A1.

The structure of 2P3 bound to ALDH2 can reliably be used to predict how structural modifications will affect the activity of the lactones for ALDH2; however, care must be taken when making future modifications in regards to activity versus ALDH1A1 and the rest of the ALDH1/2 family. The addition of a substituent to the scaffold to increase interaction with ALDH2, such as an interaction between a halogen and Met124, which is not a conserved residue, could have unintended effects on the activity versus other isoenzymes through shifting of the aromatic scaffold.

Although the complete rationale for selectivity remains unknown, two selective compounds were discovered and characterized—the ALDH1A1-selective BUC22 and the ALDH2-selective BUC27. Initial experiments with cells in 3D culture suggest that BUC22 can enter cancer cells and impact cell proliferation through inhibition of ALDH1A1, though off-target effects are still possible. Previous studies with CM037, an ALDH1A1 inhibitor, have found that both ovarian cancer and MDA-MB-468 breast cancer cells are more sensitive to ALDH1A1 inhibition in 3D culture as opposed to monolayers. This is due in part to an increase in ALDH1A1 expression in cells grown in 3D culture.^{111, 113} Based on this data, BUC22 should also have differing effects on MDA-MB-468 cells in 3D vs 2D culture and should be confirmed. BUC22 or future derivatives could be used to examine the mechanism by which ALDH1A1 inhibition leads to decreased mitochondrial function and proliferative potential. Pharmacodynamic and pharmacokinetic experiments could also be completed in mice to determine BUC22's future prospective for *in vivo* studies. Unlike CM037 and other ALDH1A1-selective inhibitors, BUC22 does not rely on Gly458, which is not conserved in rodents, for

inhibition or selectivity. BUC22 should be able to inhibit murine ALDH1A1 by binding in the more conserved NAD⁺-binding site. There are potential limitations that should be addressed before BUC22, or future derivatives, are used in animal models. Mainly, the residues Ile249 and Val242 that helped provide selectivity against human ALDH2 are substituted by a valine and isoleucine in murine ALDH2, identical to the residues in human ALDH1A1. Selectivity against ALDH2 in murine systems is potentially lost, though interactions at the second proposed binding site leave this uncertain. Likewise, BUC22 may inhibit other NAD⁺-dependent enzymes which would limit its use. The variability of the ALDH1/2 family between rodents and humans complicates the animal studies that must precede any attempts at human trials, since there are no direct models leading from rodents to humans that maintain the human ALDH1/2 structure-activity relationship. Possible solutions to this conundrum include the creation of a humanized mouse/rat line where the human target of interest is integrated in place of the rodent enzyme.

Concerning the ALDH2-selective BUC27, a crystal structure of BUC27 bound to ALDH2 would potentially provide a rationale for the selectivity against the other ALDH1/2 members. The structure may confirm the proposed interaction between the bromine and Met124 and drive development of more potent inhibitors. It would also be beneficial to examine if BUC27 is capable of inhibiting ALDH2 within cells by measuring potential effects on alcohol metabolism. Unfortunately, to this point there is no known liver cell line or primary cell which maintains expression of ALDH2 in culture, limiting future studies. For this reason prior development of ALDH2-selective

compounds have gone from *in vitro* studies straight to animal models. BUC27, or subsequent derivatives, could be examined for their ability to affect alcohol drinking of selectively bred rats to determine bioavailability and potency *in vivo*. Both BUC27, and the ALDH1A1-selective BUC22, should be further developed for use as chemical probes to study the individual functions of ALDH2 and/or ALDH1A1.

References

- [1] Vasiliou, V., Pappa, A., and Estey, T. (2004) Role of human aldehyde dehydrogenases in endobiotic and xenobiotic metabolism, *Drug metabolism reviews* 36, 279-299.
- [2] Lindahl, R. (1992) Aldehyde dehydrogenases and their role in carcinogenesis, *Crit Rev Biochem Mol Biol* 27, 283-335.
- [3] Rhinn, M., and Dolle, P. (2012) Retinoic acid signalling during development, *Development* 139, 843-858.
- [4] Zhou, X. E., Melcher, K., and Xu, H. E. (2012) Structure and activation of rhodopsin, *Acta Pharmacol Sin* 33, 291-299.
- [5] Esterbauer, H., Schaur, R. J., and Zollner, H. (1991) Chemistry and biochemistry of 4-hydroxynonenal, malonaldehyde and related aldehydes, *Free radical biology & medicine* 11, 81-128.
- [6] O'Brien, P. J., Siraki, A. G., and Shangari, N. (2005) Aldehyde sources, metabolism, molecular toxicity mechanisms, and possible effects on human health, *Critical reviews in toxicology* 35, 609-662.
- [7] Curtis, J. M., Hahn, W. S., Long, E. K., Burrill, J. S., Arriaga, E. A., and Bernlohr, D. A. (2012) Protein carbonylation and metabolic control systems, *Trends Endocrinol Metab* 23, 399-406.
- [8] Hauck, A. K., and Bernlohr, D. A. (2016) Oxidative stress and lipotoxicity, *J Lipid Res.*
- [9] Vander Jagt, D. L., Hunsaker, L. A., Vander Jagt, T. J., Gomez, M. S., Gonzales, D. M., Deck, L. M., and Royer, R. E. (1997) Inactivation of glutathione reductase by 4-hydroxynonenal and other endogenous aldehydes, *Biochemical pharmacology* 53, 1133-1140.
- [10] Kinter, M., and Roberts, R. J. (1996) Glutathione consumption and glutathione peroxidase inactivation in fibroblast cell lines by 4-hydroxy-2-nonenal, *Free radical biology & medicine* 21, 457-462.
- [11] Brooks, P. J., and Theruvathu, J. A. (2005) DNA adducts from acetaldehyde: implications for alcohol-related carcinogenesis, *Alcohol* 35, 187-193.
- [12] Cheng, G., Shi, Y., Sturla, S. J., Jalas, J. R., McIntee, E. J., Villalta, P. W., Wang, M., and Hecht, S. S. (2003) Reactions of formaldehyde plus acetaldehyde with deoxyguanosine and DNA: formation of cyclic deoxyguanosine adducts and formaldehyde cross-links, *Chemical research in toxicology* 16, 145-152.

- [13] McMahon, R. E. (1982) Chapter 5: Alcohols, aldehyde, and ketones, In *Metabolic basis of detoxication: metabolism of functional groups* (Jakoby, W. B., Bend, J. R., and Coldwell, J., Eds.), Academic Press, NY.
- [14] Penning, T. M. (2015) The aldo-keto reductases (AKRs): Overview, *Chemico-biological interactions* 234, 236-246.
- [15] Beedham, C., Peet, C. F., Panoutsopoulos, G. I., Carter, H., and Smith, J. A. (1995) Role of aldehyde oxidase in biogenic amine metabolism, *Prog Brain Res* 106, 345-353.
- [16] Vasiliou, V., Pappa, A., and Petersen, D. R. (2000) Role of aldehyde dehydrogenases in endogenous and xenobiotic metabolism, *Chemico-biological interactions* 129, 1-19.
- [17] Kavanagh, K. L., Jornvall, H., Persson, B., and Oppermann, U. (2008) Medium- and short-chain dehydrogenase/reductase gene and protein families : the SDR superfamily: functional and structural diversity within a family of metabolic and regulatory enzymes, *Cell Mol Life Sci* 65, 3895-3906.
- [18] Berhane, K., Widersten, M., Engstrom, A., Kozarich, J. W., and Mannervik, B. (1994) Detoxication of base propenals and other alpha, beta-unsaturated aldehyde products of radical reactions and lipid peroxidation by human glutathione transferases, *Proceedings of the National Academy of Sciences of the United States of America* 91, 1480-1484.
- [19] Jackson, B., Brocker, C., Thompson, D. C., Black, W., Vasiliou, K., Nebert, D. W., and Vasiliou, V. (2011) Update on the aldehyde dehydrogenase gene (ALDH) superfamily, *Human genomics* 5, 283-303.
- [20] Vasiliou, V., Bairoch, A., Tipton, K. F., and Nebert, D. W. (1999) Eukaryotic aldehyde dehydrogenase (ALDH) genes: human polymorphisms, and recommended nomenclature based on divergent evolution and chromosomal mapping, *Pharmacogenetics* 9, 421-434.
- [21] Vasiliou, V., Thompson, D. C., Smith, C., Fujita, M., and Chen, Y. (2013) Aldehyde dehydrogenases: From eye crystallins to metabolic disease and cancer stem cells, *Chemico-biological interactions* 202, 2-10.
- [22] Braun, T., Bober, E., Singh, S., Agarwal, D. P., and Goedde, H. W. (1987) Evidence for a signal peptide at the amino-terminal end of human mitochondrial aldehyde dehydrogenase, *FEBS letters* 215, 233-236.
- [23] Marchitti, S. A., Brocker, C., Stagos, D., and Vasiliou, V. (2008) Non-P450 aldehyde oxidizing enzymes: the aldehyde dehydrogenase superfamily, *Expert opinion on drug metabolism & toxicology* 4, 697-720.

- [24] Estey, T., Cantore, M., Weston, P. A., Carpenter, J. F., Petrash, J. M., and Vasiliou, V. (2007) Mechanisms involved in the protection of UV-induced protein inactivation by the corneal crystallin ALDH3A1, *The Journal of biological chemistry* 282, 4382-4392.
- [25] Vasiliou, V., Sandoval, M., Backos, D. S., Jackson, B. C., Chen, Y., Reigan, P., Lanaspas, M. A., Johnson, R. J., Koppaka, V., and Thompson, D. C. (2013) ALDH16A1 is a novel non-catalytic enzyme that may be involved in the etiology of gout via protein-protein interactions with HPRT1, *Chemico-biological interactions* 202, 22-31.
- [26] Vasiliou, V., and Nebert, D. W. (2005) Analysis and update of the human aldehyde dehydrogenase (ALDH) gene family, *Human genomics* 2, 138-143.
- [27] Emadi, A., Jones, R. J., and Brodsky, R. A. (2009) Cyclophosphamide and cancer: golden anniversary, *Nat Rev Clin Oncol* 6, 638-647.
- [28] Lassen, N., Bateman, J. B., Estey, T., Kuszak, J. R., Nees, D. W., Piatigorsky, J., Duester, G., Day, B. J., Huang, J., Hines, L. M., and Vasiliou, V. (2007) Multiple and additive functions of ALDH3A1 and ALDH1A1: cataract phenotype and ocular oxidative damage in *Aldh3a1(-)/Aldh1a1(-)* knock-out mice, *The Journal of biological chemistry* 282, 25668-25676.
- [29] Deak, K. L., Dickerson, M. E., Linney, E., Enterline, D. S., George, T. M., Melvin, E. C., Graham, F. L., Siegel, D. G., Hammock, P., Mehlretter, L., Bassuk, A. G., Kessler, J. A., Gilbert, J. R., Speer, M. C., and Group, N. T. D. C. (2005) Analysis of ALDH1A2, CYP26A1, CYP26B1, CRABP1, and CRABP2 in human neural tube defects suggests a possible association with alleles in ALDH1A2, *Birth Defects Res A Clin Mol Teratol* 73, 868-875.
- [30] Marchitti, S. A., Deitrich, R. A., and Vasiliou, V. (2007) Neurotoxicity and metabolism of the catecholamine-derived 3,4-dihydroxyphenylacetaldehyde and 3,4-dihydroxyphenylglycolaldehyde: the role of aldehyde dehydrogenase, *Pharmacological reviews* 59, 125-150.
- [31] Anastasiou, V., Ninou, E., Alexopoulou, D., Stertmann, J., Muller, A., Dahl, A., Solimena, M., Speier, S., Serafimidis, I., and Gavalas, A. (2016) Aldehyde dehydrogenase activity is necessary for beta cell development and functionality in mice, *Diabetologia* 59, 139-150.
- [32] Rizzo, W. B., and Carney, G. (2005) Sjogren-Larsson syndrome: diversity of mutations and polymorphisms in the fatty aldehyde dehydrogenase gene (ALDH3A2), *Human mutation* 26, 1-10.

- [33] Sun, X., Jia, Y., Zhang, X., Xu, Q., Shen, Y., and Li, Y. (2005) Multi-locus association study of schizophrenia susceptibility genes with a posterior probability method, *Sci China C Life Sci* 48, 263-269.
- [34] Geraghty, M. T., Vaughn, D., Nicholson, A. J., Lin, W. W., Jimenez-Sanchez, G., Obie, C., Flynn, M. P., Valle, D., and Hu, C. A. (1998) Mutations in the Delta1-pyrroline 5-carboxylate dehydrogenase gene cause type II hyperprolinemia, *Human molecular genetics* 7, 1411-1415.
- [35] Akaboshi, S., Hogema, B. M., Novelletto, A., Malaspina, P., Salomons, G. S., Maropoulos, G. D., Jakobs, C., Grompe, M., and Gibson, K. M. (2003) Mutational spectrum of the succinate semialdehyde dehydrogenase (ALDH5A1) gene and functional analysis of 27 novel disease-causing mutations in patients with SSADH deficiency, *Human mutation* 22, 442-450.
- [36] Goodwin, G. W., Rougraff, P. M., Davis, E. J., and Harris, R. A. (1989) Purification and characterization of methylmalonate-semialdehyde dehydrogenase from rat liver. Identity to malonate-semialdehyde dehydrogenase, *The Journal of biological chemistry* 264, 14965-14971.
- [37] Chambliss, K. L., Gray, R. G., Rylance, G., Pollitt, R. J., and Gibson, K. M. (2000) Molecular characterization of methylmalonate semialdehyde dehydrogenase deficiency, *J Inherit Metab Dis* 23, 497-504.
- [38] Mills, P. B., Struys, E., Jakobs, C., Plecko, B., Baxter, P., Baumgartner, M., Willemsen, M. A., Omran, H., Tacke, U., Uhlenberg, B., Weschke, B., and Clayton, P. T. (2006) Mutations in antiquitin in individuals with pyridoxine-dependent seizures, *Nature medicine* 12, 307-309.
- [39] Hu, C. A., Lin, W. W., Obie, C., and Valle, D. (1999) Molecular enzymology of mammalian Delta1-pyrroline-5-carboxylate synthase. Alternative splice donor utilization generates isoforms with different sensitivity to ornithine inhibition, *The Journal of biological chemistry* 274, 6754-6762.
- [40] Baumgartner, M. R., Rabier, D., Nassogne, M. C., Dufier, J. L., Padovani, J. P., Kamoun, P., Valle, D., and Saudubray, J. M. (2005) Delta1-pyrroline-5-carboxylate synthase deficiency: neurodegeneration, cataracts and connective tissue manifestations combined with hyperammonaemia and reduced ornithine, citrulline, arginine and proline, *Eur J Pediatr* 164, 31-36.
- [41] Perozich, J., Nicholas, H., Wang, B. C., Lindahl, R., and Hempel, J. (1999) Relationships within the aldehyde dehydrogenase extended family, *Protein Sci* 8, 137-146.

- [42] Hammen, P. K., Allali-Hassani, A., Hallenga, K., Hurley, T. D., and Weiner, H. (2002) Multiple conformations of NAD and NADH when bound to human cytosolic and mitochondrial aldehyde dehydrogenase, *Biochemistry* 41, 7156-7168.
- [43] MacGibbon, A. K., Blackwell, L. F., and Buckley, P. D. (1977) Kinetics of sheep-liver cytoplasmic aldehyde dehydrogenase, *European journal of biochemistry / FEBS* 77, 93-100.
- [44] Perez-Miller, S. J., and Hurley, T. D. (2003) Coenzyme isomerization is integral to catalysis in aldehyde dehydrogenase, *Biochemistry* 42, 7100-7109.
- [45] D'Ambrosio, K., Pailot, A., Talfournier, F., Didierjean, C., Benedetti, E., Aubry, A., Branlant, G., and Corbier, C. (2006) The first crystal structure of a thioacylenzyme intermediate in the ALDH family: new coenzyme conformation and relevance to catalysis, *Biochemistry* 45, 2978-2986.
- [46] Farres, J., Wang, T. T., Cunningham, S. J., and Weiner, H. (1995) Investigation of the active site cysteine residue of rat liver mitochondrial aldehyde dehydrogenase by site-directed mutagenesis, *Biochemistry* 34, 2592-2598.
- [47] Wang, X., and Weiner, H. (1995) Involvement of glutamate 268 in the active site of human liver mitochondrial (class 2) aldehyde dehydrogenase as probed by site-directed mutagenesis, *Biochemistry* 34, 237-243.
- [48] MacGibbon, A. K., Blackwell, L. F., and Buckley, P. D. (1977) Pre-steady-state kinetic studies on cytoplasmic sheep liver aldehyde dehydrogenase, *The Biochemical journal* 167, 469-477.
- [49] Blackwell, L. F., Motion, R. L., MacGibbon, A. K., Hardman, M. J., and Buckley, P. D. (1987) Evidence that the slow conformation change controlling NADH release from the enzyme is rate-limiting during the oxidation of propionaldehyde by aldehyde dehydrogenase, *The Biochemical journal* 242, 803-808.
- [50] Weiner, H., Hu, J. H., and Sanny, C. G. (1976) Rate-limiting steps for the esterase and dehydrogenase reaction catalyzed by horse liver aldehyde dehydrogenase, *The Journal of biological chemistry* 251, 3853-3855.
- [51] Mann, C. J., and Weiner, H. (1999) Differences in the roles of conserved glutamic acid residues in the active site of human class 3 and class 2 aldehyde dehydrogenases, *Protein Sci* 8, 1922-1929.
- [52] Feldman, R. I., and Weiner, H. (1972) Horse liver aldehyde dehydrogenase. II. Kinetics and mechanistic implications of the dehydrogenase and esterase activity, *The Journal of biological chemistry* 247, 267-272.

- [53] Sidhu, R. S., and Blair, A. H. (1975) Human liver aldehyde dehydrogenase. Esterase activity, *The Journal of biological chemistry* 250, 7894-7898.
- [54] Takahashi, K., Weiner, H., and Filmer, D. L. (1981) Effects of pH on horse liver aldehyde dehydrogenase: alterations in metal ion activation, number of functioning active sites, and hydrolysis of the acyl intermediate, *Biochemistry* 20, 6225-6230.
- [55] Perez-Miller, S., Younus, H., Vanam, R., Chen, C. H., Mochly-Rosen, D., and Hurley, T. D. (2010) Alda-1 is an agonist and chemical chaperone for the common human aldehyde dehydrogenase 2 variant, *Nature structural & molecular biology* 17, 159-164.
- [56] Koppaka, V., Thompson, D. C., Chen, Y., Ellermann, M., Nicolaou, K. C., Juvonen, R. O., Petersen, D., Deitrich, R. A., Hurley, T. D., and Vasiliou, V. (2012) Aldehyde dehydrogenase inhibitors: a comprehensive review of the pharmacology, mechanism of action, substrate specificity, and clinical application, *Pharmacological reviews* 64, 520-539.
- [57] Wang, M. F., Han, C. L., and Yin, S. J. (2009) Substrate specificity of human and yeast aldehyde dehydrogenases, *Chemico-biological interactions* 178, 36-39.
- [58] Bhat, P. V., and Samaha, H. (1999) Kinetic properties of the human liver cytosolic aldehyde dehydrogenase for retinal isomers, *Biochemical pharmacology* 57, 195-197.
- [59] Wang, X., Penzes, P., and Napoli, J. L. (1996) Cloning of a cDNA encoding an aldehyde dehydrogenase and its expression in Escherichia coli. Recognition of retinal as substrate, *The Journal of biological chemistry* 271, 16288-16293.
- [60] Duester, G. (2008) Retinoic acid synthesis and signaling during early organogenesis, *Cell* 134, 921-931.
- [61] Germain, P., Chambon, P., Eichele, G., Evans, R. M., Lazar, M. A., Leid, M., De Lera, A. R., Lotan, R., Mangelsdorf, D. J., and Gronemeyer, H. (2006) International Union of Pharmacology. LX. Retinoic acid receptors, *Pharmacological reviews* 58, 712-725.
- [62] Germain, P., Chambon, P., Eichele, G., Evans, R. M., Lazar, M. A., Leid, M., De Lera, A. R., Lotan, R., Mangelsdorf, D. J., and Gronemeyer, H. (2006) International Union of Pharmacology. LXIII. Retinoid X receptors, *Pharmacological reviews* 58, 760-772.
- [63] Kumar, S., Sandell, L. L., Trainor, P. A., Koentgen, F., and Duester, G. (2012) Alcohol and aldehyde dehydrogenases: retinoid metabolic effects in mouse knockout models, *Biochimica et biophysica acta* 1821, 198-205.

- [64] Marcato, P., Dean, C. A., Giacomantonio, C. A., and Lee, P. W. (2011) Aldehyde dehydrogenase: its role as a cancer stem cell marker comes down to the specific isoform, *Cell Cycle* 10, 1378-1384
- [65] Niederreither, K., Subbarayan, V., Dolle, P., and Chambon, P. (1999) Embryonic retinoic acid synthesis is essential for early mouse post-implantation development, *Nature genetics* 21, 444-448.
- [66] Dupe, V., Matt, N., Garnier, J. M., Chambon, P., Mark, M., and Ghyselinck, N. B. (2003) A newborn lethal defect due to inactivation of retinaldehyde dehydrogenase type 3 is prevented by maternal retinoic acid treatment, *Proceedings of the National Academy of Sciences of the United States of America* 100, 14036-14041.
- [67] Molotkov, A., and Duester, G. (2003) Genetic evidence that retinaldehyde dehydrogenase Raldh1 (Aldh1a1) functions downstream of alcohol dehydrogenase Adh1 in metabolism of retinol to retinoic acid, *The Journal of biological chemistry* 278, 36085-36090.
- [68] Canestro, C., Catchen, J. M., Rodriguez-Mari, A., Yokoi, H., and Postlethwait, J. H. (2009) Consequences of lineage-specific gene loss on functional evolution of surviving paralogs: ALDH1A and retinoic acid signaling in vertebrate genomes, *PLoS Genet* 5, e1000496.
- [69] Ziouzenkova, O., Orasanu, G., Sharlach, M., Akiyama, T. E., Berger, J. P., Viereck, J., Hamilton, J. A., Tang, G., Dolnikowski, G. G., Vogel, S., Duester, G., and Plutzky, J. (2007) Retinaldehyde represses adipogenesis and diet-induced obesity, *Nature medicine* 13, 695-702.
- [70] Reichert, B., Yasmeen, R., Jeyakumar, S. M., Yang, F., Thomou, T., Alder, H., Duester, G., Maiseyeu, A., Mihai, G., Harrison, E. H., Rajagopalan, S., Kirkland, J. L., and Ziouzenkova, O. (2011) Concerted action of aldehyde dehydrogenases influences depot-specific fat formation, *Mol Endocrinol* 25, 799-809.
- [71] Lin, M., and Napoli, J. L. (2000) cDNA cloning and expression of a human aldehyde dehydrogenase (ALDH) active with 9-cis-retinal and identification of a rat ortholog, ALDH12, *The Journal of biological chemistry* 275, 40106-40112.
- [72] Ueshima, Y., Matsuda, Y., Tsutsumi, M., and Takada, A. (1993) Role of the aldehyde dehydrogenase-1 isozyme in the metabolism of acetaldehyde, *Alcohol and alcoholism 1B*, 15-19.
- [73] King, G., and Holmes, R. (1997) Human corneal and lens aldehyde dehydrogenases. Purification and properties of human lens ALDH1 and differential expression as major soluble proteins in human lens (ALDH1) and cornea (ALDH3), *Advances in experimental medicine and biology* 414, 19-27.

- [74] Lassen, N., Black, W. J., Estey, T., and Vasiliou, V. (2008) The role of corneal crystallins in the cellular defense mechanisms against oxidative stress, *Semin Cell Dev Biol* 19, 100-112.
- [75] Zhou, J., and Weiner, H. (1997) Binding of thyroxine analogs to human liver aldehyde dehydrogenases, *European journal of biochemistry / FEBS* 245, 123-128.
- [76] Schnier, J. B., Kaur, G., Kaiser, A., Stinson, S. F., Sausville, E. A., Gardner, J., Nishi, K., Bradbury, E. M., and Senderowicz, A. M. (1999) Identification of cytosolic aldehyde dehydrogenase 1 from non-small cell lung carcinomas as a flavopiridol-binding protein, *FEBS letters* 454, 100-104.
- [77] Klyosov, A. A., Rashkovetsky, L. G., Tahir, M. K., and Keung, W. M. (1996) Possible role of liver cytosolic and mitochondrial aldehyde dehydrogenases in acetaldehyde metabolism, *Biochemistry* 35, 4445-4456.
- [78] Chen, Z., Foster, M. W., Zhang, J., Mao, L., Rockman, H. A., Kawamoto, T., Kitagawa, K., Nakayama, K. I., Hess, D. T., and Stamler, J. S. (2005) An essential role for mitochondrial aldehyde dehydrogenase in nitroglycerin bioactivation, *Proceedings of the National Academy of Sciences of the United States of America* 102, 12159-12164.
- [79] Stagos, D., Chen, Y., Brocker, C., Donald, E., Jackson, B. C., Orlicky, D. J., Thompson, D. C., and Vasiliou, V. (2010) Aldehyde dehydrogenase 1B1: molecular cloning and characterization of a novel mitochondrial acetaldehyde-metabolizing enzyme, *Drug metabolism and disposition: the biological fate of chemicals* 38, 1679-1687.
- [80] Singh, S., Chen, Y., Matsumoto, A., Orlicky, D. J., Dong, H., Thompson, D. C., and Vasiliou, V. (2015) ALDH1B1 links alcohol consumption and diabetes, *Biochemical and biophysical research communications* 463, 768-773.
- [81] Singh, S., Arcaroli, J. J., Orlicky, D. J., Chen, Y., Messersmith, W. A., Bagby, S., Purkey, A., Quackenbush, K. S., Thompson, D. C., and Vasiliou, V. (2016) Aldehyde Dehydrogenase 1B1 as a Modulator of Pancreatic Adenocarcinoma, *Pancreas* 45, 117-122.
- [82] Chen, Y., Orlicky, D. J., Matsumoto, A., Singh, S., Thompson, D. C., and Vasiliou, V. (2011) Aldehyde dehydrogenase 1B1 (ALDH1B1) is a potential biomarker for human colon cancer, *Biochemical and biophysical research communications* 405, 173-179.
- [83] Singh, S., Arcaroli, J., Chen, Y., Thompson, D. C., Messersmith, W., Jimeno, A., and Vasiliou, V. (2015) ALDH1B1 Is Crucial for Colon Tumorigenesis by Modulating Wnt/beta-Catenin, Notch and PI3K/Akt Signaling Pathways, *PLoS one* 10, e0121648.

- [84] Krupenko, S. A., Horstman, D. A., Wagner, C., and Cook, R. J. (1995) Baculovirus expression and purification of rat 10-formyltetrahydrofolate dehydrogenase, *Protein Expr Purif* 6, 457-464.
- [85] Tsybovsky, Y., Donato, H., Krupenko, N. I., Davies, C., and Krupenko, S. A. (2007) Crystal structures of the carboxyl terminal domain of rat 10-formyltetrahydrofolate dehydrogenase: implications for the catalytic mechanism of aldehyde dehydrogenases, *Biochemistry* 46, 2917-2929.
- [86] Krupenko, S. A. (2009) FDH: an aldehyde dehydrogenase fusion enzyme in folate metabolism, *Chemico-biological interactions* 178, 84-93.
- [87] Wagner, C. (2001) Biochemical role of folate in cellular metabolism (Reprinted from *Folate and Health Disease*, pgs 23-42, 1995), *Clin Res Regul Aff* 18, 161-180.
- [88] Krupenko, S. A., and Oleinik, N. V. (2002) 10-formyltetrahydrofolate dehydrogenase, one of the major folate enzymes, is down-regulated in tumor tissues and possesses suppressor effects on cancer cells, *Cell Growth Differ* 13, 227-236.
- [89] Skrzydlewska, E. (2003) Toxicological and metabolic consequences of methanol poisoning, *Toxicol Mech Methods* 13, 277-293.
- [90] Reya, T., Morrison, S. J., Clarke, M. F., and Weissman, I. L. (2001) Stem cells, cancer, and cancer stem cells, *Nature* 414, 105-111.
- [91] Friedmann-Morvinski, D., and Verma, I. M. (2014) Dedifferentiation and reprogramming: origins of cancer stem cells, *EMBO Rep* 15, 244-253.
- [92] Sell, S. (2004) Stem cell origin of cancer and differentiation therapy, *Crit Rev Oncol Hematol* 51, 1-28.
- [93] Lapidot, T., Sirard, C., Vormoor, J., Murdoch, B., Hoang, T., Caceres-Cortes, J., Minden, M., Paterson, B., Caligiuri, M. A., and Dick, J. E. (1994) A cell initiating human acute myeloid leukaemia after transplantation into SCID mice, *Nature* 367, 645-648.
- [94] Al-Hajj, M., Wicha, M. S., Benito-Hernandez, A., Morrison, S. J., and Clarke, M. F. (2003) Prospective identification of tumorigenic breast cancer cells, *Proceedings of the National Academy of Sciences of the United States of America* 100, 3983-3988.
- [95] Taipale, J., and Beachy, P. A. (2001) The Hedgehog and Wnt signalling pathways in cancer, *Nature* 411, 349-354.
- [96] Wicha, M. S., Liu, S., and Dontu, G. (2006) Cancer stem cells: an old idea--a paradigm shift, *Cancer research* 66, 1883-1890; discussion 1895-1886.

- [97] Douville, J., Beaulieu, R., and Balicki, D. (2009) ALDH1 as a functional marker of cancer stem and progenitor cells, *Stem Cells Dev* 18, 17-25.
- [98] Tomita, H., Tanaka, K., Tanaka, T., and Hara, A. (2016) Aldehyde dehydrogenase 1A1 in stem cells and cancer, *Oncotarget* 7, 11018-11032.
- [99] Levi, B. P., Yilmaz, O. H., Duester, G., and Morrison, S. J. (2009) Aldehyde dehydrogenase 1a1 is dispensable for stem cell function in the mouse hematopoietic and nervous systems, *Blood* 113, 1670-1680.
- [100] Chanda, B., Ditadi, A., Iscove, N. N., and Keller, G. (2013) Retinoic acid signaling is essential for embryonic hematopoietic stem cell development, *Cell* 155, 215-227.
- [101] Qiu, J. J., Zeisig, B. B., Li, S., Liu, W., Chu, H., Song, Y., Giordano, A., Schwaller, J., Gronemeyer, H., Dong, S., and So, C. W. (2015) Critical role of retinoid/rexinoid signaling in mediating transformation and therapeutic response of NUP98-RARG leukemia, *Leukemia* 29, 1153-1162.
- [102] Ginestier, C., Wicinski, J., Cervera, N., Monville, F., Finetti, P., Bertucci, F., Wicha, M. S., Birnbaum, D., and Charafe-Jauffret, E. (2009) Retinoid signaling regulates breast cancer stem cell differentiation, *Cell Cycle* 8, 3297-3302.
- [103] Singh, S., Brocker, C., Koppaka, V., Chen, Y., Jackson, B. C., Matsumoto, A., Thompson, D. C., and Vasiliou, V. (2013) Aldehyde dehydrogenases in cellular responses to oxidative/electrophilic stress, *Free radical biology & medicine* 56, 89-101.
- [104] Miyata, T., Takizawa, S., and van Ypersele de Strihou, C. (2011) Hypoxia. 1. Intracellular sensors for oxygen and oxidative stress: novel therapeutic targets, *Am J Physiol Cell Physiol* 300, C226-231.
- [105] Moreb, J., Zucali, J. R., Zhang, Y., Colvin, M. O., and Gross, M. A. (1992) Role of aldehyde dehydrogenase in the protection of hematopoietic progenitor cells from 4-hydroperoxycyclophosphamide by interleukin 1 beta and tumor necrosis factor, *Cancer research* 52, 1770-1774.
- [106] Kastan, M. B., Schlaffer, E., Russo, J. E., Colvin, O. M., Civin, C. I., and Hilton, J. (1990) Direct demonstration of elevated aldehyde dehydrogenase in human hematopoietic progenitor cells, *Blood* 75, 1947-1950.
- [107] Saw, Y. T., Yang, J., Ng, S. K., Liu, S., Singh, S., Singh, M., Welch, W. R., Tsuda, H., Fong, W. P., Thompson, D., Vasiliou, V., Berkowitz, R. S., and Ng, S. W. (2012) Characterization of aldehyde dehydrogenase isozymes in ovarian cancer tissues and sphere cultures, *BMC Cancer* 12, 329.

- [108] Charafe-Jauffret, E., Ginestier, C., Iovino, F., Tarpin, C., Diebel, M., Esterni, B., Houvenaeghel, G., Extra, J. M., Bertucci, F., Jacquemier, J., Xerri, L., Dontu, G., Stassi, G., Xiao, Y., Barsky, S. H., Birnbaum, D., Viens, P., and Wicha, M. S. (2010) Aldehyde dehydrogenase 1-positive cancer stem cells mediate metastasis and poor clinical outcome in inflammatory breast cancer, *Clin Cancer Res* 16, 45-55.
- [109] Lukacs, R. U., Lawson, D. A., Xin, L., Zong, Y., Garraway, I., Goldstein, A. S., Memarzadeh, S., and Witte, O. N. (2008) Epithelial stem cells of the prostate and their role in cancer progression, *Cold Spring Harb Symp Quant Biol* 73, 491-502.
- [110] Sodek, K. L., Ringuette, M. J., and Brown, T. J. (2009) Compact spheroid formation by ovarian cancer cells is associated with contractile behavior and an invasive phenotype, *Int J Cancer* 124, 2060-2070.
- [111] Condello, S., Morgan, C. A., Nagdas, S., Cao, L., Turek, J., Hurley, T. D., and Matei, D. (2015) beta-Catenin-regulated ALDH1A1 is a target in ovarian cancer spheroids, *Oncogene* 34, 2297-2308.
- [112] Polakis, P. (2012) Wnt signaling in cancer, *Cold Spring Harb Perspect Biol* 4.
- [113] Martien, M. F. (2015) Bidirectional Regulation of YAP and ALDH1A1, In *Biochemistry and Molecular Biology*, Indiana University.
- [114] Rodriguez-Zavala, J. S., and Weiner, H. (2002) Structural aspects of aldehyde dehydrogenase that influence dimer-tetramer formation, *Biochemistry* 41, 8229-8237.
- [115] Eriksson, C. J. (1977) Acetaldehyde metabolism in vivo during ethanol oxidation, *Advances in experimental medicine and biology* 85A, 319-341.
- [116] Stewart, M. J., Malek, K., Xiao, Q., Dipple, K. M., and Crabb, D. W. (1995) The novel aldehyde dehydrogenase gene, ALDH5, encodes an active aldehyde dehydrogenase enzyme, *Biochemical and biophysical research communications* 211, 144-151.
- [117] Brooks, P. J., Enoch, M. A., Goldman, D., Li, T. K., and Yokoyama, A. (2009) The alcohol flushing response: an unrecognized risk factor for esophageal cancer from alcohol consumption, *PLoS medicine* 6, e50.
- [118] Luo, H. R., Wu, G. S., Pakstis, A. J., Tong, L., Oota, H., Kidd, K. K., and Zhang, Y. P. (2009) Origin and dispersal of atypical aldehyde dehydrogenase ALDH2487Lys, *Gene* 435, 96-103.
- [119] Goedde, H. W., Agarwal, D. P., Fritze, G., Meier-Tackmann, D., Singh, S., Beckmann, G., Bhatia, K., Chen, L. Z., Fang, B., Lisker, R., and et al. (1992) Distribution of ADH2 and ALDH2 genotypes in different populations, *Hum Genet* 88, 344-346.

- [120] Farres, J., Wang, X., Takahashi, K., Cunningham, S. J., Wang, T. T., and Weiner, H. (1994) Effects of changing glutamate 487 to lysine in rat and human liver mitochondrial aldehyde dehydrogenase. A model to study human (Oriental type) class 2 aldehyde dehydrogenase, *The Journal of biological chemistry* 269, 13854-13860.
- [121] Larson, H. N., Zhou, J., Chen, Z., Stamler, J. S., Weiner, H., and Hurley, T. D. (2007) Structural and functional consequences of coenzyme binding to the inactive asian variant of mitochondrial aldehyde dehydrogenase: roles of residues 475 and 487, *The Journal of biological chemistry* 282, 12940-12950.
- [122] Larson, H. N., Weiner, H., and Hurley, T. D. (2005) Disruption of the coenzyme binding site and dimer interface revealed in the crystal structure of mitochondrial aldehyde dehydrogenase "Asian" variant, *The Journal of biological chemistry* 280, 30550-30556.
- [123] Chao, Y. C., Liou, S. R., Tsai, S. F., and Yin, S. J. (1993) Dominance of the mutant ALDH2(2) allele in the expression of human stomach aldehyde dehydrogenase-2 activity, *Proceedings of the National Science Council, Republic of China. Part B, Life sciences* 17, 98-102.
- [124] Higuchi, S., Matsushita, S., Murayama, M., Takagi, S., and Hayashida, M. (1995) Alcohol and aldehyde dehydrogenase polymorphisms and the risk for alcoholism, *Am J Psychiatry* 152, 1219-1221.
- [125] Higuchi, S., Matsushita, S., Imazeki, H., Kinoshita, T., Takagi, S., and Kono, H. (1994) Aldehyde dehydrogenase genotypes in Japanese alcoholics, *Lancet* 343, 741-742.
- [126] Asakage, T., Yokoyama, A., Haneda, T., Yamazaki, M., Muto, M., Yokoyama, T., Kato, H., Igaki, H., Tsujinaka, T., Kumagai, Y., Yokoyama, M., Omori, T., and Watanabe, H. (2007) Genetic polymorphisms of alcohol and aldehyde dehydrogenases, and drinking, smoking and diet in Japanese men with oral and pharyngeal squamous cell carcinoma, *Carcinogenesis* 28, 865-874.
- [127] Enomoto, N., Takase, S., Takada, N., and Takada, A. (1991) Alcoholic liver disease in heterozygotes of mutant and normal aldehyde dehydrogenase-2 genes, *Hepatology* 13, 1071-1075.
- [128] (2014) National Survey on Drug Use and Health, Substance Abuse and Mental Health Services Administration.
- [129] Sacks, J. J., Gonzales, K. R., Bouchery, E. E., Tomedi, L. E., and Brewer, R. D. (2015) 2010 National and State Costs of Excessive Alcohol Consumption, *Am J Prev Med* 49, e73-79.

- [130] Baan, R., Straif, K., Grosse, Y., Secretan, B., El Ghissassi, F., Bouvard, V., Altieri, A., Coglianò, V., and Group, W. H. O. I. A. f. R. o. C. M. W. (2007) Carcinogenicity of alcoholic beverages, *Lancet Oncol* 8, 292-293.
- [131] Chen, Y. C., Peng, G. S., Tsao, T. P., Wang, M. F., Lu, R. B., and Yin, S. J. (2009) Pharmacokinetic and pharmacodynamic basis for overcoming acetaldehyde-induced adverse reaction in Asian alcoholics, heterozygous for the variant ALDH2*2 gene allele, *Pharmacogenetics and genomics* 19, 588-599.
- [132] Vakevainen, S., Tillonen, J., Agarwal, D. P., Srivastava, N., and Salaspuro, M. (2000) High salivary acetaldehyde after a moderate dose of alcohol in ALDH2-deficient subjects: strong evidence for the local carcinogenic action of acetaldehyde, *Alcoholism, clinical and experimental research* 24, 873-877.
- [133] Yokoyama, A., Tsutsumi, E., Imazeki, H., Suwa, Y., Nakamura, C., Mizukami, T., and Yokoyama, T. (2008) Salivary acetaldehyde concentration according to alcoholic beverage consumed and aldehyde dehydrogenase-2 genotype, *Alcoholism, clinical and experimental research* 32, 1607-1614.
- [134] Lorenti Garcia, C., Mechilli, M., Proietti De Santis, L., Schinoppi, A., Kobos, K., and Palitti, F. (2009) Relationship between DNA lesions, DNA repair and chromosomal damage induced by acetaldehyde, *Mutation research* 662, 3-9.
- [135] Cho, Y. J., Wang, H., Kozekov, I. D., Kurtz, A. J., Jacob, J., Voehler, M., Smith, J., Harris, T. M., Lloyd, R. S., Rizzo, C. J., and Stone, M. P. (2006) Stereospecific formation of interstrand carbinolamine DNA cross-links by crotonaldehyde- and acetaldehyde-derived alpha-CH3-gamma-OH-1,N2-propano-2'-deoxyguanosine adducts in the 5'-CpG-3' sequence, *Chemical research in toxicology* 19, 195-208.
- [136] Stein, S., Lao, Y., Yang, I. Y., Hecht, S. S., and Moriya, M. (2006) Genotoxicity of acetaldehyde- and crotonaldehyde-induced 1,N2-propanodeoxyguanosine DNA adducts in human cells, *Mutation research* 608, 1-7.
- [137] Nagayoshi, H., Matsumoto, A., Nishi, R., Kawamoto, T., Ichiba, M., and Matsuda, T. (2009) Increased formation of gastric N(2)-ethylidene-2'-deoxyguanosine DNA adducts in aldehyde dehydrogenase-2 knockout mice treated with ethanol, *Mutation research* 673, 74-77.
- [138] Boffetta, P., and Hashibe, M. (2006) Alcohol and cancer, *Lancet Oncol* 7, 149-156.
- [139] Seitz, H. K., and Meier, P. (2007) The role of acetaldehyde in upper digestive tract cancer in alcoholics, *Transl Res* 149, 293-297.
- [140] Yokoyama, A., Muramatsu, T., Ohmori, T., Higuchi, S., Hayashida, M., and Ishii, H. (1996) Esophageal cancer and aldehyde dehydrogenase-2 genotypes in Japanese males, *Cancer Epidemiol Biomarkers Prev* 5, 99-102.

- [141] Matsuda, T., Yabushita, H., Kanaly, R. A., Shibutani, S., and Yokoyama, A. (2006) Increased DNA damage in ALDH2-deficient alcoholics, *Chemical research in toxicology* 19, 1374-1378.
- [142] O'Shea, K. S., and Kaufman, M. H. (1979) The teratogenic effect of acetaldehyde: implications for the study of the fetal alcohol syndrome, *J Anat* 128, 65-76.
- [143] Langevin, F., Crossan, G. P., Rosado, I. V., Arends, M. J., and Patel, K. J. (2011) Fancd2 counteracts the toxic effects of naturally produced aldehydes in mice, *Nature* 475, 53-58.
- [144] Moldovan, G. L., and D'Andrea, A. D. (2009) How the fanconi anemia pathway guards the genome, *Annu Rev Genet* 43, 223-249.
- [145] Kutler, D. I., Auerbach, A. D., Satagopan, J., Giampietro, P. F., Batish, S. D., Huvos, A. G., Goberdhan, A., Shah, J. P., and Singh, B. (2003) High incidence of head and neck squamous cell carcinoma in patients with Fanconi anemia, *Arch Otolaryngol Head Neck Surg* 129, 106-112.
- [146] Duan, J., McFadden, G. E., Borgerding, A. J., Norby, F. L., Ren, B. H., Ye, G., Epstein, P. N., and Ren, J. (2002) Overexpression of alcohol dehydrogenase exacerbates ethanol-induced contractile defect in cardiac myocytes, *American journal of physiology. Heart and circulatory physiology* 282, H1216-1222.
- [147] Hintz, K. K., Relling, D. P., Saari, J. T., Borgerding, A. J., Duan, J., Ren, B. H., Kato, K., Epstein, P. N., and Ren, J. (2003) Cardiac overexpression of alcohol dehydrogenase exacerbates cardiac contractile dysfunction, lipid peroxidation, and protein damage after chronic ethanol ingestion, *Alcoholism, clinical and experimental research* 27, 1090-1098.
- [148] Ma, H., Li, J., Gao, F., and Ren, J. (2009) Aldehyde dehydrogenase 2 ameliorates acute cardiac toxicity of ethanol: role of protein phosphatase and forkhead transcription factor, *Journal of the American College of Cardiology* 54, 2187-2196.
- [149] Zhang, Y., and Ren, J. (2011) ALDH2 in alcoholic heart diseases: molecular mechanism and clinical implications, *Pharmacology & therapeutics* 132, 86-95.
- [150] Ge, W., Guo, R., and Ren, J. (2011) AMP-dependent kinase and autophagic flux are involved in aldehyde dehydrogenase-2-induced protection against cardiac toxicity of ethanol, *Free radical biology & medicine* 51, 1736-1748.
- [151] Chen, C. H., Budas, G. R., Churchill, E. N., Disatnik, M. H., Hurley, T. D., and Mochly-Rosen, D. (2008) Activation of aldehyde dehydrogenase-2 reduces ischemic damage to the heart, *Science* 321, 1493-1495.

- [152] Chen, C. H., Sun, L., and Mochly-Rosen, D. (2010) Mitochondrial aldehyde dehydrogenase and cardiac diseases, *Cardiovascular research* 88, 51-57.
- [153] Radovanovic, S., Savic-Radojevic, A., Pljesa-Ercegovac, M., Djukic, T., Suvakov, S., Krotin, M., Simic, D. V., Matic, M., Radojicic, Z., Pekmezovic, T., and Simic, T. (2012) Markers of oxidative damage and antioxidant enzyme activities as predictors of morbidity and mortality in patients with chronic heart failure, *J Card Fail* 18, 493-501.
- [154] Roede, J. R., and Jones, D. P. (2010) Reactive species and mitochondrial dysfunction: mechanistic significance of 4-hydroxynonenal, *Environmental and molecular mutagenesis* 51, 380-390.
- [155] Chen, C. H., Ferreira, J. C., Gross, E. R., and Mochly-Rosen, D. (2014) Targeting aldehyde dehydrogenase 2: new therapeutic opportunities, *Physiological reviews* 94, 1-34.
- [156] Endo, J., Sano, M., Katayama, T., Hishiki, T., Shinmura, K., Morizane, S., Matsushashi, T., Katsumata, Y., Zhang, Y., Ito, H., Nagahata, Y., Marchitti, S., Nishimaki, K., Wolf, A. M., Nakanishi, H., Hattori, F., Vasiliou, V., Adachi, T., Ohsawa, I., Taguchi, R., Hirabayashi, Y., Ohta, S., Suematsu, M., Ogawa, S., and Fukuda, K. (2009) Metabolic remodeling induced by mitochondrial aldehyde stress stimulates tolerance to oxidative stress in the heart, *Circ Res* 105, 1118-1127.
- [157] Ma, H., Guo, R., Yu, L., Zhang, Y., and Ren, J. (2011) Aldehyde dehydrogenase 2 (ALDH2) rescues myocardial ischaemia/reperfusion injury: role of autophagy paradox and toxic aldehyde, *Eur Heart J* 32, 1025-1038.
- [158] Doorn, J. A., Hurley, T. D., and Petersen, D. R. (2006) Inhibition of human mitochondrial aldehyde dehydrogenase by 4-hydroxynon-2-enal and 4-oxonon-2-enal, *Chemical research in toxicology* 19, 102-110.
- [159] Takagi, S., Iwai, N., Yamauchi, R., Kojima, S., Yasuno, S., Baba, T., Terashima, M., Tsutsumi, Y., Suzuki, S., Morii, I., Hanai, S., Ono, K., Baba, S., Tomoike, H., Kawamura, A., Miyazaki, S., Nonogi, H., and Goto, Y. (2002) Aldehyde dehydrogenase 2 gene is a risk factor for myocardial infarction in Japanese men, *Hypertension research : official journal of the Japanese Society of Hypertension* 25, 677-681.
- [160] Xu, F., Chen, Y. G., Xue, L., Li, R. J., Zhang, H., Bian, Y., Zhang, C., Lv, R. J., Feng, J. B., and Zhang, Y. (2011) Role of aldehyde dehydrogenase 2 Glu504lys polymorphism in acute coronary syndrome, *J Cell Mol Med* 15, 1955-1962.

- [161] Kato, N., Takeuchi, F., Tabara, Y., Kelly, T. N., Go, M. J., Sim, X., Tay, W. T., Chen, C. H., Zhang, Y., Yamamoto, K., Katsuya, T., Yokota, M., Kim, Y. J., Ong, R. T., Nabika, T., Gu, D., Chang, L. C., Kokubo, Y., Huang, W., Ohnaka, K., Yamori, Y., Nakashima, E., Jaquish, C. E., Lee, J. Y., Seielstad, M., Isono, M., Hixson, J. E., Chen, Y. T., Miki, T., Zhou, X., Sugiyama, T., Jeon, J. P., Liu, J. J., Takayanagi, R., Kim, S. S., Aung, T., Sung, Y. J., Zhang, X., Wong, T. Y., Han, B. G., Kobayashi, S., Ogihara, T., Zhu, D., Iwai, N., Wu, J. Y., Teo, Y. Y., Tai, E. S., Cho, Y. S., and He, J. (2011) Meta-analysis of genome-wide association studies identifies common variants associated with blood pressure variation in east Asians, *Nature genetics* 43, 531-538.
- [162] Marsh, N., and Marsh, A. (2000) A short history of nitroglycerine and nitric oxide in pharmacology and physiology, *Clin Exp Pharmacol Physiol* 27, 313-319.
- [163] Abrams, J. (1985) Hemodynamic effects of nitroglycerin and long-acting nitrates, *American heart journal* 110, 216-224.
- [164] Chen, Z., Zhang, J., and Stamler, J. S. (2002) Identification of the enzymatic mechanism of nitroglycerin bioactivation, *Proceedings of the National Academy of Sciences of the United States of America* 99, 8306-8311.
- [165] Lang, B. S., Gorren, A. C., Oberdorfer, G., Wenzl, M. V., Furdui, C. M., Poole, L. B., Mayer, B., and Gruber, K. (2012) Vascular bioactivation of nitroglycerin by aldehyde dehydrogenase-2: reaction intermediates revealed by crystallography and mass spectrometry, *The Journal of biological chemistry* 287, 38124-38134.
- [166] Kosugi, M., Nakagomi, A., Shibui, T., Kato, K., Kusama, Y., Atarashi, H., and Mizuno, K. (2011) Effect of long-term nitrate treatment on cardiac events in patients with vasospastic angina, *Circulation journal : official journal of the Japanese Circulation Society* 75, 2196-2205.
- [167] Munzel, T., Daiber, A., and Mulsch, A. (2005) Explaining the phenomenon of nitrate tolerance, *Circ Res* 97, 618-628.
- [168] Chen, Z., and Stamler, J. S. (2006) Bioactivation of nitroglycerin by the mitochondrial aldehyde dehydrogenase, *Trends Cardiovasc Med* 16, 259-265.
- [169] Kollau, A., Hofer, A., Russwurm, M., Koesling, D., Keung, W. M., Schmidt, K., Brunner, F., and Mayer, B. (2005) Contribution of aldehyde dehydrogenase to mitochondrial bioactivation of nitroglycerin: evidence for the activation of purified soluble guanylate cyclase through direct formation of nitric oxide, *The Biochemical journal* 385, 769-777.

- [170] Sydow, K., Daiber, A., Oelze, M., Chen, Z., August, M., Wendt, M., Ullrich, V., Mulsch, A., Schulz, E., Keaney, J. F., Jr., Stamler, J. S., and Munzel, T. (2004) Central role of mitochondrial aldehyde dehydrogenase and reactive oxygen species in nitroglycerin tolerance and cross-tolerance, *The Journal of clinical investigation* 113, 482-489.
- [171] Li, Y., Zhang, D., Jin, W., Shao, C., Yan, P., Xu, C., Sheng, H., Liu, Y., Yu, J., Xie, Y., Zhao, Y., Lu, D., Nebert, D. W., Harrison, D. C., Huang, W., and Jin, L. (2006) Mitochondrial aldehyde dehydrogenase-2 (ALDH2) Glu504Lys polymorphism contributes to the variation in efficacy of sublingual nitroglycerin, *The Journal of clinical investigation* 116, 506-511.
- [172] Mackenzie, I. S., Maki-Petaja, K. M., McEniery, C. M., Bao, Y. P., Wallace, S. M., Cheriyan, J., Monteith, S., Brown, M. J., and Wilkinson, I. B. (2005) Aldehyde dehydrogenase 2 plays a role in the bioactivation of nitroglycerin in humans, *Arterioscler Thromb Vasc Biol* 25, 1891-1895.
- [173] Beretta, M., Gorren, A. C., Wenzl, M. V., Weis, R., Russwurm, M., Koesling, D., Schmidt, K., and Mayer, B. (2010) Characterization of the East Asian variant of aldehyde dehydrogenase-2: bioactivation of nitroglycerin and effects of Alda-1, *The Journal of biological chemistry* 285, 943-952.
- [174] Sun, L., Ferreira, J. C., and Mochly-Rosen, D. (2011) ALDH2 activator inhibits increased myocardial infarction injury by nitroglycerin tolerance, *Science translational medicine* 3, 107ra111.
- [175] Reed, T. T. (2011) Lipid peroxidation and neurodegenerative disease, *Free radical biology & medicine* 51, 1302-1319.
- [176] Zhu, X., Smith, M. A., Perry, G., and Aliev, G. (2004) Mitochondrial failures in Alzheimer's disease, *Am J Alzheimers Dis Other Demen* 19, 345-352.
- [177] Farrer, M. J. (2006) Genetics of Parkinson disease: paradigm shifts and future prospects, *Nat Rev Genet* 7, 306-318.
- [178] Michotte, A. (2003) Recent developments in the neuropathological diagnosis of Parkinson's disease and parkinsonism, *Acta Neurol Belg* 103, 155-158.
- [179] Panneton, W. M., Kumar, V. B., Gan, Q., Burke, W. J., and Galvin, J. E. (2010) The neurotoxicity of DOPAL: behavioral and stereological evidence for its role in Parkinson disease pathogenesis, *PloS one* 5, e15251.
- [180] Tarazi, F. I., Sahli, Z. T., Wolny, M., and Mousa, S. A. (2014) Emerging therapies for Parkinson's disease: from bench to bedside, *Pharmacology & therapeutics* 144, 123-133.

- [181] Yoritaka, A., Hattori, N., Uchida, K., Tanaka, M., Stadtman, E. R., and Mizuno, Y. (1996) Immunohistochemical detection of 4-hydroxynonenal protein adducts in Parkinson disease, *Proceedings of the National Academy of Sciences of the United States of America* 93, 2696-2701.
- [182] MacKerell, A. D., Jr., and Pietruszko, R. (1987) Chemical modification of human aldehyde dehydrogenase by physiological substrate, *Biochimica et biophysica acta* 911, 306-317.
- [183] Florang, V. R., Rees, J. N., Brogden, N. K., Anderson, D. G., Hurley, T. D., and Doorn, J. A. (2007) Inhibition of the oxidative metabolism of 3,4-dihydroxyphenylacetaldehyde, a reactive intermediate of dopamine metabolism, by 4-hydroxy-2-nonenal, *Neurotoxicology* 28, 76-82.
- [184] Fitzmaurice, A. G., Rhodes, S. L., Lulla, A., Murphy, N. P., Lam, H. A., O'Donnell, K. C., Barnhill, L., Casida, J. E., Cockburn, M., Sagasti, A., Stahl, M. C., Maidment, N. T., Ritz, B., and Bronstein, J. M. (2013) Aldehyde dehydrogenase inhibition as a pathogenic mechanism in Parkinson disease, *Proceedings of the National Academy of Sciences of the United States of America* 110, 636-641.
- [185] Galter, D., Buervenich, S., Carmine, A., Anvret, M., and Olson, L. (2003) ALDH1 mRNA: presence in human dopamine neurons and decreases in substantia nigra in Parkinson's disease and in the ventral tegmental area in schizophrenia, *Neurobiol Dis* 14, 637-647.
- [186] Werner, C. J., Heyny-von Haussen, R., Mall, G., and Wolf, S. (2008) Proteome analysis of human substantia nigra in Parkinson's disease, *Proteome Sci* 6, 8.
- [187] Wey, M. C., Fernandez, E., Martinez, P. A., Sullivan, P., Goldstein, D. S., and Strong, R. (2012) Neurodegeneration and motor dysfunction in mice lacking cytosolic and mitochondrial aldehyde dehydrogenases: implications for Parkinson's disease, *PLoS one* 7, e31522.
- [188] Yu, H. S., Oyama, T., Isse, T., Kitakawa, K., Ogawa, M., Pham, T. T., and Kawamoto, T. (2009) Characteristics of aldehyde dehydrogenase 2 (Aldh2) knockout mice, *Toxicol Mech Methods* 19, 535-540.
- [189] Anderson, D. W., Schray, R. C., Duester, G., and Schneider, J. S. (2011) Functional significance of aldehyde dehydrogenase ALDH1A1 to the nigrostriatal dopamine system, *Brain Res* 1408, 81-87.
- [190] Norfray, J. F., and Provenzale, J. M. (2004) Alzheimer's disease: neuropathologic findings and recent advances in imaging, *AJR Am J Roentgenol* 182, 3-13.
- [191] Brookmeyer, R., Johnson, E., Ziegler-Graham, K., and Arrighi, H. M. (2007) Forecasting the global burden of Alzheimer's disease, *Alzheimers Dement* 3, 186-191.

- [192] Williams, T. I., Lynn, B. C., Markesbery, W. R., and Lovell, M. A. (2006) Increased levels of 4-hydroxynonenal and acrolein, neurotoxic markers of lipid peroxidation, in the brain in Mild Cognitive Impairment and early Alzheimer's disease, *Neurobiol Aging* 27, 1094-1099.
- [193] McGrath, L. T., McGleenon, B. M., Brennan, S., McColl, D., Mc, I. S., and Passmore, A. P. (2001) Increased oxidative stress in Alzheimer's disease as assessed with 4-hydroxynonenal but not malondialdehyde, *QJM* 94, 485-490.
- [194] Hao, P. P., Chen, Y. G., Wang, J. L., Wang, X. L., and Zhang, Y. (2011) Meta-analysis of aldehyde dehydrogenase 2 gene polymorphism and Alzheimer's disease in East Asians, *Can J Neurol Sci* 38, 500-506.
- [195] Kamino, K., Nagasaka, K., Imagawa, M., Yamamoto, H., Yoneda, H., Ueki, A., Kitamura, S., Namekata, K., Miki, T., and Ohta, S. (2000) Deficiency in mitochondrial aldehyde dehydrogenase increases the risk for late-onset Alzheimer's disease in the Japanese population, *Biochemical and biophysical research communications* 273, 192-196.
- [196] Ohsawa, I., Nishimaki, K., Yasuda, C., Kamino, K., and Ohta, S. (2003) Deficiency in a mitochondrial aldehyde dehydrogenase increases vulnerability to oxidative stress in PC12 cells, *Journal of neurochemistry* 84, 1110-1117.
- [197] Ohsawa, I., Nishimaki, K., Murakami, Y., Suzuki, Y., Ishikawa, M., and Ohta, S. (2008) Age-dependent neurodegeneration accompanying memory loss in transgenic mice defective in mitochondrial aldehyde dehydrogenase 2 activity, *The Journal of neuroscience : the official journal of the Society for Neuroscience* 28, 6239-6249.
- [198] Solito, R., Corti, F., Chen, C. H., Mochly-Rosen, D., Giachetti, A., Ziche, M., and Donnini, S. (2013) Mitochondrial aldehyde dehydrogenase-2 activation prevents beta-amyloid-induced endothelial cell dysfunction and restores angiogenesis, *Journal of cell science* 126, 1952-1961.
- [199] Berke, J. D., and Hyman, S. E. (2000) Addiction, dopamine, and the molecular mechanisms of memory, *Neuron* 25, 515-532.
- [200] Yao, L., Fan, P., Arolfo, M., Jiang, Z., Olive, M. F., Zablocki, J., Sun, H. L., Chu, N., Lee, J., Kim, H. Y., Leung, K., Shryock, J., Blackburn, B., and Diamond, I. (2010) Inhibition of aldehyde dehydrogenase-2 suppresses cocaine seeking by generating THP, a cocaine use-dependent inhibitor of dopamine synthesis, *Nature medicine* 16, 1024-1028.

- [201] Arolfo, M. P., Overstreet, D. H., Yao, L., Fan, P., Lawrence, A. J., Tao, G., Keung, W. M., Vallee, B. L., Olive, M. F., Gass, J. T., Rubin, E., Anni, H., Hodge, C. W., Besheer, J., Zablocki, J., Leung, K., Blackburn, B. K., Lange, L. G., and Diamond, I. (2009) Suppression of heavy drinking and alcohol seeking by a selective ALDH-2 inhibitor, *Alcoholism, clinical and experimental research* 33, 1935-1944.
- [202] Soyka, M., and Rosner, S. (2010) Emerging drugs to treat alcoholism, *Expert Opin Emerg Drugs* 15, 695-711.
- [203] Keung, W. M., and Vallee, B. L. (1993) Daidzin: a potent, selective inhibitor of human mitochondrial aldehyde dehydrogenase, *Proceedings of the National Academy of Sciences of the United States of America* 90, 1247-1251.
- [204] Lowe, E. D., Gao, G. Y., Johnson, L. N., and Keung, W. M. (2008) Structure of daidzin, a naturally occurring anti-alcohol-addiction agent, in complex with human mitochondrial aldehyde dehydrogenase, *Journal of medicinal chemistry* 51, 4482-4487.
- [205] Lam, J. P., Mays, D. C., and Lipsky, J. J. (1997) Inhibition of recombinant human mitochondrial and cytosolic aldehyde dehydrogenases by two candidates for the active metabolites of disulfiram, *Biochemistry* 36, 13748-13754.
- [206] Mays, D. C., Ortiz-Bermudez, P., Lam, J. P., Tong, I. H., Fauq, A. H., and Lipsky, J. J. (1998) Inhibition of recombinant human mitochondrial aldehyde dehydrogenase by two intermediate metabolites of disulfiram, *Biochemical pharmacology* 55, 1099-1103.
- [207] Barth, K. S., and Malcolm, R. J. (2010) Disulfiram: an old therapeutic with new applications, *CNS Neurol Disord Drug Targets* 9, 5-12.
- [208] Schroeder, J. P., Cooper, D. A., Schank, J. R., Lyle, M. A., Gaval-Cruz, M., Ogbonmwan, Y. E., Pozdeyev, N., Freeman, K. G., Iuvone, P. M., Edwards, G. L., Holmes, P. V., and Weinshenker, D. (2010) Disulfiram attenuates drug-primed reinstatement of cocaine seeking via inhibition of dopamine beta-hydroxylase, *Neuropsychopharmacology* 35, 2440-2449.
- [209] Lin, L. Z., and Lin, J. (2011) Antabuse (disulfiram) as an affordable and promising anticancer drug, *Int J Cancer* 129, 1285-1286; author reply 1286-1287.
- [210] Morgan, C. A., Parajuli, B., Buchman, C. D., Dria, K., and Hurley, T. D. (2015) N,N-diethylaminobenzaldehyde (DEAB) as a substrate and mechanism-based inhibitor for human ALDH isoenzymes, *Chemico-biological interactions* 234, 18-28.

- [211] Rekha, G. K., and Sladek, N. E. (1997) Inhibition of human class 3 aldehyde dehydrogenase, and sensitization of tumor cells that express significant amounts of this enzyme to oxazaphosphorines, by the naturally occurring compound gossypol, *Advances in experimental medicine and biology* 414, 133-146.
- [212] Staub, R. E., Quistad, G. B., and Casida, J. E. (1998) Mechanism for benomyl action as a mitochondrial aldehyde dehydrogenase inhibitor in mice, *Chemical research in toxicology* 11, 535-543.
- [213] Amory, J. K., Muller, C. H., Shimshoni, J. A., Isoherranen, N., Paik, J., Moreb, J. S., Amory, D. W., Sr., Evanoff, R., Goldstein, A. S., and Griswold, M. D. (2011) Suppression of spermatogenesis by bisdichloroacetyldiamines is mediated by inhibition of testicular retinoic acid biosynthesis, *J Androl* 32, 111-119.
- [214] Parajuli, B., Georgiadis, T. M., Fishel, M. L., and Hurley, T. D. (2014) Development of selective inhibitors for human aldehyde dehydrogenase 3A1 (ALDH3A1) for the enhancement of cyclophosphamide cytotoxicity, *Chembiochem : a European journal of chemical biology* 15, 701-712.
- [215] Parajuli, B., Fishel, M. L., and Hurley, T. D. (2014) Selective ALDH3A1 inhibition by benzimidazole analogues increase mafosfamide sensitivity in cancer cells, *Journal of medicinal chemistry* 57, 449-461.
- [216] Morgan, C. A., and Hurley, T. D. (2015) Characterization of two distinct structural classes of selective aldehyde dehydrogenase 1A1 inhibitors, *Journal of medicinal chemistry* 58, 1964-1975.
- [217] Belmont-Diaz, J. A., Calleja-Castaneda, L. F., Yoval-Sanchez, B., and Rodriguez-Zavala, J. S. (2015) Tamoxifen, an anticancer drug, is an activator of human aldehyde dehydrogenase 1A1, *Proteins* 83, 105-116.
- [218] Kotraiah, V., Pallares, D., Toema, D., Kong, D., and Beausoleil, E. (2012) Identification of aldehyde dehydrogenase 1A1 modulators using virtual screening, *Journal of enzyme inhibition and medicinal chemistry*.
- [219] Bell, R. G., and Smith, H. W. (1949) Preliminary report on clinical trials of antabuse, *Canadian Medical Association journal* 60, 286-288.
- [220] Morgan, C. A., and Hurley, T. D. (2015) Development of a high-throughput in vitro assay to identify selective inhibitors for human ALDH1A1, *Chemico-biological interactions* 234, 29-37.
- [221] Zheng, C. F., Wang, T. T., and Weiner, H. (1993) Cloning and expression of the full-length cDNAs encoding human liver class 1 and class 2 aldehyde dehydrogenase, *Alcoholism, clinical and experimental research* 17, 828-831.

- [222] Parajuli, B., Kimble-Hill, A. C., Khanna, M., Ivanova, Y., Meroueh, S., and Hurley, T. D. (2011) Discovery of novel regulators of aldehyde dehydrogenase isoenzymes, *Chemico-biological interactions* 191, 153-158.
- [223] Klyosov, A. A. (1996) Kinetics and specificity of human liver aldehyde dehydrogenases toward aliphatic, aromatic, and fused polycyclic aldehydes, *Biochemistry* 35, 4457-4467.
- [224] Otwinowski, Z., and Minor, W. (1997) Processing of X-ray diffraction data collected in oscillation mode, *Method Enzymol* 276, 307-326.
- [225] Bailey, S. (1994) The Ccp4 Suite - Programs for Protein Crystallography, *Acta Crystallogr D* 50, 760-763.
- [226] Emsley, P., and Cowtan, K. (2004) Coot: model-building tools for molecular graphics, *Acta Crystallogr D* 60, 2126-2132.
- [227] Painter, J., and Merritt, E. A. (2006) Optimal description of a protein structure in terms of multiple groups undergoing TLS motion, *Acta Crystallogr D* 62, 439-450.
- [228] Painter, J., and Merritt, E. A. (2005) A molecular viewer for the analysis of TLS rigid-body motion in macromolecules, *Acta Crystallogr D* 61, 465-471.
- [229] Kimble-Hill, A. C., Parajuli, B., Chen, C. H., Mochly-Rosen, D., and Hurley, T. D. (2014) Development of selective inhibitors for aldehyde dehydrogenases based on substituted indole-2,3-diones, *Journal of medicinal chemistry* 57, 714-722.
- [230] dos Santos, D. J., and Eriksson, L. A. (2006) Permeability of psoralen derivatives in lipid membranes, *Biophys J* 91, 2464-2474.

Curriculum vitae

Cameron D. Buchman

Education

Ph.D., Biochemistry and Molecular Biology 2011-2016
Indiana University, Indianapolis, IN
Thesis Title: *Discovery and characterization of small molecule inhibitors of the aldehyde dehydrogenase 1/2 family*

B.S., Biochemistry (*summa cum laude*) 2007-2011
Marshall University, Huntington, WV
Capstone Title: *Understanding how photosynthesis functions at a molecular level: assembly of the water-splitting catalyst*

Research Experience

Graduate Student Research Scientist 2011-Present
Department of Biochemistry and Molecular Biology, Indiana University School of Medicine

Research Advisor: Dr. Thomas D. Hurley

- Performed *in vitro* high-throughput screen to identify novel small molecule modulators of ALDH2.
- Characterized compounds further using steady-state kinetics to determine mode of inhibition, protein X-ray crystallography to determine molecular bases for selectivity and potency, and mammalian cell culture to determine compound bioavailability. Determined structure activity relationships with several isoenzymes using enzyme kinetics and protein expression and purification.

Undergraduate Student Research Scientist 2010-2011

Department of Chemistry, Marshall University

Research Advisor: Dr. Derrick R.J. Kolling

- Investigated relationship between manganese concentration and the rate of photoassembly in photosynthesis organisms. Used 3,3',5,5'-tetramethylbenzidine to measure the manganese concentration of *Chlamydomonas reinhardtii*.
- Learned skills include UV spectroscopy, molecular biology, and bacterial cell culture.

Teaching Experience

Teaching Assistant

Principles of Chemistry Lab, Marshall University 2009-2010

- Graded lab reports and helped with in-lab training of students

Biochemistry Lab, Marshall University 2011

- Prepared the reagents used in each week's experiment
- Helped develop new experiments to be used within the class

Awards and Grants

- Trainee Award, 17th International Workshop of the Enzymology and Molecular Biology of Carbonyl Metabolism 2014
- NASA WV Space Grant Recipient 2010-2011
- Completion of Marshall University Honors Program 2011
- Marshall University Outstanding Graduating Chemist 2011
- Marshall University Outstanding Freshman Chemist 2008

Publications

- **Buchman CD**, Hurley TD. Inhibition of the Aldehyde Dehydrogenase 1/2 Family by Psoralen and Coumarin Derivatives. Submitted to *Journal of Medicinal Chemistry*
- **Buchman CD**, Mahalingan KK, Hurley TD. (2015) Discovery of a series of aromatic lactones as ALDH1/2-directed inhibitors. *Chem. Biol. Interact.* 234:38-44
- Morgan CA, Parajuli B, **Buchman CD**, Dria K, Hurley TD. (2015) N,N-diethylaminobenzaldehyde(DEAB) as a substrate and mechanism-based inhibitor for human ALDH isoenzymes. *Chem. Biol. Interact.* 234:18-28
- Wang B, **Buchman CD**, Li L, Hurley TD, Meroueh SO. (2014) Enrichment of chemical libraries docked to protein conformational ensembles and application to aldehyde dehydrogenase 2. *J. Chem. Inf. Model.* 54(7):2105-16

Abstracts, Posters, Presentations

- **Buchman CD**, Mahalingan KK, Hurley TD. "Inhibition of Aldehyde Dehydrogenase 2 by a Class of Aromatic Lactones", Department of Biochemistry and Molecular Biology, Indiana University School of Medicine, February 2015
- **Buchman CD**, Mahalingan KK, Hurley TD. "Inhibition of Aldehyde Dehydrogenase 2 by a Class of Aromatic Lactones", Indiana University School of Medicine Biochemistry Research Day, November 2014
- **Buchman CD**, Mahalingan KK, Hurley TD. "Inhibition of Aldehyde Dehydrogenase 2 by a Class of Aromatic Lactones" 17th International Workshop on the Enzymology and Molecular Biology of Carbonyl Metabolism, Poconos, PA, July 2014
- **Buchman CD**, Zeid Y, Kolling DRJ. "Understanding How Photosynthesis Functions at a Molecular Level: Assembly of the Water-Splitting Catalyst" 8th Annual Undergraduate Research Day at the Capitol, Charleston, WV, January 2011